THE RADIAL DISTRIBUTION FUNCTION AND THE THERMODYNAMIC PROPERTIES OF MONATOMIC LIQUIDS

A STATISTICAL MECHANICAL THEORY OF THE COEFFICIENT OF THERMAL CONDUCTIVITY OF MONATOMIC LIQUIDS

Thesis by

Berni Julian Alder

In Partial Fulfillment of the Requirements
For the Degree of
Doctor of Philosophy

California Institute of Technology
Pasadena, California
1952

ACKNOWLEDGMENT

A project such as the first part of this thesis represents is only possible through the cooperation of many people. I was indeed fortunate to have the help and suggestions during this work of a very splendid group of persons to whom I wish to express herewith my sincere gratitude.

Foremost my acknowledgment goes to Professor Kirkwood who first introduced to me and patiently taught me the principles of statistical mechanics and without whose constant guidance, inspiration, and encouragement no part of this work would ever have seen the light of day. I am thankful to have been able to profit by this rewarding association.

I feel indeed obliged to Dr. J. H. Irving who helped me start on the first part of the thesis and who assisted me greatly in the theory of the thermal conductivity. The ideas and patient labor of Dr. E. K. Maun and Dr. V. A. Lewinson largely contributed to the success of this venture as did Dr. S. P. Frankel's ingenious use of the I.B.M. machines. I am greatly indebted to Mrs. V. F. Alfonte for cheerful and competent assistance. I am also indebted to Mr. W. Chaplin, Mr. G. Nazarian, and Mr. R. Zwanzig for their contributions during various phases of this project.

I am thankful furthermore to the Office of Naval Research, which bore the main financial burdens and which kindly provided me with a research fellowship for the year 1949-1950. Finally, I gratefully acknowledge the Shell fellowship for the year 1950-1951.

ABSTRACT

A fluid consisting of molecules interacting with the Lennard-Jones intermolecular potential but with rigid cores is treated by the Kirkwood and the Born-Green statistical-mechanical formulations. The integral equation for the radial distribution function of this fluid is solved numerically by a series expansion of all temperature dependent quantities in the reciprocal of the temperature. The first three terms of this series for the radial distribution function have been evaluated over a wide range of densities for the Born-Green integral equation.

The distribution functions so obtained have been used to calculate the equation of state, the excess internal energy, and the excess entropy of this fluid. The two phase region of this equation of state is determined. For reasonable values of the parameters in the potential, these calculated quantities agree within 10% to 20% with experimental data available for argon.

At one density a comparison between the Kirkwood and the Born-Green theories shows that the two formulations agree closely.

A molecular theory of the coefficient of heat conductivity of monatomic liquids is developed on the basis of the general theory of transport processes presented by Kirkwood in 1946. The coefficient is expressed in terms of the intermolecular force and the equilibrium radial distribution function. Substituting for these, respectively, the Lennard-Jones

potential and a reasonable analytic approximation to the experimental radial distribution function, the product of the thermal conductivity and the friction constant has been evaluated~~,~~ for liquid argon at 89°K. With a preliminary estimate of the friction constant, the value of the coefficient of thermal conductivity is then given.

TABLE OF CONTENTS

TABLE OF CONTENTS (Cont.)

PART I

THE RADIAL DISTRIBUTION FUNCTION AND THE THERMODYNAMIC PROPERTIES OF MONATOMIC LIQUIDS

THE RADIAL DISTRIBUTION FUNCTION AND THE THERMODYNAMIC PROPERTIES OF MONATOMIC LIQUIDS

Introduction

Although statistical mechanics has had considerable success in the interpretation of properties of rarefied gases and of crystalline solids, practical difficulties have retarded its application to dense gases and to liquids. Theories for the condensed fluid phase have recently been developed by Kirkwood(1), Born and Green(2), Mayer(3), and Yvon(4) in almost equivalent form. In the first part of this thesis we will give a brief resume' of these statistical mechanical treatments of fluids, and subsequently apply the theory to evaluate the thermodynamic functions of the condensed state.

These methods assume that classical statistical mechanics is competent to describe the dependence of the thermodynamic functions of fluids upon intermolecular force. This assumption is justified when certain conditions involving masses, moments of inertia, the intermolecular potential, and temperature are satisfied. Furthermore, early in the derivation of the theory, we restrict ourselves to fluids composed of molecules with a potential of intermolecular force depending only on the relative distance, R_{ik}, of molecular pairs,

$$V_N = \sum_{\substack{i<k \\ =1}}^{N} V(R_{ik}). \tag{1}$$

The restriction of the potential to the form of equation (1) implies that the molecules of the fluid are spherical. The fluids, then, with which experimental comparisons are justified are the single-component condensed rare-gases, and other liquids satisfying the law of corresponding states, at temperatures high enough so that quantum effects can be neglected. Liquid metals and polar liquids can not be treated by this theory since their potentials of intermolecular force are not adequately represented by (1).

Under the above restrictions we will evaluate the important radial distribution function, g(R), which characterizes the liquid structure, as a solution to an integral equation. g(R) Is so defined that $\frac{N}{v}$ g(R) is the average local molecular density at a distance R from a specified molecule in a system of N molecules occupying a volume v. Kirkwood$^{(1)}$ has called attention to the close relation which exists between the distribution function and the potential of average force.

$$g(R) = e^{-W^{(2)}(R)/kT} , \qquad (2)$$

where $W^{(2)}(R)$ is the potential of mean force acting on the molecular pair, the resultant of their direct interaction and the average interaction with the other (N-2) molecules of the liquid. T is the temperature and k is the Boltzmann constant.

By these theories$^{(1,2)}$, the thermodynamic functions of a liquid can be expressed in terms of the radial distribution function and the potential of intermolecular force, V(R). The equation of state is given by

$$\frac{pv}{NkT} = 1 - \frac{2\pi N}{3vkT}\int_0^\infty R^3 \frac{dV}{dR} g(R)\, dR, \qquad (3)$$

and the internal energy, E, by

$$\frac{E}{NkT} = \frac{3}{2} + \frac{2\pi N}{vkT}\int_0^\infty R^2 V(R)\, g(R)\, dR. \qquad (4)$$

These thermodynamic functions may be calculated when the radial distribution function has been evaluated from the integral equation which determines it. The major problem resolved in the first part of this thesis is the numerical solution of this equation for the radial distribution function over a wide range of density and temperature.

For the noble gas fluids the potential of intermolecular force

$$V(R) = \frac{A}{R^{12}} - \frac{B}{R^6} \qquad (5)$$

due to Lennard-Jones$^{(5)}$ is generally substituted in the integral equation as well as in (3) and (4). A and B are constants characteristic of the substance. The attractive part of the interaction energy is taken to be proportional to

R^{-6} in accordance with the Heitler-London theory of intermolecular force. From a comparison between theoretical and experimental values of the second virial coefficient, the value of the repulsive power exponent, as well as A and B, can be determined for each substance.

The non-equilibrium properties of the fluid state may also be expressed in terms of the equilibrium radial distribution function and the potential of intermolecular force(6). The general theory of transport processes has already been applied to the coefficient of viscosity by Kirkwood, Buff, and Green(7), and in the second part of this thesis, the detailed derivation of the coefficient of thermal conductivity is developed.

In addition to the above applications of the radial distribution function, it is also of particular interest since it can be determined experimentally from the angular distribution of x-ray scattering. If x-rays of wave length λ are scattered by an array of atoms which are separated by distances R_{ik}, the intensity of radiation, I, at the scattering angle 2θ is given by(8):

$$I = \sum_i \sum_k f_i f_k \frac{\sin sR_{ik}}{sR_{ik}}, \tag{6}$$

where f is the atomic structure factor and $s = \dfrac{4\pi \sin\theta}{\lambda}$.

If we assume a continuous distribution of a single kind of atom, I reduces to:

$$I = Nf^2\left[1 + \int_0^\infty 4\pi R^2 \frac{N}{v}\left(g(R) - 1\right)\frac{\sin sR}{sR}\, dR\right]. \tag{7}$$

The radial distribution function can then be calculated from the observed intensities by a Fourier integral transformation of (7):

$$\frac{N}{V}\left[g(R)-1\right] = \frac{1}{2\pi^2 R}\int_0^\infty \left(\frac{I}{Nf^2}-1\right) s \sin Rs \, ds . \qquad (8)$$

The basic theory was developed by Zernicke and Prins(9), and Debye and Mencke(8), and has been applied extensively by Warren(10) and Eisenstein and Gingrich(11) to many liquids. Of particular interest in the present work are the x-ray scattering data available for argon(11), which are used in the comparison with the theoretically determined radial distribution function.

Derivation of the Equations for the Radial Distribution Function

The radial distribution function is calculable from a system of integro-differential equations developed in equivalent form by Kirkwood(1), Born and Green(2), Mayer(3), and Yvon(4). The starting point in all these derivations is the canonical ensemble of Gibbs, which gives an expression for the equilibrium probability density, $f^{(N)}(\vec{R}_1 \cdots \vec{R}_N, \vec{p}_1 \cdots \vec{p}_N)$, in phase space for a system of N molecules:

$$f^{(N)}(\vec{R}_1 \cdots \vec{R}_N, \vec{p}_1 \cdots \vec{p}_N) = e^{\beta\left[A - H(\vec{R}_1 \cdots \vec{R}_N, \vec{p}_1 \cdots \vec{p}_N)\right]}, \qquad (9)$$

where $\vec{R}_1$ is the distance vector from some origin to particle 1, $\vec{p}_1$ is the momentum of particle 1, and $\beta = \frac{1}{kT}$. Also H is the classical Hamiltonian, and A is the normalization constant, which is determined so that

$$\iint f^{(N)}(\vec{R}_1 \cdots \vec{R}_N, \vec{p}_1 \cdots \vec{p}_N) \prod_{k=1}^{N} d\vec{R}_k \, d\vec{p}_k = 1. \qquad (10)$$

A is furthermore identified with the Helmholtz free energy. Integration over momentum space after substitution of the Hamiltonian

$$H = V^{(N)}(\vec{R}_1 \cdots \vec{R}_N) + \sum_{k=1}^{N} \frac{\vec{P}_k^{\,2}}{2m_k} \qquad (11)$$

results in the equilibrium probability density, $P^{(N)}(\vec{R}_1 \cdots \vec{R}_N)$, in configuration space.

$$P^{(N)}(\vec{R}_1 \cdots \vec{R}_N) = e^{\beta[\bar{A} - V^{(N)}(\vec{R}_1 \cdots \vec{R}_N)]}, \tag{12}$$

where $V^{(N)}(\vec{R}_1 \cdots \vec{R}_N)$ is the intermolecular potential and m_k is the mass of particle k. $\bar{A}$ is the new normalization constant. The probability density $P^{(n)}(\vec{R}_1 \cdots \vec{R}_n)$ of n molecules in a system of N molecules is in the subspace of the entire configuration space and is obtained by integration over the space of N-n molecules.

$$P^{(n)}(\vec{R}_1 \cdots \vec{R}_n) = \underbrace{\int \cdots \int}_{N-n} e^{\beta[\bar{A} - V^{(N)}(\vec{R}_1 \cdots \vec{R}_N)]} \prod_{k=n+1}^{N} d\vec{R}_k \,. \tag{13}$$

As a special case of this, integration over N-2 particles yields the important probability density $P^{(2)}(\vec{R}_1, \vec{R}_2)$ in the configuration space of molecular pairs, to which the radial distribution function is simply related:

$$P^{(2)}(\vec{R}_1, \vec{R}_2) = \underbrace{\int \cdots \int}_{N-2} e^{\beta[\bar{A} - V^{(N)}(\vec{R}_1 \cdots \vec{R}_N)]} \prod_{k=3}^{N} d\vec{R}_k \,. \tag{14}$$

The exact numerical value of this multiple integral can not be directly computed by present methods except for the very simple case of the perfect gas where $V^{(N)}(\vec{R}_1 \cdots \vec{R}_N)$ is independent of the distances. In all other cases integration over the coordinates of a large number of molecules has to be carried out. Mayer(3) has shown that a variational method leads to integral equations involving integration over fewer molecules. In both the Kirkwood and the Born-Green derivations a particular case of the variation of the potential is taken.

A. Derivation of Born-Green System of Integral Equations

The Born-Green equation, which is to be numerically solved here, utilizes a potential of the form:

$$V^{(N)}(\vec{R}_1 \cdots \vec{R}_N) = \sum_{\substack{i<k \\ =1}}^{N} V(\vec{R}_{ik}) . \tag{15}$$

The particular variation is the gradient with respect to the position of any molecule in the set of n molecules. This molecule is arbitrarily chosen here as molecule one. Thus

$$\nabla_{\vec{R}_1} P^{(n)}(\vec{R}_1 \cdots \vec{R}_n) = -\beta \int_{N-n}\!\!\cdots\!\int \left[\nabla_{\vec{R}_1} V^{(N)}(\vec{R}_1 \cdots \vec{R}_N)\right] e^{\beta[\bar{A} - V^{(N)}]} \prod_{k=n+1}^{N} d\vec{R}_k \tag{16}$$

$$= -\beta(n-1)\left[\nabla_{\vec{R}_1} V(\vec{R}_{12})\right] P^{(n)}(\vec{R}_1 \cdots \vec{R}_n) -$$
$$-\beta(N-n)\int \left[\nabla_{\vec{R}_1} V(\vec{R}_{13})\right] P^{(n+1)}(\vec{R}_1 \cdots \vec{R}_{n+1})\, d\vec{R}_3 .$$

The last equality follows since the gradient of the potential can be broken up into two parts.

$$\nabla_{\vec{R}_1} V^{(N)}(\vec{R}_1 \cdots \vec{R}_N) = \sum_{k=2}^{n} \nabla_{\vec{R}_1} V(\vec{R}_{1k}) + \sum_{k=n+1}^{N} \nabla_{\vec{R}_1} V(\vec{R}_{1k}) . \tag{17}$$

Upon substitution of this expression, the first term of the gradient of the potential can be taken outside of the integral. The sum over k gives n-1 identical terms, so that k can be arbitrarily called 2. The second term of the gradient of the potential, when substituted, can also be reduced as a result of the fact that for any k the integral is the same. k is here arbitrarily called 3.

The solution of this set of integro-differential equations (16) would probably be as difficult as the evaluation of the integral itself, if it were not easier to introduce an approximation in this new formulation. The root of the difficulty in the solution of the set of equation (16) is that the nth equation depends on the $(n+1)^{st}$. Thus, to solve for $P^{(2)}$ a knowledge of $P^{(3)}$ is essential, and in this fashion a whole chain is set up. This can be broken if $P^{(3)}$ could somehow be related to $P^{(2)}$ by an additional expression. Substitution of such an expression would result in an integro-differential expression involving $P^{(2)}$ only. Kirkwood's superposition approximation accomplishes precisely that. Its physical foundation as well as its name rests essentially on the proposition that the probability densities in triplet space are independent. They can therefore be expressed in terms of probability densities in pair space. A more precise statement can be given if the following theorem is recalled:

$$P^{(n)}(\vec{R}_1 \cdots \vec{R}_n) = e^{-\beta W^{(n)}(\vec{R}_1 \cdots \vec{R}_n)} \Big/ v^n, \qquad (18)$$

where $W^{(n)}$ is the potential of mean force acting on the system of n molecules and v is the volume of the system. The approximation can now be stated in the form that the mean force acting on molecule three due to molecule one and two in its vicinity, is equal to the sum of the mean forces if molecules one and two were each present alone. Or, in terms of probabilities:

$$\frac{P^{(3)}(\vec{R}_1, \vec{R}_2, \vec{R}_3)}{P^{(1)}(\vec{R}_1)\, P^{(1)}(\vec{R}_2)\, P^{(1)}(\vec{R}_3)} = \frac{P^{(2)}(\vec{R}_1, \vec{R}_2)}{P^{(1)}(\vec{R}_1)\, P^{(1)}(\vec{R}_2)} \times \frac{P^{(2)}(\vec{R}_1, \vec{R}_3)}{P^{(1)}(\vec{R}_1)\, P^{(1)}(\vec{R}_3)} \times \frac{P^{(2)}(\vec{R}_2, \vec{R}_3)}{P^{(1)}(\vec{R}_2)\, P^{(1)}(\vec{R}_3)} . \qquad (19)$$

This means that the probability density of simultaneous occurrence of a triple of molecules 1, 2, and 3 at $\vec{R}_1, \vec{R}_2, + \vec{R}_3$,, relative to the probability density that the molecules be singly at those positions, is just the relative probability density of independent occurrence of each of the three pairs involved.

For convenience, we introduce the number density and the radial distribution function. The number density differs from the probability density by the indistinguishability of the particles, and is therefore given by:

$$\rho^{(n)}(\vec{R}_1 \cdots \vec{R}_n) = \frac{N!}{(N-n)!} P^{(n)}(\vec{R}_1 \cdots \vec{R}_n) . \qquad (20)$$

The advantage of introducing this definition into (16) is that the (N-n) factor is removed, if the approximation is made that (N-n) ≅ N. The radial distribution function or pair correlation function, $g^{(2)}(\vec{R}_1, \vec{R}_{12})$, is related to the number density through the definition:

$$\frac{\rho^{(2)}(\vec{R}_1, \vec{R}_2)}{\rho^{(1)}(\vec{R}_1)\, \rho^{(1)}(\vec{R}_2)} = g^{(2)}(\vec{R}_1, \vec{R}_{12}), \qquad (21)$$

where $\vec{R}_{12} = \vec{R}_1 - \vec{R}_2$. For a fluid, by definition, $\rho^{(1)}(\vec{R})$ is considered to be uniform and equal to the reciprocal of the volume per molecule.

$$\rho^{(1)} = \frac{N}{v} . \tag{22}$$

The restriction imposed by this homogeneous singlet density quite obviously leaves the crystalline state out of the consideration of this theory. The uniform singlet density also has an effect on the two-phase region between the gas and liquid states where the equilibrium density is not uniform. The solutions of the equation under the above restraint can only be interpreted as corresponding to the uniform metastable density of the supersaturated vapor or the superheated liquid.

The statement of the superposition approximation in terms of forces immediately follows, now, since, by (18), we can write (19) as:

$$W^{(3)}(\vec{R}_1, \vec{R}_2, \vec{R}_3) = W^{(2)}(\vec{R}_2, \vec{R}_3) + W^{(2)}(\vec{R}_1, \vec{R}_3) + W^{(2)}(\vec{R}_1, \vec{R}_2) . \tag{23}$$

Taking the gradients of (23) results in

$$\nabla_{\vec{R}_1} W^{(3)}(\vec{R}_1, \vec{R}_2, \vec{R}_3) = \nabla_{\vec{R}_1} W^{(2)}(\vec{R}_1, \vec{R}_2) + \nabla_{\vec{R}_1} W^{(2)}(\vec{R}_1, \vec{R}_3) . \tag{24}$$

It is quite evident how an equivalent superposition approximation could be written in a general n-dimensional configuration space. It is also reasonable from the physical nature of the approximation that, the higher the dimensionality of the space in which the approximation is used, the more closely the resulting probability density corresponds to the correct one. In connection with this, it is interesting to note that Kirkwood was able to show(12) that the use of superposition in singlet space leads to the simple free volume theory of liquids.

We restrict our considerations further to an isotropic homogeneous liquid, that is to the bulk of a fluid. This simplification makes $g^{(2)}$ a function only of the relative distance between molecular pairs, and independent of the absolute location and direction in the fluid:

$$g^{(2)} = g^{(2)}(R_{12}) \,. \tag{25}$$

Utilization in (16), written in pair space, of the superposition approximation and the definitions given by (20) and (21) yields:

$$\begin{aligned} &\nabla_{\vec{R}_1}\left[\log g^{(2)}(R_{12}) + \beta V(R_{12})\right] = \\ &-\beta \rho^{(1)} \int \left[\nabla_{\vec{R}_1} V(R_{13})\right] g^{(2)}(R_{13})\, g^{(2)}(R_{23})\, d\vec{R}_3 . \end{aligned} \tag{26}$$

Equation (16) in singlet space becomes:

$$\int \left[\nabla_{\vec{R}_1} V(R_{13})\right] g^{(2)}(R_{13})\, d\vec{R}_3 = 0, \tag{27}$$

since $\rho^{(1)} = \frac{1}{V}$ is a constant. For convenience (27) is subtracted from (26), so that:

$$\nabla_{\vec{R}_1}\left[\log g^{(2)}(R_{12}) + \beta V(R_{12})\right] = - \beta \rho^{(1)} \int \left[\nabla_{\vec{R}_1} V(R_{13})\right] g^{(2)}(R_{13}) \left[g^{(2)}(R_{23}) - 1\right] d\vec{R}_3 . \qquad (28)$$

A great number of mathematical operations are now performed on (28) including a change to bipolar coordinates. The details of these are given in Appendix A. The final result is the following equation:

$$\log g(R) = -\beta V(R) + \frac{\pi \rho^{(1)}}{R} \int_{-\infty}^{\infty} K(R-r)\, r \left[g(r)-1\right] dr , \qquad (29)$$

where R_{12} has been called R, and where the kernel of the integral equation, $K(z)$, is given by:

$$K(z) = \beta \int_{|z|}^{\infty} (y^2 - z^2) \frac{dV(y)}{d(y)} g(y)\, dy . \qquad (30)$$

B. Derivation of Kirkwood's System of Integral Equations

Kirkwood, on the other hand, proceeds from a potential of the form

$$V^{(N)}(\xi_1 \cdots \xi_N , \vec{R}_1 \cdots \vec{R}_N) = \sum_{\substack{i<k \\ =1}}^{N} \xi_i \xi_k V(\vec{R}_{ik}) , \qquad (31)$$

where the ξ's are coupling parameters. They allow the force between any two molecules to be continuously changed from no force at all when ξ is zero, to the full value of the force when ξ equals unity. For example, if all molecules are fully coupled except molecule one (i.e., $\xi_2 = \xi_3 = \cdots = \xi_N = 1$), the potential would correspond to

$$V^{(N)}(\vec{R}_1 \cdots \vec{R}_N, \xi_1) = V^{(N-1)}(\vec{R}_2 \cdots \vec{R}_N) + \sum_{k=2}^{N} \xi_1 V(\vec{R}_{1k}). \qquad (32)$$

The introduction of such a potential quite obviously makes the probability density, the radial distribution function, and also $\bar{A}_N$ in (12), functions of these coupling parameters.

The particular variation of the potential carried out is the differentiation with respect to the coupling parameter of one of the set of n molecules. This molecule is again arbitrarily labeled molecule one. Substitution of (31) into (14), followed by the differentiation, results in:

$$\frac{\partial P^{(n)}(\xi_1 \cdots \xi_N, \vec{R}_1 \cdots \vec{R}_N)}{\partial \xi_1} = \beta \underbrace{\int \cdots \int}_{N-n} \left\{ \frac{\partial \bar{A}_N(\xi_1 \cdots \xi_N)}{\partial \xi_1} - \right. \qquad (33)$$

$$\left. - \sum_{k=2}^{n} \xi_k V(\vec{R}_{1k}) - \sum_{k=n+1}^{N} \xi_k V(\vec{R}_{1k}) \right\} e^{\beta\left[\bar{A}_N - V^{(N)}\right]} \prod_{k=n+1}^{N} d\vec{R}_k ,$$

where the potential has been broken up into two parts. Specialization to the pair probability distribution function for molecule one with an arbitrary molecule 2 transforms (33) to the following:

$$\frac{\partial P^{(2)}(\xi,\vec{R}_1,\vec{R}_2)}{\partial \xi} = \beta\left[\frac{\partial \bar{A}_N(\xi)}{\partial \xi} - V(\vec{R}_{12})\right] P^{(2)}(\xi,\vec{R}_1,\vec{R}_2) - \beta(N-2)\int V(\vec{R}_{13})\, P^{(3)}(\xi,\vec{R}_1,\vec{R}_2,\vec{R}_3)\, d\vec{R}_3, \qquad (34)$$

where $\xi_1 = \xi;\ \xi_2 = \xi_3 = \cdots = \xi_N = 1$. This simplification makes all the N-2 integrals of the last term identical. The representative integral is written for molecule three.

The procedure from here on is the same as in the Born-Green derivation. The only exception is that the term $\frac{\partial \bar{A}_N}{\partial \xi}$ in (34) must first be eliminated. This is accomplished by substituting the expression for $\frac{\partial \bar{A}_N}{\partial \xi}$ obtained from (33) when it is restricted to the singlet space. That is,

$$\frac{\partial P^{(1)}(\xi,\bar{R}_1)}{\partial \xi} = 0 = \beta\,\frac{\partial \bar{A}_N(\xi)}{\partial \xi}\cdot\frac{1}{v} - \beta(N-1)\int V(\vec{R}_{13})\,P^{(2)}(\xi,\vec{R}_1,\vec{R}_3)\,d\vec{R}_3, \qquad (35)$$

where again $P^{(1)}$ is presumed uniform and equal to $\frac{1}{v}$.

The same problem of the cyclic character of the set of integro-differential equations is faced. Again it is resolved by the superposition of the probability density (19). However, the probability densities concerned with molecule one involve the coupling parameter. Thus, the superposition approximation is introduced differently. The error caused by it will consequently not be the same in the Kirkwood and the Born-Green derivations, even though the original sets of integro-differential equations are identical.

For an isotropic homogeneous liquid the combination of (34) and (35), with the introduction of (19) and (21), results in:

$$\frac{\partial \ln g^{(2)}(R_{12},\xi)}{\partial \xi} + \beta V(R_{12}) = -\beta\rho^{(1)}\int V(R_{13})\, g^{(2)}(R_{13},\xi)\left[g^{(2)}(R_{23})-1\right] d\vec{R}_3. \tag{36}$$

A series of mathematical operations similar to those used in the Born-Green case converts this equation into the following integral equation:

$$\log g(R,\xi) = -\beta V(R) + \frac{\pi\rho^{(1)}}{R}\int_{-\infty}^{\infty} K(R-r,\xi)\, r\left[g(r)-1\right] dr, \tag{37}$$

where

$$K(z,\xi) = -2\beta\int_0^{\xi}\int_{|z|}^{\infty} y\, V(y)\, g(y,\xi)\, dy\, d\xi. \tag{38}$$

The details are given in Appendix A.

(37) becomes formally identical with its Born-Green equivalent (29), when ξ is set equal to one, that is, if molecule one is fully coupled as in the actual physical situation. The Born-Green equations implicitly have the coupling constant always equal to one. However, the kernels of the two integral equations are different even if $\xi = 1$, reflecting the influence of the manner in which the superposition approximation was introduced.

Methods of Solution of the Equation

It is convenient before proceeding to solve (29) to convert it to a non-dimensional or reduced form. It will be shown that the solutions then apply generally to all substances whose potentials of interaction differ only in the value of two parameters. The two characteristic values, ε and a, occurring in the potential have the units of energy and distance respectively, since the potential itself has the dimensions of energy and is a function of the distance of separation of the two molecules. In reduced units

$$V(R) = \varepsilon\,\gamma(x)\ ; \quad x = \frac{R}{a}\ . \tag{39}$$

Therefore

$$\log g(x) + \beta\varepsilon\,\gamma(x) = \frac{\lambda_0}{4x}\int_{-\infty}^{\infty} K(x-s)\, s\left[g(s)-1\right] ds, \tag{40}$$

where

$$\lambda_0 = \frac{4\pi N a^3}{v}\ , \quad g^{(2)}(x) = g(x),$$

and

$$K(t) = \beta\varepsilon\int_{|t|}^{\infty} (s^2 - t^2)\,\frac{d\gamma(s)}{ds}\,g(s)\,ds. \tag{41}$$

Besides the parameters $\beta\varepsilon$ and λ_0, the form of the potential assumed influences the solution for g(x). The one adopted quite generally for the fluids under consideration is the Lennard-Jones potential(5)

$$\gamma_1(x) = \frac{4}{x^n} - \frac{4}{x^6} \tag{42}$$

where n is an exponent in the neighborhood of 12. The exponent 6 in the attractive part of the potential is well established quantum mechanically. However, there exists some uncertainty on how to take into account the repulsion of the atoms. Therefore n is empirically fixed, as are ε and a, to give best agreement with the experimentally determined second virial coefficient and other data. With the potential (42), ε determines the depth of the potential well, and a is the finite value of R for which the potential vanishes.

The mathematical solution of the integral equation (40) with the Lennard-Jones potential, by direct iteration or by the method of Fourier transforms, proved to be difficult (see Appendix B-1). To obtain integral equations which could be solved, the Lennard-Jones potential was modified, and g(x) was expanded in powers of the reciprocal of temperature.

The modified Lennard-Jones potential has the form:

$$\begin{aligned} &\gamma(x) = \gamma_0(x) + \gamma_1(x) \\ &\gamma_0(x) = 0 \quad |x| > 1, \quad \gamma_0(x) = \infty \quad |x| < 1 \\ &\gamma_1(x) = 0 \quad |x| < 1, \quad \gamma_1(x) = \frac{4}{x^{12}} - \frac{4}{x^6} \quad |x| > 1. \end{aligned} \tag{43}$$

The repulsive part of the Lennard-Jones potential, which is uncertain anyway, has been altered in (43) in the region where it is positive. The steep $\frac{1}{x^{12}}$ rise has been replaced by an abrupt step. The effect of this change is that the potential, and therefore the radial distribution function, is discontinuous at that point. Since the point of crossover for the potential has been chosen as the unit of distance a, the discontinuity occurs at x = 1. There is also a discontinuity at x = 2 in the distribution function. However, the net effect on the properties of the fluid, calculated under these circumstances, should be slight except perhaps at very high compression, where the repulsive part of the potential plays a more important role.

The series expansion in powers of the reciprocal of temperature is carried out on $\psi(x)$.

$$\psi(x) = \psi_0(x) + (\beta\varepsilon)\,\psi_1(x) + (\beta\varepsilon)^2\,\psi_2(x) + \cdots, \qquad (44)$$

where $\psi(x)$ is defined by

$$g(x) = e^{-\beta\varepsilon\gamma_0(x) + \psi(x)/x} . \qquad (45)$$

Therefore, the radial distribution function can also be expressed by a series in inverse powers of T.

$$g(x) = g_0(x)\left[1 + \beta\varepsilon\,\frac{\psi_1(x)}{x} + (\beta\varepsilon)^2\left[\frac{\psi_1^2(x)}{2x^2} + \frac{\psi_2(x)}{x}\right]\cdots\right], \qquad (46)$$

where

$$g_0(x) = e^{-\beta\varepsilon\gamma_0(x) + \frac{\psi_0(x)}{x}} . \qquad (47)$$

Substitution of (43) and (45) into the integral equation (40) results in :

$$\Psi(x) = -\beta\varepsilon\gamma_1(x) + \frac{\lambda_0}{4}\int_{-\infty}^{\infty} K(x-u)\, u\,[g(u)-1]\,du, \qquad x>1 \tag{48}$$

where

$$K(t) = \beta\varepsilon\int_{|t|}^{\infty}(s^2-t^2)\frac{d\gamma_1}{ds}g(s)ds + \beta\varepsilon\int_{|t|}^{\infty}(s^2-t^2)\frac{d\gamma_0}{ds}g(s)ds. \tag{49}$$

The second integral in the kernel (49) can be simplified by utilizing the properties of $\gamma_0(x)$. Since

$$\begin{aligned} e^{-\beta\varepsilon\gamma_0(x)} &= 0 \qquad 0\leq x\leq 1 \\ &= 1 \qquad x>1 \end{aligned} \tag{50}$$

$$\frac{d}{ds}e^{-\beta\varepsilon\gamma_0(s)} = \delta(s-1) = -\beta\varepsilon\frac{d\gamma_0}{ds}e^{-\beta\varepsilon\gamma_0(s)},$$

where $\delta(S-1)$ represents the Dirac delta function. Thus, upon introducing (50),

$$\beta\varepsilon\int_{|t|}^{\infty}(s^2-t^2)\frac{d\gamma_0}{ds}g(s)ds = g(1)K_0(t), \tag{51}$$

where

$$\begin{aligned} K_0(t) &= t^2-1 \qquad \text{if } t^2\leq 1 \\ K_0(t) &= 0 \qquad \text{if } t^2>1. \end{aligned} \tag{52}$$

(49) then takes the form

$$K(t) = \beta\varepsilon\int_{|t|}^{\infty}(s^2-t^2)\frac{d\gamma_1}{ds}g(s)ds + g(1)K_0(t). \tag{53}$$

Substitution of the temperature expansion (44) into (48) results in:

$$\Psi_0(x) + (\beta\varepsilon)(\Psi_1(x)) + (\beta\varepsilon)^2\Psi_2(x) + \cdots = -\beta\varepsilon\, x\,\gamma_1(x) + \frac{\lambda_0}{4}\int_{-\infty}^{\infty} K(x-u)\,u\Big\{g_0(u) - 1 + (\beta\varepsilon)g_0(u)\frac{\Psi_1(u)}{u} + (\beta\varepsilon)^2\Big[\frac{\Psi_1^2(u)}{2u^2} + \frac{\Psi_2(u)}{u}\Big] + \cdots\Big\}\,du. \tag{54}$$

K(t) can be expanded into the series:

$$K(t) = (\beta\varepsilon)K_1(t) + (\beta\varepsilon)^2K_2(t) + \cdots + g_0(1)\Big\{1 + (\beta\varepsilon)\Psi_1(1) + (\beta\varepsilon)^2\Big[\frac{\Psi_1^2(1)}{2} + \Psi_2(1)\Big] + \cdots\Big\}K_0(t), \tag{55}$$

where

$$K_1(t) = \int_{|t|}^{\infty}(s^2 - t^2)\,g_0(s)\,\frac{d\gamma_1(s)}{ds}\,ds,$$
$$K_2(t) = \int_{|t|}^{\infty}(s^2 - t^2)\,g_0(s)\,\frac{\Psi_1(s)}{s}\,\frac{d\gamma_1(s)}{ds}\,ds. \tag{56}$$

If equal powers of $\beta\varepsilon$ are collected, the terms in $(\beta\varepsilon)^0$ give the hard-sphere integral equation already solved(13) (see Appendix D)

$$\Psi_0(x) = \frac{\lambda}{4}\int_{-\infty}^{\infty}K_0(x-s)\big[s[g(s)-1]\big]\,ds, \tag{57}$$

where $\lambda = \lambda_0\, g_0(1)$.

The terms in $(\beta\varepsilon)^1$ make up the following integral equation:

$$\Psi_1(x) = -x\,\gamma_1(x) + \Psi_1(1)\Psi_0(x) + \frac{\lambda_0}{4}\int_{-\infty}^{\infty}K_1(x-s)\,s\,[g_0(s) - 1]\,ds + \frac{\lambda}{4}\int_{-\infty}^{\infty}K_0(x-s)\,g_0\,\Psi_1\,ds. \tag{58}$$

This equation is of the same general form as all succeeding equations in higher powers of $\beta\varepsilon$:

$$\Psi_r(x) = m_r(x) + \Psi_r(1)\,\Psi_0(x) + \frac{\lambda}{4}\int_{-\infty}^{\infty}ds\,K_0(x-s)\,g_0(s)\,\Psi_r(s). \tag{59}$$

The equation (58) for r = 1 contains the very large term $-x\,\gamma_1(x)$ in its inhomogeneous part. It should therefore express the principal effect of adding the Lennard-Jones potential to the hard-sphere core. For higher values of r, $m_r(x)$ involves more and more terms. Thus for r = 2:

$$\begin{aligned} m_2(x) = {} & \frac{\varphi_1^2(1)}{2}\varphi_0(x) + \frac{\lambda_0}{4}\int_{-\infty}^{\infty} K_2(x-s)\, s\left[g(s)-1\right] ds + \\ & + \frac{\lambda_0}{4}\int_{-\infty}^{\infty} K_1(x-s)\, g_0(s)\, \varphi_1(s)\, ds + \\ & + \frac{\lambda}{4}\int_{-\infty}^{\infty} K_0(x-s)\, g_0(s)\, \frac{\varphi_1^2(s)}{2s}\, ds + \\ & + \frac{\lambda}{4}\int_{-\infty}^{\infty} \varphi_1(1)\, K_0(x-s)\, g_0(s)\, \varphi_1(s)\, ds. \end{aligned} \tag{60}$$

Only the last term has been evaluated previously in the equation for r = 1. Thus the work involved in calculating $m_r(x)$ from previously determined functions becomes more complicated with increasing r; but the form of the integral equation remains the same.

The equations for $\varphi_r(x)$ (59) depend only upon the choice of the reduced volume, that is, on the parameter λ. Once the terms in the series are known for some value of the volume, the radial distribution function can be evaluated for any desired temperature (i.e., value of the parameter $\beta\varepsilon$) at that volume. Thus the expansion has the advantage that the radial distribution function can be calculated for a whole net of temperatures and volumes, knowing only the expansion terms for several volumes. Unfortunately, however, no mathematical test on the convergence of the series is available. We must await the numerical results of the next section to tell us how soon the terms in the series become negligibly small. But we know we can not depend on powers of $\beta\varepsilon$ to make the terms in the series decrease rapidly, since $\beta\varepsilon$ is around unity or higher for conditions corresponding to the liquid state.

The schemes developed for the numerical solution of the integral equations (59) and (57) are identical and depend quite decisively on the properties of the hard-sphere kernel. The method was devised with the aim of allowing the use of I.B.M. machines. Thus, any iterative procedure should involve only simple steps, even though possibly the convergence per iteration is not rapid. The theorem upon which this method is based has unfortunately not been put into rigorous mathematical form. It can, however, be stated that in the mean the true solution lies between the input and the output. That is, on the average the solution can be bounded between iterates. The reason for this becomes apparent if we suppose that the input $g^{(in)}$ differs by $\omega(x)$ from the true solution $g^{(t)}(x)$:

$$g^{(in)}(x) = g^{(t)}(x) + \omega(x) \tag{61}$$

or

$$\varphi^{(in)}(x) = \varphi^{(t)}(x) + \omega'(x), \tag{62}$$

where $\omega'(x) = \frac{\omega(x)\,x}{g^{(t)}(x)}$ if the exponential $e^{\omega'/x}$ can be linearized. Since x and $g^{(t)}(x)$ are always positive, $\omega'(x)$ and $\omega(x)$ have the same sign. On the average, $g^{(t)}(x) \cong 1$, so that

$$\psi^{(in)}(x) \cong \psi^{(t)}(x) + x\,\omega(x). \qquad (63)$$

Substituting (61) into the hard-sphere integral equation (57) yields:

$$\psi^{(out)}(x) = \psi^{(t)}(x) + \frac{\lambda}{4}\int_{-\infty}^{\infty} k_0(x-s)\, s\,\omega(s)\, ds. \qquad (64)$$

$k_0(t)$ has its minimum value of -1 at t = 0 and rises parabolically to zero at t = ±1. In so far as this function can be represented as a delta-function at t = 0, or x = s, (64) becomes:

$$\psi^{(out)}(x) = \psi^{(t)}(x) - \frac{\lambda}{3}\, x\,\omega(x), \qquad (65)$$

using the fact that

$$\int_{-\infty}^{\infty} k_0(t)\, dt = \int_{-1}^{1} (t^2-1)\, dt = -\frac{4}{3}. \qquad (66)$$

This is, of course, a very crude approximation, but comparison of (63) and (65) does support the idea that the true solution lies between the input and the output. It furthermore illustrates how the solutions behave for various values of λ. Certainly for $\lambda \geq 3$ (roughly), direct iteration should fail. This has already been noted. The case of $\lambda = 5$, treated later, showed that rapid convergence was obtained if the output and input were averaged. This is also indicated by (65) and (63). For values of $\lambda = 20$ to $\lambda = 30$, pertaining to the liquid state, the averaging of input and output should fail to converge. This was found to be the case. Instead one had to take 80 to 90% of the input and only 20 to 10% of the output in order to approach the true solution.

The procedure is equally applicable to the integral equation (59) for the higher terms in the expansion. The inhomogeneous part in no way alters the arguments. As a first approximation, the $\psi_r(1)\,\psi_0(x)$ term can be included in the inhomogeneous part, since $\psi_r(1)$ can be considered a constant over a period of a few iterations. Hence, if we define $\omega_r'(x)$ by:

$$\psi_r^{(in)}(x) = \psi_r^{(t)}(x) + \omega_r'(x), \tag{67}$$

then

$$\psi_r^{(out)}(x) = \psi_r^{(t)}(x) - \frac{\lambda}{3}\, g_0(x)\, \omega_r'(x). \tag{68}$$

The linearization of the exponent is not necessary here. Qualitatively (68) behaves similarly to (65) since again the average value of $g_0(x)$ can be set equal to one. The n^th^

iteration is expressed by the following equation:

$$\psi_r^{(n)(out)}(x) = m_r(x) + \psi_r^{(n-1)}(x)\,\psi_0(x) + \frac{\lambda}{4}\int_{-\infty}^{\infty} K_0(x-s)\, g_0\, \psi_r^{(n)(in)}\, ds, \tag{69}$$

and the next trial $\psi_r^{(n+1)(in)}$ by:

$$\psi_r^{(n+1)(in)}(x) = \alpha^{(n)}\,\psi_r^{(n)(out)} + \left(1-\alpha^{(n)}\right)\psi_r^{(n)(in)}. \tag{70}$$

Here $\alpha^{(n)}$ is a constant whose choice depends on the value of λ. It is safest to pick, at first, too low a value of α and increase it if the convergence proceeds too slowly. The details of this procedure and the set up of the I.B.M. machines are described in the Appendix (B-2 and B-3)

With the above method $\psi_1(x)$ and $\psi_2(x)$ were calculated for several values of λ. The problem arises now of how the radial distribution functions can then be improved in the original unexpanded integral equation (40) so as to avoid the great labor of calculating higher terms in the series. The kernel (41) is usually positive and has two maxima, so that the solution is no longer necessarily bounded between input and output. A further difficulty is that the kernel depends also on the distribution function. Since the dependence is not too sensitive, this complication can be overcome. The kernel can be calculated with the distribution function correct to terms in $\psi_2(x)$, and (40) can be solved with this kernel kept fixed. Then a new kernel can be evaluated and kept fixed till a new solution is obtained. This double series should eventually converge to the point where the distribution function used to calculate the kernel is the same as the next iterated output.

The kernel (41) is mainly negative for low values of λ and $\beta\varepsilon$. Thus the value of α is certain to be positive and can be used to combine the input and output till iteration converges upon a solution in each of the series of fixed kernel integral equations. With the radial distribution function correct to terms in $\Psi_2(x)$, the first kernel was calculated for $\lambda = 5$, $\beta\varepsilon = .60$ and a value of $\alpha = .50$ was used to iterate. Two changes of the kernel brought the radial distribution function within the desired accuracy. At $\lambda = 1$ and $\beta\varepsilon = .60$ and $\beta\varepsilon = 1.00$ this method converged even though the procedure was started with $g(x) = e^{-\beta\varepsilon\, \gamma_1(x)}$. For $\lambda = 5$, $\beta\varepsilon = 1.00$, however, the kernel is positive and therefore the value of α is uncertain. α can be calculated so as to minimize the sum of the square of the differences between direct iterates, as explained in Appendices B-1 and D. Whether this procedure would converge will have to be tried in the future since time did not permit us to investigate the method thoroughly.

Radial Distribution Functions

As outlined in the previous section, the solution~~s~~ of the Born-Green integral equation depends upon the radial distribution function for a hard-sphere intermolecular potential. These solutions for the hard-sphere radial distribution function have been published (Appendix D). The solutions cover a wide range of the parameter λ , i.e., of densities. However, before the Lennard-Jones intermolecular potential was introduced, the accuracy of the solutions was improved by method (70). In addition the solution for $\lambda = 1$ was obtained by direct iteration. The more precise solutions are tabulated in Table I. The accuracies are such that direct iteration causes a discrepancy in the radial distribution function of ± .002 between input and output for $\lambda = 1$, 5, 10, 20, and 27.4 and ± .01 for $\lambda = 33$.

With these distribution functions the inhomogeneous part of (58) was evaluated and the equation was solved for Ψ_1 (x) on I.B.M. machines (Appendices B-2 and B-3). The accuracy demanded was that direct iterates of Ψ_1 agree within ±.002 for $\lambda = 5$, 10, and 20, and ±.004 for $\lambda = 27.4$. The series was carried one step further by the evaluation of Ψ_2 . The I.B.M. machines were told to stop when Ψ_2 (x) was within ±.002 of its direct iterate for $\lambda = 5$ and 10, ±.003 for $\lambda = 20$, and ±.004 for $\lambda = 27.4$. These functions are also tabulated in Table I.

Figures 1 and 2 are representative graphs of the radial distribution function correct to terms in Ψ_2 . Figure 1 illustrates the variation of the radial distribution function with density at fixed temperature ($\beta\varepsilon$ = .80). Curves A, B and C correspond respectively to λ = 27.4, 20, and 5. Figure 1 shows clearly that the amplitude in the oscillation is larger for higher densities, indicating more orderly packing of the molecules of the fluid. As Figure 2 demonstrates, the peaks in the radial distribution function are also higher when the temperature is decreased at fixed density (λ = 20). Curve C, having the largest swings, corresponds to $\beta\varepsilon$ = 1.20; curves B and C are at $\beta\varepsilon$ = .60 and .00 respectively.

It turns out that Ψ_2 (x) is gratifyingly small compared to Ψ_1 (x) even if $x\gamma_1$ (x) is subtracted from Ψ_1 (x) to make a fairer test. How large the effect of the neglected terms in the series might be can be checked by substitution of the approximate radial distribution function in the integral equation (40). A calculation was carried out for λ = 5, $\beta\varepsilon$ = 1.00, using the first two and then also the first three terms of the series. For the radial distribution function correct to the Ψ_1 term, the right hand side was greater than the left hand side by .163 at x = 1.00 and by .171 at x = 1.12. Including the next term of the series hardly improved the deviation between direct iterates (.147 at x = 1.00 and .159 at x = 1.12). For higher values of λ and $\beta\varepsilon$ = 1.00 the difference between direct iterates was of the same sign and nature but somewhat smaller in magnitude. For λ = 10, $\beta\varepsilon$ = 1.00, and x = 1.00, the difference was .111 while for λ = 27.4, $\beta\varepsilon$ = 1.00, at x = 1.00, it was .110. This indicates that the solutions are probably more accurate for higher values of λ , both because the differences are smaller and because the equations are more sensitive due to the factor λ (65). The difference between direct iterates diminishes greatly as $\beta\varepsilon$ is lowered, as would be expected from the expansion (44), since the terms containing higher powers of $\beta\varepsilon$ decrease rapidly. Thus at $\lambda = 5$, $\beta\varepsilon = .60$, the difference was only .033 at x = 1.00 and .035 at x = 1.12.

In the above comparison the radial distribution function (45), where Ψ (x) was calculated by (44), was substituted on the right hand side. This g(x) is not strictly correct if only terms up to the second power in $\beta\varepsilon$ are to be included, since the above formula for the radial distribution function includes the terms in higher powers of $\beta\varepsilon$ containing only Ψ_1 and Ψ_2 . However this procedure is justified if, as one hopes, Ψ_3 (x) and higher terms are small. The difference between (45) and the strictly correct radial distribution function (46) is small at large distances. The values are different only near x = 1, where Ψ_1 (x) is large.

The solutions do not appear as accurate as is desirable, since the equation of state and the transport properties are sensitive to the radial distribution function. To calculate the next term in the series, Ψ_3 (x), does not seem worthwhile because of the large amount of labor involved with no guarantee of greatly increasing the agreement of direct iterates. However, it is hoped that the solutions including terms up to

Ψ_2 are close enough to the true solutions to be improved by other methods. (See pages 26 and 27, this thesis.)

Such a method was successful in improving the radial distribution function at $\lambda = 5$, $\beta\varepsilon = .60$. The radial distribution function, tabulated in Table II, and its iterate agree within ± .005 when substituted into (40). Also included in this table are the exact solutions for $\lambda = 1.00$, $\beta\varepsilon = .60$ and $\beta\varepsilon = 1.00$, $\lambda = 1.00$ obtained by the same method. (See pages 26 and 27, this thesis.) Again direct iterates agree within ± .005.

TABLE I

The functions Ψ which determine the radial distribution function as a function of x for several values of the parameter λ in the Born and Green equation; $\Psi(x) = x \log g(x)$

$x \geq 1$

$$\Psi(x) = \Psi_0(x) + (\beta\varepsilon)\Psi_1(x) + (\beta\varepsilon)^2\Psi_2(x)$$

	$\lambda=1$	$\lambda=5$			$\lambda=10.$		
x	Ψ_0	Ψ_0	Ψ_1	Ψ_2	Ψ_0	Ψ_1	Ψ_2
1.00	.095	.368	-.586	.078	.587	-.789	.025
1.04	.092	.349	.099	.075	.552	-.095	.024
1.08	.088	.329	.414	.073	.515	.230	.024
1.12	.083	.305	.529	.069	.476	.353	.023
1.16	.079	.283	.534	.067	.436	.367	.021
1.20	.074	.260	.486	.065	.392	.330	.019
1.24	.069	.236	.411	.063	.350	.266	.018
1.28	.064	.212	.330	.061	.305	.196	.017
1.32	.059	.188	.250	.058	.261	.127	.015
1.36	.053	.164	.175	.055	.218	.063	.014
1.40	.048	.141	.109	.053	.174	.008	.013
1.44	.042	.115	.053	.050	.130	-.036	.012
1.48	.037	.091	.006	.048	.089	-.074	.011
1.52	.032	.072	-.034	.045	.049	-.101	.010
1.56	.027	.048	-.064	.045	.013	-.123	.010
1.60	.022	.029	-.088	.044	-.022	-.135	.010
1.64	.017	.011	-.105	.044	-.052	-.142	.010
1.68	.013	-.006	-.116	.043	-.080	-.142	.011
1.72	.009	-.020	-.123	.044	-.101	-.139	.012
1.76	.005	-.034	-.124	.044	-.120	-.129	.013

TABLE I (cont.)

	$\lambda = 1$	$\lambda = 5$			$\lambda = 10$		
x	ψ_0	ψ_0	ψ_1	ψ_2	ψ_0	ψ_1	ψ_2
1.80	.002	-.041	-.120	.046	-.131	-.117	.015
1.84	.000	-.048	-.111	.047	-.136	-.102	.017
1.88	-.002	-.051	-.101	.049	-.133	-.084	.020
1.92	-.003	-.055	-.086	.052	-.123	-.066	.023
1.96	-.004	-.051	-.070	.055	-.106	-.046	.027
2.00	-.004	-.040	-.053	.059	-.077	-.026	.030
2.04	-.003	-.032	-.030	.063	-.051	.003	.031
2.08	-.003	-.022	-.007	.066	-.027	.036	.032
2.12	-.002	-.016	.014	.069	-.007	.063	.033
2.16	-.002	-.011	.031	.069	.010	.082	.034
2.20	-.002	-.003	.041	.067	.021	.094	.033
2.24	-.001	.001	.048	.064	.030	.096	.029
2.28	-.001	.003	.051	.057	.037	.092	.023
2.32	-.001	.005	.053	.050	.040	.085	.016
2.36	-.001	.007	.051	.042	.041	.073	.009
2.40	.000	.008	.045	.034	.041	.060	.001
2.44		.008	.040	.026	.039	.044	-.005
2.48		.009	.035	.017	.035	.030	-.010
2.52		.008	.029	.011	.030	.017	-.015
2.56		.007	.023	.006	.025	.004	-.019
2.60		.006	.017	.001	.019	-.008	-.021
2.64		.005	.011	-.004	.013	-.017	-.011
2.68		.004	.006	-.006	.008	-.026	-.002

TABLE I (cont.)

	$\lambda = 1$	$\lambda = 5$			$\lambda = 10$		
x	ψ_0	ψ_0	ψ_1	ψ_2	ψ_0	ψ_1	ψ_2
2.72	.000	.004	.001	-.007	.003	-.031	.003
2.76		.003	-.003	-.008	-.003	-.035	.007
2.80		.002	-.005	-.007	-.006	-.037	.009
2.84		.001	-.007	-.007	-.010	-.037	.009
2.88		.000	-.008	-.006	-.011	-.035	.008
2.92		.000	-.009	-.005	-.012	-.033	.005
2.96		-.001	-.010	-.003	-.013	-.028	.002
3.00		-.001	-.009	-.001	-.014	-.022	.001
3.04		-.001	-.008	.001	-.013	-.015	.005
3.08		-.002	-.007	.003	-.011	-.010	.007
3.12		-.002	-.006	.005	-.010	-.004	.009
3.16		-.002	-.004	.007	-.008	.003	.010
3.20		-.001	-.003	.009	-.006	.007	.011
3.24		-.001	-.002	.010	-.003	.010	.012
3.28		-.001	-.001	.011	-.002	.015	.011
3.32		-.001	.000	.011	.000	.016	.010
3.36		.000	.001	.011	.001	.018	.009
3.40			.002	.010	.002	.017	.007
3.44			.003	.010	.003	.016	.005
3.48			.003	.009	.004	.014	.003
3.52			.003	.008	.005	.012	.001
3.56			.004	.007	.004	.009	-.001
3.60			.004	.006	.004	.007	-.003
3.64			.003	.005	.003	.005	-.005

TABLE I (cont.)

	$\lambda = 1$	$\lambda = 5$			$\lambda = 10$		
x	ψ_0	ψ_0	ψ_1	ψ_2	ψ_0	ψ_1	ψ_2
3.68	.000	.000	.003	.004	.003	.002	-.006
3.72			.003	.003	.002	.001	-.006
3.76			.002	.002	.002	-.002	-.004
3.80			.002	.002	.001	-.003	-.002
3.84			.001	.001	.001	-.005	.000
3.88			.001	.000	.000	-.005	.002
3.92			.001	.000	.000	-.007	.002
3.96			.001	-.001	.000	-.006	.002
4.00			.001	-.001	-.001	-.006	.002
4.04			.001	-.001	-.001	-.005	.001
4.08			.001	-.001	-.001	-.004	.001
4.12			.000	-.001	-.001	-.004	.000
4.16				.000	-.001	-.003	.000
4.20				.000	-.001	-.002	.001
4.24				.000	-.001	-.001	.002
4.28				.000	.000	-.001	.002
4.32				.001		.001	.002
4.36				.001		.001	.002
4.40				.001		.002	.002
4.44				.001		.002	.003
4.48				.001		.003	.002
4.52				.001		.002	.002
4.56				.002		.002	.002
4.60				.002		.002	.001

TABLE I (cont.)

	$\lambda = 1$	$\lambda = 5$			$\lambda = 10$		
x	ψ_0	ψ_0	ψ_1	ψ_2	ψ_0	ψ_1	ψ_2
4.64	.000	.000	.000	.002	.000	.002	.001
4.68				.002		.001	.001
4.72				.001		.001	.000
4.76				.001		.001	.000
4.80				.001		.000	.000
4.84				.001			.000
4.88				.001			-.001
4.92				.001			-.001
4.96				.001			-.001
5.00				.001			-.001
5.04				.001			-.001
5.08				.001			-.001
5.12				.000			-.001
5.16							-.001
5.20							-.001
5.24							-.001
5.28							-.001
5.32							.000
5.36							.000
5.40							.001
5.44							.001
5.48							.001
5.52							.001
5.56							.001

TABLE I (cont.)

	$\lambda = 1$	$\lambda = 5$			$\lambda = 10$		
x	ψ_0	ψ_0	ψ_1	ψ_2	ψ_0	ψ_1	ψ_2
5.60	.000	.000	.000	.000	.000	.000	.001
5.64							.001
5.68							.001
5.72							.000

TABLE I (cont.)

	$\lambda = 20$			$\lambda = 27.4$			$\lambda = 33$
x	ψ_0	ψ_1	ψ_2	ψ_0	ψ_1	ψ_2	ψ_0
1.00	.859	-.920	-.038	.980	-.956	-.048	1.040
1.04	.808	-.218	-.034	.933	-.247	-.044	1.016
1.08	.751	.119	-.031	.879	.095	-.041	.980
1.12	.691	.253	-.028	.817	.236	-.038	.928
1.16	.627	.280	-.025	.745	.268	-.036	.861
1.20	.556	.255	-.023	.665	.245	-.034	.778
1.24	.483	.203	-.021	.575	.196	-.033	.673
1.28	.406	.143	-.019	.476	.138	-.030	.552
1.32	.329	.081	-.017	.371	.079	-.028	.414
1.36	.250	.026	-.015	.261	.026	-.025	.264
1.40	.170	-.019	-.013	.148	-.019	-.022	.108
1.44	.090	-.056	-.010	.034	-.055	-.018	-.047
1.48	.014	-.085	-.008	-.077	-.082	-.013	-.204
1.52	-.060	-.104	-.005	-.185	-.098	-.008	-.354
1.56	-.128	-.115	-.002	-.281	-.109	-.001	-.491
1.60	-.188	-.121	.001	-.368	-.110	.004	-.610
1.64	-.240	-.120	.003	-.441	-.108	.010	-.709
1.68	-.283	-.114	.006	-.498	-.098	.017	-.783
1.72	-.313	-.105	.009	-.536	-.086	.024	-.828
1.76	-.332	-.092	.013	-.554	-.070	.032	-.822
1.80	-.338	-.077	.018	-.548	-.055	.040	-.816
1.84	-.329	-.060	.024	-.517	-.041	.047	-.723
1.88	-.301	-.045	.029	-.460	-.027	.054	-.657
1.92	-.256	-.031	.034	-.376	-.017	.061	-.518

TABLE I (cont.)

	$\lambda = 20$			$\lambda = 27.4$			$\lambda = 33$
x	ψ_0	ψ_1	ψ_2	ψ_0	ψ_1	ψ_2	ψ_0
1.96	-.194	-.019	.039	-.264	-.011	.069	-.341
2.00	-.110	-.010	.043	-.122	-.009	.074	-.125
2.04	-.030	.022	.034	.021	.019	.056	.094
2.08	.037	.068	.024	.137	.077	.036	.270
2.12	.089	.106	.020	.227	.127	.025	.412
2.16	.130	.128	.019	.292	.154	.020	.514
2.20	.155	.137	.017	.333	.159	.015	.580
2.24	.170	.131	.014	.353	.146	.008	.607
2.28	.175	.116	.010	.354	.118	-.002	.600
2.32	.172	.093	.003	.337	.082	-.013	.559
2.36	.161	.066	-.005	.305	.043	-.024	.493
2.40	.143	.038	-.013	.261	.003	-.032	.406
2.44	.124	.008	-.017	.207	-.033	-.039	.302
2.48	.096	-.015	-.020	.148	-.066	-.044	.181
2.52	.069	-.036	-.022	.083	-.091	-.046	.061
2.56	.040	-.054	-.023	.019	-.110	-.044	-.061
2.60	.013	-.067	-.023	-.042	-.123	-.038	-.173
2.64	-.014	-.076	-.021	-.099	-.128	-.031	-.277
2.68	-.037	-.082	-.017	-.150	-.125	-.022	-.369
2.72	-.058	-.083	-.012	-.190	-.118	-.011	-.443
2.76	-.074	-.080	-.008	-.221	-.105	.001	-.495
2.80	-.086	-.074	-.003	-.240	-.088	.012	-.524
2.84	-.093	-.064	.003	-.247	-.066	.022	-.522
2.88	-.094	-.053	.009	-.241	-.043	.031	-.499

TABLE I (cont.)

	$\lambda = 20$			$\lambda = 27.4$			$\lambda = 33$
x	ψ_0	ψ_1	ψ_2	ψ_0	ψ_1	ψ_2	ψ_0
2.92	-.090	-.041	.013	-.222	-.019	.039	-.448
2.96	-.081	-.026	.017	-.193	.007	.046	-.374
3.00	-.071	-.009	.020	-.155	.032	.048	-.283
3.04	-.056	.007	.022	-.110	.057	.048	-.177
3.08	-.039	.022	.023	-.061	.080	.046	-.067
3.12	-.023	.037	.023	-.013	.099	.041	.043
3.16	-.005	.047	.022	.033	.112	.036	.142
3.20	.009	.056	.019	.074	.118	.028	.230
3.24	.021	.062	.016	.108	.117	.019	.303
3.28	.031	.063	.011	.134	.108	.010	.358
3.32	.040	.059	.006	.151	.093	-.001	.388
3.36	.044	.054	.002	.159	.074	-.012	.399
3.40	.048	.044	-.002	.160	.049	-.022	.385
3.44	.047	.034	-.006	.151	.023	-.031	.351
3.48	.046	.022	-.010	.135	-.002	-.038	.299
3.52	.040	.012	-.013	.114	-.027	-.042	.236
3.56	.036	-.001	-.015	.087	-.049	-.043	.164
3.60	.027	-.010	-.017	.061	-.070	-.043	.083
3.64	.021	-.021	-.018	.030	-.083	-.040	.001
3.68	.011	-.027	-.016	.000	-.093	-.036	-.073
3.72	.004	-.034	-.014	-.028	-.097	-.028	-.147
3.76	-.005	-.035	-.011	-.053	-.097	-.018	-.210
3.80	-.011	-.038	-.008	-.075	-.090	-.008	-.261
3.84	-.016	-.038	-.004	-.091	-.080	.002	-.296

TABLE I (cont.)

	$\lambda = 20$			$\lambda = 27.4$			$\lambda = 33$
x	ψ_0	ψ_1	ψ_2	ψ_0	ψ_1	ψ_2	ψ_0
3.88	-.019	-.037	-.001	-.102	-.066	.012	-.319
3.92	-.023	-.032	.000	-.107	-.049	.020	-.327
3.96	-.025	-.026	.002	-.106	-.030	.027	-.314
4.00	-.024	-.021	.005	-.100	-.011	.033	-.282
4.04	-.023	-.014	.008	-.089	.007	.037	-.245
4.08	-.020	-.008	.010	-.074	.025	.039	-.190
4.12	-.017	-.001	.011	-.057	.043	.039	-.130
4.16	-.013	.006	.012	-.038	.058	.037	-.066
4.20	-.009	.012	.013	-.018	.070	.033	.005
4.24	-.005	.017	.012	.002	.077	.027	.067
4.28	-.003	.023	.010	.020	.080	.020	.120
4.32	.001	.025	.007	.037	.077	.012	.170
4.36	.004	.025	.005	.051	.071	.004	.208
4.40	.007	.024	.002	.061	.061	-.005	.236
4.44	.010	.022	.000	.068	.047	-.013	.245
4.48	.011	.020	.000	.070	.032	-.020	.246
4.52	.012	.016	-.002	.068	.018	-.026	.230
4.56	.012	.013	-.003	.064	.002	-.031	.203
4.60	.011	.008	-.005	.056	-.012	-.032	.172
4.64	.011	.003	-.006	.046	-.026	-.033	.130
4.68	.009	-.001	-.006	.035	-.038	-.033	.083
4.72	.007	-.004	-.006	.022	-.048	-.029	.035
4.76	.006	-.008	-.006	.009	-.055	-.026	-.018
4.80	.004	-.011	-.006	-.004	-.058	-.020	-.061

TABLE I (cont.)

x	$\lambda = 20$			$\lambda = 27.4$			$\lambda = 33$
	ψ_0	ψ_1	ψ_2	ψ_0	ψ_1	ψ_2	ψ_0
4.84	.002	-.013	-.005	-.016	-.058	-.013	-.103
4.88	-.001	-.013	-.003	-.026	-.056	-.006	-.139
4.92	-.002	-.014	-.001	-.034	-.050	.001	-.167
4.96	-.003	-.014	.000	-.040	-.042	.008	-.189
5.00	-.004	-.013	.000	-.043	-.032	.015	-.198
5.04	-.005	-.011	.000	-.044	-.024	.020	-.195
5.08	-.006	-.009	.001	-.043	-.013	.024	-.183
5.12	-.007	-.006	.002	-.040	-.002	.026	-.165
5.16	-.006	-.004	.003	-.034	.010	.028	-.133
5.20	-.005	-.002	.004	-.027	.020	.028	-.104
5.24	-.005	.000	.004	-.019	.028	.026	-.064
5.28	-.004	.003	.004	-.012	.036	.023	-.027
5.32	-.003	.005	.003	-.005	.043	.019	.014
5.36	-.002	.006	.002	.003	.044	.014	.052
5.40	-.001	.007	.001	.010	.044	.008	.083
5.44	.000	.007	.000	.017	.041	.002	.113
5.48	.001	.007	.000	.022	.036	-.004	.134
5.52	.002	.007	.000	.025	.030	-.009	.146
5.56	.002	.007	.000	.027	.023	-.014	.152
5.60	.002	.006	.000	.027	.015	-.017	.148
5.64	.003	.004	.000	.026	.004	-.020	.139
5.68	.003	.004	.000	.024	-.002	-.022	.126
5.72	.003	.003	.000	.020	-.009	-.023	.100
5.76	.003	.001	-.001	.016	-.015	-.021	.074

TABLE I (cont.)

	$\lambda = 20$			$\lambda = 27.4$			$\lambda = 33$
x	ψ_0	ψ_1	ψ_2	ψ_0	ψ_1	ψ_2	ψ_0
5.80	.002	.000	-.001	.013	-.021	-.020	.047
5.84	.002	-.001	-.001	.008	-.026	-.017	.017
5.88	.002	-.002	-.001	.002	-.027	-.013	-.013
5.92	.001	-.003	-.001	-.003	-.029	-.008	-.041
5.96	.000	-.003	.000	-.007	-.030	-.003	-.066
6.00	.000	-.003	.000	-.011	-.027	.000	-.084
6.04	.000	-.003	.000	-.014	-.023	.005	-.105
6.08	.000	-.004	.000	-.015	-.019	.009	-.122
6.12	-.001	-.003	.000	-.016	-.015	.012	-.126
6.16	-.001	-.003	.000	-.016	-.010	.015	-.121
6.20	-.001	-.003	.000	-.015	-.004	.016	-.110
6.24	-.001	-.002	.000	-.014	.001	.017	-.096
6.28	.000	-.002	.001	-.012	.005	.017	-.075
6.32		-.001	.001	-.009	.009	.016	-.057
6.36		-.001	.001	-.007	.014	.015	-.033
6.40		.000	.001	-.004	.016	.012	-.008
6.44		.000	.001	-.001	.018	.009	.014
6.48		.000	.000	.001	.020	.006	.036
6.52		.000		.004	.019	.002	.055
6.56		.001		.006	.018	-.001	.069
6.60		.001		.007	.016	-.004	.079
6.64		.001		.009	.012	-.007	.087
6.68		.001		.009	.009	-.010	.090
6.72		.001		.009	.006	-.011	.089

TABLE I (cont.)

	$\lambda=20$			$\lambda=27.4$			$\lambda=33$
x	ψ_0	ψ_1	ψ_2	ψ_0	ψ_1	ψ_2	ψ_0
6.76	.000	.001	.000	.009	.004	-.012	.080
6.80		.001		.008	.000	-.012	.072
6.84		.002		.007	-.004	-.012	.060
6.88		.001		.005	-.006	-.011	.044
6.92		.001		.004	-.007	-.009	.026
6.96		.001		.002	-.009	-.008	.009
7.00		.001		-.001	-.009	-.006	-.009
7.04		.000		-.001	-.011	-.003	-.026
7.08				-.001	-.013	-.001	-.040
7.12				-.002	-.012	.001	-.052
7.16				-.003	-.011	.004	-.059
7.20				-.004	-.008	.006	-.063
7.24				-.005	-.006	.007	-.066
7.28				-.005	-.005	.008	-.065
7.32				-.005	-.003	.009	-.057
7.36				-.005	.000	.009	-.050
7.40				-.005	.002	.008	-.044
7.44				-.004	.004	.007	-.033
7.48				-.003	.005	.006	-.020
7.52				-.002	.006	.005	-.007
7.56				-.001	.007	.004	.007
7.60				.000	.007	.002	.018
7.64				.001	.007	.000	.029
7.68				.002	.007	-.001	.035

TABLE I (cont.)

	$\lambda = 20$			$\lambda = 27.4$			$\lambda = 33$
x	ψ_0	ψ_1	ψ_2	ψ_0	ψ_1	ψ_2	ψ_0
7.72	.000	.000	.000	.002	.006	-.003	.038
7.76				.002	.005	-.004	.042
7.80				.002	.004	-.004	.043
7.84				.002	.003	-.006	.044
7.88				.003	.002	-.006	.043
7.92				.002	.000	-.006	.038
7.96				.002	-.001	-.006	.031
8.00				.002	-.002	-.005	.019
8.04				.002	-.004	-.005	.015
8.08				.001	-.004	-.003	.012
8.12				.001	-.005	-.002	.007
8.16				.001	-.005	-.001	-.006
8.20				.001	-.005	-.001	-.020
8.24				.000	-.004	.000	-.025
8.28				-.001	-.004	.002	-.026
8.32				-.001	-.003	.003	-.028
8.36				-.001	-.003	.003	-.029
8.40				-.001	-.002	.003	-.031
8.44				-.001	-.001	.004	-.030
8.48				-.001	-.001	.004	-.028
8.52				-.002	.000	.003	-.022
8.56				-.002	.001	.003	-.017
8.60				-.001	.001	.003	-.009
8.64				-.001	.002	.002	-.003

TABLE I (cont.)

	$\lambda = 20$			$\lambda = 27.4$			$\lambda = 33$
x	ψ_0	ψ_1	ψ_2	ψ_0	ψ_1	ψ_2	ψ_0
8.68	.000	.000	.000	-.001	.002	.002	.000
8.72				-.001	.003	.001	.004
8.76				.000	.002	.000	.009
8.80				.000	.002	-.001	.013
8.84				.000	.003	-.001	.015
8.88				.001	.001	-.001	.016
8.92				.001	.001	-.002	.017
8.96				.001	.001	-.002	.018
9.00				.001	.001	-.002	.021
9.04				.000	.001	-.002	.016
9.08					.001	-.002	.012
9.12					.001	-.002	.007
9.16					.000	-.002	.003
9.20					.000	-.002	.002
9.24					-.001	-.001	.001
9.28					-.001	-.001	-.001
9.32					-.001	.000	-.004
9.36					-.001	.000	-.008
9.40					.000	.001	-.009
9.44					-.001	.001	-.012
9.48					-.001	.001	-.010
9.52					-.001	.001	-.009
9.56					-.001	.001	-.008
9.60					-.001	.001	-.007
9.64					.000	.001	-.003

TABLE I (cont.)

	$\lambda = 20$			$\lambda = 27.4$			$\lambda = 33$
x	ψ_0	ψ_1	ψ_2	ψ_0	ψ_1	ψ_2	ψ_0
9.68	.000	.000	.000	.000	.000	.000	-.002
9.72							-.001
9.76							.000
9.80							.000
9.84							.001
9.88							.001
9.92							.002
9.96							.002
10.00							.003
10.04							.004
10.08							.005
10.12							.003
10.16							.002
10.20							.001
10.24							.001
10.28							.000

TABLE II

Exact radial distribution functions for several values of the parameters λ and $\beta\varepsilon$.

g(x) as a function of x.

x	$\lambda = 1$ $\beta\varepsilon = .6$	$\lambda = 1$ $\beta\varepsilon = 1.0$	$\lambda = 5$ $\beta\varepsilon = .6$	x	$\lambda = 1$ $\beta\varepsilon = .6$	$\lambda = 1$ $\beta\varepsilon = 1.0$	$\lambda = 5$ $\beta\varepsilon = .6$
1.00	1.022	1.162	1.092	1.80	1.042	1.201	.965
1.04	1.512	2.230	1.585	1.84	1.036	1.190	.965
1.08	1.764	2.868	1.824	1.88	1.032	1.182	.968
1.12	1.825	3.034	1.853	1.92	1.030	1.178	.972
1.16	1.782	2.910	1.783	1.96	1.031	1.180	.981
1.20	1.692	2.673	1.674	2.00	1.031	1.182	.992
1.24	1.590	2.418	1.554	2.04	1.031	1.184	1.004
1.28	1.495	2.184	1.449	2.08	1.031	1.186	1.017
1.32	1.412	1.977	1.355	2.12	1.031	1.188	1.026
1.36	1.339	1.821	1.274	2.16	1.030	1.191	1.034
1.40	1.280	1.697	1.208	2.20	1.030	1.191	1.040
1.44	1.232	1.576	1.151	2.24	1.028	1.186	1.043
1.48	1.192	1.490	1.105	2.28	1.026	1.179	1.044
1.52	1.159	1.420	1.070	2.32	1.025	1.170	1.044
1.56	1.132	1.367	1.039	2.36	1.024	1.162	1.042
1.60	1.109	1.325	1.015	2.40	1.022	1.155	1.038
1.64	1.089	1.288	.998	2.44	1.021	1.145	1.035
1.68	1.073	1.256	.982	2.48	1.020	1.138	1.031
1.72	1.060	1.233	.972	2.52	1.019	1.129	1.027
1.76	1.049	1.216	.965	2.56	1.018	1.122	1.023

TABLE II (cont.)

x	$\lambda=1$ $\beta\varepsilon=.6$	$\lambda=1$ $\beta\varepsilon=1.0$	$\lambda=5$ $\beta\varepsilon=.6$	x	$\lambda=1$ $\beta\varepsilon=.6$	$\lambda=1$ $\beta\varepsilon=1.0$	$\lambda=5$ $\beta\varepsilon=.6$
2.60	1.016	1.116	1.020	3.56	1.003	1.040	1.006
2.64	1.015	1.110	1.017	3.60	1.003	1.038	1.006
2.68	1.014	1.104	1.015	3.64	1.003	1.037	1.006
2.72	1.013	1.098	1.014	3.68	1.003	1.035	1.006
2.76	1.012	1.092	1.012	3.72	1.003	1.034	1.006
2.80	1.011	1.086	1.010	3.76	1.002	1.032	1.006
2.84	1.010	1.081	1.009	3.80	1.002	1.031	1.006
2.88	1.009	1.079	1.008	3.84	1.002	1.029	1.005
2.92	1.009	1.076	1.007	3.88	1.002	1.028	1.005
2.96	1.008	1.072	1.007	3.92	1.002	1.027	1.005
3.00	1.008	1.070	1.006	3.96	1.002	1.026	1.005
3.04	1.007	1.067	1.007	4.00	1.002	1.025	1.004
3.08	1.007	1.064	1.006	4.04	1.002	1.024	1.004
3.12	1.006	1.062	1.007	4.08	1.002	1.023	1.004
3.16	1.006	1.060	1.007	4.12	1.001	1.022	1.004
3.20	1.006	1.058	1.007	4.16	1.001	1.021	1.004
3.24	1.005	1.055	1.007	4.20	1.001	1.020	1.003
3.28	1.005	1.053	1.007	4.24	1.001	1.020	1.003
3.32	1.005	1.051	1.007	4.28	1.001	1.019	1.003
3.36	1.004	1.049	1.007	4.32	1.001	1.018	1.003
3.40	1.004	1.047	1.007	4.36	1.001	1.018	1.003
3.44	1.004	1.045	1.007	4.40	1.001	1.017	1.003
3.48	1.003	1.043	1.007	4.48	1.001	1.016	1.003
3.52	1.003	1.041	1.007	4.48	1.001	1.016	1.003

TABLE II (cont.)

x	$\lambda=1$ $\beta\varepsilon=.6$	$\lambda=1$ $\beta\varepsilon=1.0$	$\lambda=5$ $\beta\varepsilon=.6$	x	$\lambda=1$ $\beta\varepsilon=.6$	$\lambda=1$ $\beta\varepsilon=1.0$	$\lambda=5$ $\beta\varepsilon=.6$
4.52	1.001	1.015	1.002	5.48	1.000	1.006	1.001
4.56	1.001	1.015	1.002	5.52		1.006	1.001
4.60	1.001	1.014	1.002	5.56		1.005	1.001
4.64	1.001	1.014	1.002	5.60		1.005	1.001
4.68	1.001	1.013	1.002	5.64		1.005	1.001
4.72	1.001	1.012	1.002	5.68		1.005	1.001
4.76	1.001	1.012	1.002	5.72		1.004	1.001
4.80	1.001	1.011	1.002	5.76		1.004	1.001
4.84	1.001	1.011	1.002	5.80		1.004	1.001
4.88	1.001	1.011	1.002	5.84		1.004	1.001
4.92	1.001	1.010	1.002	5.88		1.004	1.001
4.96	1.001	1.010	1.002	5.92		1.004	1.001
5.00	1.001	1.010	1.002	5.96		1.003	1.001
5.04	1.001	1.009	1.002	6.00		1.003	1.001
5.08	1.001	1.009	1.002	6.04		1.003	1.001
5.12	1.000	1.008	1.002	6.08		1.003	1.001
5.16		1.008	1.002	6.12		1.003	1.001
5.20		1.008	1.002	6.16		1.003	1.000
5.24		1.008	1.001	6.20		1.003	
5.28		1.007	1.001	6.24		1.003	
5.32		1.007	1.001	6.28		1.002	
5.36		1.007	1.001	6.32		1.002	
5.40		1.006	1.001	6.36		1.002	
5.44		1.006	1.001	6.40		1.002	

TABLE II (cont.)

x	$\lambda = 1$ $\beta\varepsilon = .6$	$\lambda = 1$ $\beta\varepsilon = 1.0$	$\lambda = 5$ $\beta\varepsilon = .6$	x	$\lambda = 1$ $\beta\varepsilon = .6$	$\lambda = 1$ $\beta\varepsilon = 1.0$	$\lambda = 5$ $\beta\varepsilon = .6$
6.44	1.000	1.002	1.000	7.40	1.000	1.001	1.000
6.48		1.002		7.44		1.001	
6.52		1.002		7.48		1.000	
6.56		1.002					
6.60		1.002					
6.64		1.002					
6.68		1.002					
6.72		1.002					
6.76		1.002					
6.80		1.002					
6.84		1.001					
6.88		1.001					
6.92		1.001					
6.96		1.001					
7.00		1.001					
7.04		1.001					
7.08		1.001					
7.12		1.001					
7.16		1.001					
7.20		1.001					
7.24		1.001					
7.28		1.001					
7.32		1.001					
7.36		1.001					

Figure 1. The variation of the radial distribution function correct to Ψ_2 with volume for $\beta\varepsilon$ = .80 on the Born-Green basis.

A for λ = 27.4
B for λ = 20.
C for λ = 5.

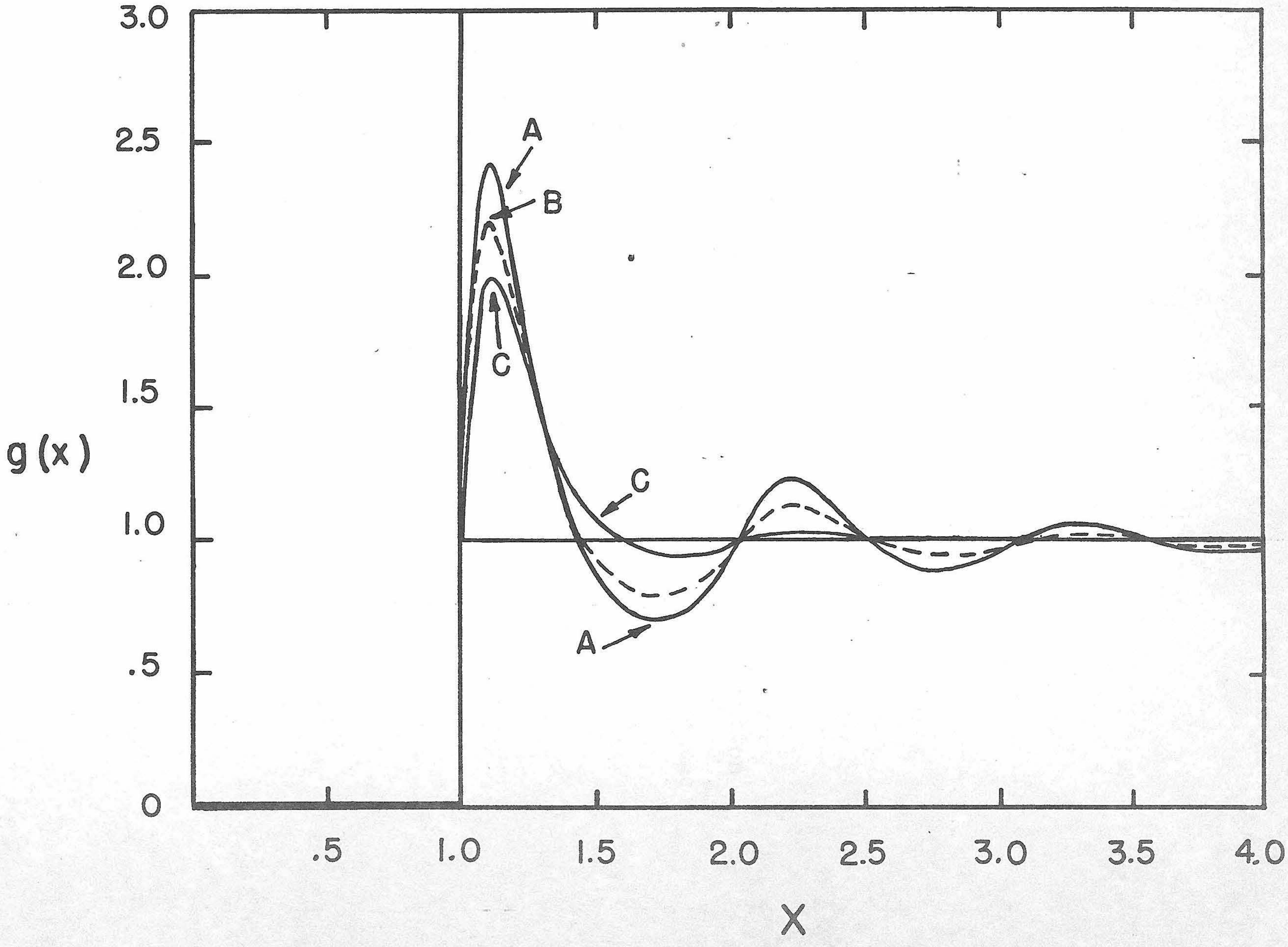
3.0
2.5
2.0
1.5
1.0
.5
0
g(x)
.5
1.0
1.5
2.0
2.5
3.0
3.5
4.0
X
A
B
C
C
A

Figure 2. The variation of the radial distribution function correct to Ψ_2 with temperature for λ = 20 on the Born-Green basis:

A for $\beta\varepsilon$ = .00

B for $\beta\varepsilon$ = .60

C for $\beta\varepsilon$ =1.20

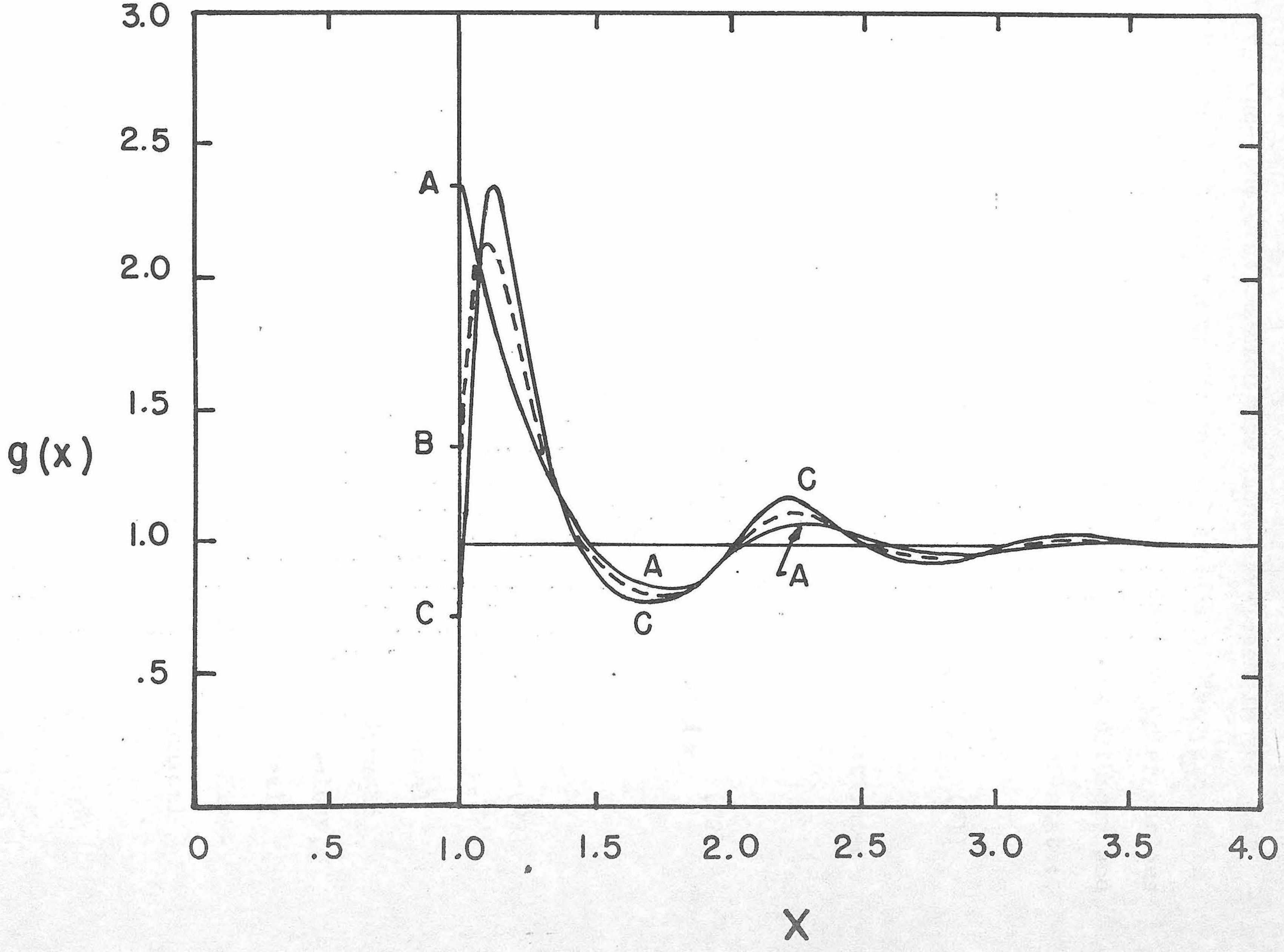
3.0
2.5
2.0
1.5
1.0
.5
g(x)
0
.5
1.0
1.5
2.0
2.5
3.0
3.5
4.0
X
A
B
C
C
A
A
C
A

Calculation of Thermodynamic Functions

Once the distribution functions developed in the previous section are known for several values of the parameters, the calculations of the thermodynamic functions under various conditions is an easy matter. Both the Born-Green theory and the Kirkwood theory lead to the following equation of state:

$$\frac{PV}{NkT} = 1 - \frac{\lambda_0 \beta \varepsilon}{6} \int_0^\infty x^3 \frac{d\gamma}{dx} g(x)\, dx. \qquad (71)$$

If the modified Lennard-Jones potential (48) is substituted then (71) becomes:

$$\frac{PV}{NkT} = 1 + \frac{\lambda_0 g(1)}{6} - \frac{\beta \varepsilon \lambda_0}{6} \int_0^\infty x^3 \frac{d\gamma_1}{dx} g(x)\, dx. \qquad (72)$$

The internal energy, E, is given by:

$$\frac{E}{NkT} = \frac{3}{2} + \frac{\lambda_0 \beta \varepsilon}{2} \int_0^\infty x^2 \gamma_1(x)\, g(x)\, dx. \qquad (73)$$

The knowledge of the equation of state and the internal energy allows the calculation of all other thermodynamic quantities through thermodynamic relations. Nevertheless, it is desirable to have explicit statistical mechanical expressions for the other thermodynamic quantities. Kirkwood's theory yields such an expression for the chemical potential, μ_*:

$$\frac{\mu}{NkT} = \log p + \frac{\mu^E}{NkT} + \frac{\mu_p^I}{NkT} ;$$
$$\mu_p^I(T) = \lim_{p \to 0}\left[\mu - NkT \log p\right] ; \qquad (74)$$
$$\mu^E/NkT = \lambda_0 \beta\varepsilon \int_0^1 \int_0^\infty x^2 \gamma(x)\, g(x,\xi)\, dx\, d\xi - \log \frac{pV}{NkT} .$$

It is convenient to work with reduced variables, since this leaves open the choice of the parameters a and ε in the potential. The reduced variables used are:

$$p^* = p\left(\frac{a^3}{\varepsilon}\right) ; \qquad v^* = \frac{4\pi}{\lambda_0} = \frac{V}{Na^3} ; \qquad (75)$$
$$T^* = \frac{1}{\beta\varepsilon} = \frac{RT}{N\varepsilon} .$$

In terms of p*, v* and T*, the calculated equation of state applies for any fluid under corresponding-state conditions. In Table III, p* is tabulated for various values of v* and T*, and for various approximations to the radial distribution function. The values of v* for which p* can be evaluated are restricted to those values for which the radial distribution f. was obtained. However, due to the expansion (44), p* can be calculated for any T*. The radial distribution f. (45), where Ψ (x) is given by (44), were calculated for values of $\beta\varepsilon$ from 0 to 1.20 by steps of .20. They were then substituted into the integral in (72). Again we have not kept strictly within the powers of $\beta\varepsilon$ to which we know the radial distribution function.

The interval in x found necessary for the evaluation of the integral was .04 throughout except near x = 1, where $\frac{d\gamma(x)}{dx}$ is a very rapidly changing function. g(x) was there interpolated to a .01 interval in x between x = 1.00 and 1.12

$$\frac{\mu}{NkT} = \log p + \frac{\mu^E}{NkT} + \frac{\mu_p^I}{NkT} \; ;$$
$$\mu_p^I(T) = \lim_{p \to 0} \left[\mu - NkT \log p \right] ; \qquad (74)$$
$$\mu^E / NkT = \lambda_0 \beta \varepsilon \int_0^1 \int_0^\infty x^2 \gamma(x)\, g(x,\xi)\, dx\, d\xi - \log \frac{pV}{NkT} .$$

It is convenient to work with reduced variables, since this leaves open the choice of the parameters a and ε in the potential. The reduced variables used are:

$$p^* = p\left(\frac{a^3}{\varepsilon}\right) ; \qquad v^* = \frac{4\pi}{\lambda_0} = \frac{v}{Na^3} ; \qquad (75)$$
$$T^* = \frac{1}{\beta\varepsilon} = \frac{RT}{N\varepsilon} .$$

In terms of p*, v* and T*, the calculated equation of state applies for any fluid under corresponding-state conditions. In Table III, p* is tabulated for various values of v* and T*, and for various approximations to the radial distribution function. The values of v* for which p* can be evaluated are restricted to those values for which the radial distribution f. was obtained. However, due to the expansion (44), p* can be calculated for any T*. The radial distribution f. (45), where Ψ (x) is given by (44), were calculated for values of $\beta\varepsilon$ from 0 to 1.20 by steps of .20. They were then substituted into the integral in (72). Again we have not kept strictly within the powers of $\beta\varepsilon$ to which we know the radial distribution function.

The interval in x found necessary for the evaluation of the integral was .04 throughout except near x = 1, where $\frac{d\gamma(x)}{dx}$ is a very rapidly changing function. g(x) was there interpolated to a .01 interval in x between x = 1.00 and 1.12

TABLE III

The Equation of State

The reduced pressure, p*, as a function of the reduced temperature, T*, and reduced volume, v*.

(A) With a radial distribution function correct to terms in Ψ_1 for the Born-Green equation.

		λ	5	10	20	27.4
T*	$\beta\varepsilon$	v*	3.633	2.261	1.484	1.223
5.000	.2		1.998	4.418	10.943	17.30
2.500	.4		.727	1.460	3.635	5.906
1.667	.6		.301	.472	1.190	2.091
1.250	.8		.084	-.028	-.041	.169
1.000	1.0		-.048	-.332	-.786	-.993

(B) With a radial distribution function correct to terms in Ψ_2 for the Born-Green equation.

		λ	5	10	20	27.4
T*	$\beta\varepsilon$	v*	3.633	2.261	1.484	1.223
5.000	.2		2.005	4.421	10.930	17.265
2.500	.4		.732	1.466	3.602	5.836
1.667	.6		.307	.478	1.144	2.001
1.250	.8		.091	-.021	-.098	.053
1.000	1.0		-.043	-.325	-.854	-1.130
.833	1.2		-.136	-.532	-1.366	-1.928

TABLE III (Cont.)

(C) With the exact radial distribution function for the Born-Green equation.

		λ	1	5
T*	$\beta\varepsilon$	v*	13.823	3.633
1.667	.6		.106	.314
1.000	1.0		.046	---

and to a .02 interval between $x = 1.12$ and 1.28.

The same intervals, values of v^* and T^*, and radial distribution functions were used to evaluate the integral in (73). The results are given in Table IV. The quantity tabulated, E^E, is the excess of the internal energy of the fluid above that of a perfect gas at the same temperature:

$$\frac{E^E}{N\varepsilon} = \frac{E}{N\varepsilon} - \frac{3RT}{2N\varepsilon} = \frac{\lambda_0}{2}\int_1^\infty x^2\,\gamma_1(x)\,g(x)\,dx. \qquad (76)$$

The difference between p^* for the various approximate radial distribution functions is relatively small. If we compare, for example, p^* at $\lambda = 5$, $\beta\varepsilon = .60$, using the distribution functions correct to $\psi_1(x)$, to $\psi_2(x)$, and the exact one, we find $p^* = 0.301$, 0.307, and 0.314, respectively. As $\beta\varepsilon$ increases, of course, the neglected terms in (44) become more important, since the higher powers of $\beta\varepsilon$ increase rapidly. A small error in the radial distribution function can make a rather large difference in the condensation region, since p^* for those values of the parameters is the difference between two large quantities and is therefore very sensitive to small changes in the radial distribution function.

Of great interest is the establishment of the critical point and the condensation region for a fluid with this calculated equation of state. The ratio $\frac{p^* v^*}{T^*}$ at the critical point, for example, furnishes an absolute check on the theory since that quantity is independent of the choice

TABLE IV

The Excess Internal Energy

$-\frac{E^E}{N\varepsilon}$ as a function of the reduced temperature, T*, and reduced volume, v*.

(A) With a radial distribution function correct to terms in Ψ_2 for the Born-Green equation.

T*	v* 3.633	2.261	1.484	1.223
5.000	1.787	2.990	4.822	6.066
2.500	1.856	3.050	4.873	6.125
1.667	1.939	3.118	4.925	6.181
1.250	2.035	3.193	4.975	6.232
1.000	2.148	3.277	5.025	6.280
.833	2.280	3.370	5.073	6.313

(B) With the exact radial distribution function for the Born-Green equation.

T*	v* 13.823	3.633
1.667	.537	1.992
1.000	.741	

of the parameters $\mathcal{E}$ and a. The difference between the experimental and calculated values of this ratio thus reflects the error caused by the superposition approximation, by the form of the potential, and by the inaccuracies in the radial distribution function. This ratio was first calculated on the basis of the equation of state obtained with the radial distribution function correct to terms in $\Psi_1(x)$. In order to carry out this calculation, the equation of state was fitted with an empirical equation, using the fact that p* is to a very good approximation a linear function of T*, and fitting the coefficients of the linear isometrics as a function of volume. The critical point can be determined by differentiating this empirical equation. Setting

$$\left(\frac{\partial p^*}{\partial v^*}\right)_{T^*} = 0 \qquad \text{and} \qquad \left(\frac{\partial^2 p^*}{\partial v^{*2}}\right)_{T^*} = 0$$

yielded: $p^*_c = .197$, $v^*_c = 3.077$, $T^*_c = 1.465$,

$$\left(\frac{p^*v^*}{T^*}\right)_c = \left(\frac{pv}{NkT}\right)_c = .414,$$

as opposed to the experimental(14)*

$$\left(\frac{pv}{NkT}\right)_c = .303 \text{ for argon.}$$

The same job was repeated with the equation of state which results from the radial distribution function correct to terms in $\Psi_2(x)$. With linear isometrics the empirical equation of state given in Appendix E, equation (157) resulted. At the critical point

$$p^*_c = .183, \qquad v^*_c = 2.674,$$

$$T^*_c = 1.318, \qquad \left(\frac{p^*v^*}{T^*}\right)_c = .371.$$

---

* X = 78

The isometrics are however not quite linear; the maximum deviation is 1 per cent in p^* near the critical region. Since the derivatives used to determine the critical point, and therefore the critical point itself, are sensitive to small changes in curvature, quadratic isometrics were also tried. This empirical equation of state (see Appendix E, equation (158)) exactly fits the points at $\beta\varepsilon = .60$, $.80$, and 1.00 for $\lambda = 5$, 10, 20, and 27.4.

The disadvantage of this equation of state is that for $\beta\varepsilon \leq .40$ the fit is imperfect. The maximum percentage error in p^* at $\beta\varepsilon = .40$ is 2% at $\lambda = 10$. The critical point given by (158) is:

$$p^*_c = .199\,, \quad v^*_c = 2.585\,,$$
$$T^*_c = 1.433\,, \left(\frac{p^*v^*}{T^*}\right)_c = .358.$$

This ratio is probably more reliable than the one with linear isometrics, since the critical point lies within the exactly fitted range. The difference is not very great.

(158) was used to determine the two phase region of the phase diagram. To make a complete determination of this region, however, the equation of state for $\lambda < 5$ is required also. For this purpose, the solutions at $\lambda = 1$ are already available, but another point is desirable for even lower λ. Without solving for any more radial distribution functions we can make use of the information the second virial coefficient furnishes at $\lambda = 0$. However, first, the second virial coefficient has to be calculated with the modified Lennard-Jones potential to which the equation of state corresponds.

The second virial coefficient, $B^{(5)}$, is given by:

$$B = -\frac{2\pi\beta\varepsilon a^3}{3}\int_0^\infty \frac{d\gamma}{dx} e^{-\beta\varepsilon\gamma(x)} x^3\,dx . \tag{77}$$

Introducing the potential (43):

$$B = -\frac{2\pi\beta\varepsilon a^3}{3}\int_1^\infty \frac{d\gamma_1}{dx} e^{-\beta\varepsilon\gamma_1(x)} x^3\,dx + \frac{2\pi}{3}a^3. \tag{78}$$

A switch of variables and expansion of one of the exponentials in the integrand makes it possible to express the integral in terms of incomplete gamma functions, $\Gamma(a,b)$, so that

$$B = \frac{2\pi a^3}{3}\sqrt{y}\left[\Gamma\left(\tfrac{3}{4},\sqrt{y}\right) - \frac{1}{4}\sum_{\tau=1}^{\infty}\frac{y^\tau}{\tau!}\Gamma\left(\tfrac{2\tau-1}{4},\sqrt{y}\right)\right] + \frac{2\pi}{3}a^3 e^{-y^2}, \tag{79}$$

where

$$y = 2\sqrt{\beta\varepsilon},$$

and where

$$\Gamma(a,b) = \int_0^b t^{a-1}e^{-t}\,dt. \tag{80}$$

The quantity $b_1 = \frac{B}{4\pi a^3}$ is tabulated below for the same values of $\beta\varepsilon$ that were used previously. Also tabulated for comparison is the corresponding b_2 for the complete Lennard-Jones potential (42).

TABLE V

Second Virial Coefficient

$\beta\varepsilon$	b_1	b_2
.20	.0735	.0406
.40	-.0290	-.0521
.60	-.1426	-.1607
.80	-.2689	-.2840
1.00	-.4100	-.4231

These data at $\beta\varepsilon$ = .60, .80, and 1.00 were now combined with the data at λ = 1 and λ = 5 previously cited, and an equation of state in the virial form was fitted to agree with all this information (see Appendix E, equation (159)). It is interesting to note that the third virial coefficient obtained in this fashion agrees very closely at $\beta\varepsilon$ = .60 and .80 with the one calculated by Bird, Spotz, and Hirschfelder$^{(15)}$ with the complete Lennard-Jones potential (42).

With these empirical equations of state (158, 159) we are now able to find the conditions under which the liquid and gas phase are in equilibrium. The thermodynamic conditions for this equilibrium are that the pressure, the temperature, and the chemical potential of the two phases be identical. We proceed by fixing our attention on an isotherm below the critical point and try to find the two volumes for which the fluid has the same pressure and chemical potential.

The formula for the chemical potential is obtained through integration of the equation of state. Defining the chemical potential on a volume basis:

$$\mu + RT \log v + \mu_v^I(T) = \int_v^\infty \left(p - \frac{RT}{v}\right) dv + pv - RT$$

$$\mu_v^I(T) = \lim_{v \to \infty} \left(\mu + RT \log v\right). \tag{81}$$

It was convenient to find the two volumes at a given temperature with equal values of

$$\frac{\mu'}{RT} = \frac{\mu - \mu_v^I(T) + RT \log 4\pi}{RT} \tag{82}$$

This is permissible since μ and μ' differ only by a constant at a given temperature. The table below gives the values of p*, T*, and $\frac{\mu'}{RT}$, for the two reduced volumes.

TABLE VI

Conditions for Equilibrium between Gas and Liquid.

T*	p*	$\frac{\mu'}{RT}$	(v*) liquid	(v*) gas
1.43	.199		2.589	2.589
1.39	.163	.032	1.860	4.649
1.35	.127	-.113	1.634	6.798
1.30	.102	-.285	1.407	8.608
1.25	.074	-.511	1.193	12.566

At $T^* = 1.23$ it is no longer possible to find two volumes which will make p^* and μ' equal, since we do not have a radial distribution function for low enough volumes. Figure III shows the attainable two phase region, with several isotherms in that region as well as some isotherms slightly above the critical point. The dome representing the states of vapor and liquid in equilibrium is plotted and extrapolated to low values of p^* on the liquid side by the dotted curve. On the gaseous side the dome, if extended, would gradually approach $p^* = 0$ at very large values of v^*. Figure III qualitatively at least strongly resembles the experimental equations of state of many fluids.

To find the internal energy of transition, the excess internal energy was fitted empirically as a function of volume and temperature (see Appendix E, equation (160)). Putting in the λ_0 and $\beta\varepsilon$ values for the liquid and gas phase, we find the energy of vaporization, $\Delta E_v/N\varepsilon$, to be the following:

TABLE VII

Energy of Vaporization

T^*	$\frac{\Delta E_v}{N\varepsilon}$
1.25	-5.704
1.30	-4.338
1.35	-3.305
1.39	-2.283

Finally, the entropy was also calculated with the aid of the equation of state and is tabulated in Table VIII, for the same values of λ and $\beta\varepsilon$ for which the internal energy and the pressure were evaluated. The table actually gives the excess entropy defined on a volume basis as follows:

$$S = R \log v + S_v^I(T) + S_v^E, \tag{83}$$

where

$$S_v^I(T) = \lim_{v \to \infty} \left[S - R \log v \right], \tag{84}$$

and where

$$S_v^E = \int_\infty^v \left[\left(\frac{\partial p}{\partial T} \right)_v - \frac{R}{v} \right] dv. \tag{85}$$

For the equation of state in the interval of $\beta\varepsilon$ between .60 and 1.00, (158) and (159) were used. For $\beta\varepsilon$ = .20 and .40, (157) was used for $\lambda > 5$. For $\lambda < 5$ the equation of state was calculated from the $\lambda = 5$ point and the second virial coefficients tabulated previously (see Appendix E, equation (161)).

TABLE VIII

The Excess Entropy

$+\frac{S_v^E}{R}$, as a function of the reduced temperature, T* , and v* with a radial distribution function correct to terms in Ψ_2 .

T*	v*	13.823	3.633	2.261	1.484	1.223
5.000		-.168	-.729	-1.317	-2.343	-3.123
2.500		-.168	-.729	-1.317	-2.343	-3.123
1.667		-.066	-.275	- .852	-1.862	-2.638
1.250		-.308	-1.211	-1.816	-2.859	-3.651
1.000		-.273	-1.089	-1.712	-2.774	-3.576

Figure 3. The reduced equation of state showing the two phase region with several isotherms.

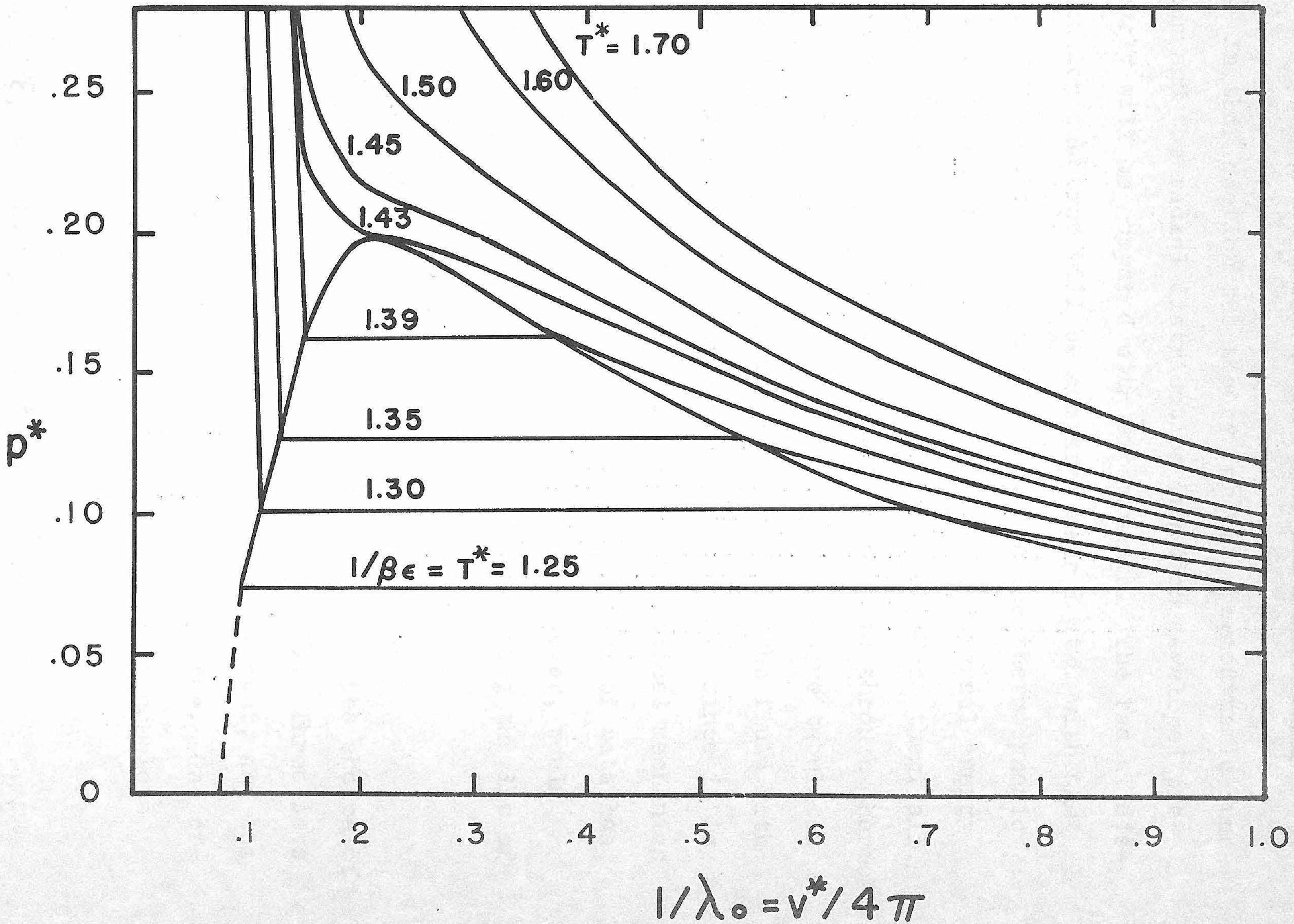
$T^* = 1.70$
1.60
1.50
1.45
1.43
1.39
1.35
1.30
$1/\beta\epsilon = T^* = 1.25$
p^*
.25
.20
.15
.10
.05
0
.1
.2
.3
.4
.5
.6
.7
.8
.9
1.0
$1/\lambda_o = v^*/4\pi$

Comparison with Experiments and Conclusions

In this section the theory for the thermodynamic functions and the radial distribution function developed previously will be compared with experiments. The radial distribution function will be compared near 1 atm. with the data of Eisenstein and Gingrich(11). In the thermodynamic comparison, the equation of state and the internal energy will be the two key quantities to analyze. From them, all other equilibrium properties can be evaluated through thermodynamic relations (e.g. the vapor pressure curve tabulated in this section). Argon has been chosen as the fluid with which experimental comparisons are to be made, since it is a monatomic fluid for which classical statistical mechanics ought to be applicable, and since a great deal of data has been gathered about it. The comparison, however, would work out equally well for any other fluid obeying the law of corresponding states with respect to argon.

(A) Comparison of Thermodynamic Data

The thermodynamic comparison depends upon the choice of a and ε which are to be substituted into (75). Three sets of these parameters were thought to be significant, and the comparison has been carried through for all three. One of these sets is that given by Michels(16) for the complete Lennard-Jones potential (39,42):

$$\begin{aligned} \varepsilon_L &= 165.3 \times 10^{-16} \text{ ergs.} \\ a_L &= 3.405 \times 10^{-8} \text{ cm.} \end{aligned} \qquad (86)$$

These two parameters were adjusted so that, for a region near room temperature, the calculated and experimental second virial coefficients for argon agree, where the second virial coefficient was calculated with the complete Lennard-Jones potential (39,42) and where the data were brought into correspondence by the method of least squares. However, due to the modified Lennard-Jones potential (43) used in our theory, the calculated second virial coefficient is different (78). Thus, the more significant parameters, a_M and ε_M , would be the ones where the modified second virial coefficients are brought into agreement with experimental data. What was actually done is almost equivalent to the above suggestion. a_M and ε_M were determined so that at $\beta\varepsilon = .60$, .80, and 1.00 the two theoretical virial coefficients coincide as well as the criterion of least squares permits. By plotting log b against log $\beta\varepsilon$, the shift necessary to make the two curves coincide determines the ratio of $\frac{\varepsilon_M}{\varepsilon_L}$ and $\frac{a_M}{a_L}$.

$$\frac{\varepsilon_M}{\varepsilon_L} = 1.171 \qquad ; \qquad \frac{a_L}{a_M} = 1.086. \tag{87}$$

These two ratios, as a matter of fact, bring the two curves in good agreement all the way down to $\beta\varepsilon = .20$.

The third set of parameters is fixed by the requirement that the theoretical and experimental critical volume and temperature be brought into agreement. This causes the calculated critical pressure to be in error (56.6 instead of 48 atm). Not too much reliance, however, can be placed upon these values, a_c and ε_c , because the error introduced by the incomplete knowledge of the radial distribution function and the uncertainty in the method of location of the critical point might shift the theoretical critical point considerably. The table below compares the three sets of values.

TABLE IX

Different Choices for the Parameters a and ε

	Na^3 cc.	$N\varepsilon$ cal.
Michels' complete Lennard-Jones potential	$Na_L^3 = 23.777$	$N\varepsilon_L = 237.84$
Modified Lennard-Jones potential	$Na_M^3 = 18.569$	$N\varepsilon_M = 278.56$
Critical point adjustment	$Na_c^3 = 30.298$	$N\varepsilon_c = 209.37$

A comparison of pv/NkT, calculated and experimental, is illustrated below for two temperatures and the three sets of parameters. (Table X)

TABLE X

pv/NkT Comparison

A) Michels' (ε_L, a_L)

	T = 0°C			T = 150°C		
λ	calc.	expt.(16)	% diff.	calc.	expt.	% diff.
5	.982	.925	+ 6.2	1.290	1.161	11.1
10	1.186	1.122	5.7	1.714	1.486	15.3
20	1.907	2.138	-10.8	2.776	2.556	8.6
27.4	2.586	3.661	-29.8	3.644	---	

B) Modified Lennard-Jones potential (ε_M, a_M)

	T = 0°C			T = 150°C		
λ	calc.	expt.	% diff.	calc.	expt.	% diff.
5	.841	.984	-14.5	1.199	1.281	-6.4
10	.943	1.510	-37.6	1.557	1.937	-19.6

C) Critical point adjustment (ε_c, a_c)

	T = 0°C			T = 150°C		
λ	calc.	expt.	% diff.	calc.	expt.	% diff.
5	1.092	.909	20.1	1.361	1.097	24.1
10	1.374	.978	40.5	1.834	1.271	44.3
20	2.217	1.362	62.8	2.974	1.776	67.5
27.4	2.952	1.915	54.2	3.889	2.345	65.9

The Michels a_L and ε_L agree best. The curve calculated with his parameters has to be moved in the direction of the parameters for the Lennard-Jones potential with the hard core (a_M, ε_M). At ~~the~~ relatively high temperatures (low $\beta\varepsilon$) the radial distribution functions ought to be very good and the deviations can be attributed to the superposition approximation, but also partly at least to the form of the potential used. At high temperatures, molecules with the modified Lennard-Jones potential behave essentially as a van der Waals gas with only the volume of the molecules themselves excluded. Probably at these temperatures the collisions are actually interpenetrating, and thus the modified Lennard-Jones potential does not represent the actual situation. Therefore, it appears reasonable that the best a and ε for the equation of state should lie somewhere between a_L, ε_L and a_M, ε_M.

A comparison of vapor pressure data was also carried out. Data are given in Table XI for log p vs. 1/T for the experimental points and the three calculated cases.

TABLE XI

Vapor Pressure Comparison

expt.(14)		Michels		Modified		Critical	
1000/T	log p	1000/T	log p	1000/T	log p	1000/T	log p
6.635	1.681	5.796	1.914	4.984	2.090	6.632	1.771
6.772	1.628	5.962	1.828	5.127	2.004	6.822	1.685
6.977	1.554	6.144	1.721	5.284	1.897	7.030	1.578
7.223	1.466	6.376	1.626	5.483	1.801	7.296	1.483
7.555	1.346	6.633	1.488	5.705	1.664	7.590	1.345
8.157	1.137						
8.934	0.871						
11.429	0.000						

The calculated curves are all straight lines, roughly in agreement with experiment. The critical point adjustment agrees best here, since we are comparing data near the critical point.

A comparison of the excess internal energy in units of cal. is illustrated in Table XII for two temperatures and the three separate values of the parameters.

TABLE XII

Excess Internal Energy Comparison

A) Michels (ε_L, a_L)

	T = 0°C			T = 150°C		
λ	calc.	expt.(17)	% diff.	calc.	expt.	% diff.
5	445	399	11.4	431	359	20.3
10	729	625	16.5	717	560	28.0
20	1163	918	26.5	1153	782	47.4

B) Modified Lennard-Jones potential (ε_M, a_M)

	T = 0°C			T = 150°C		
λ	calc.	expt.	% diff.	calc.	expt.	% diff.
5	530	504	5.0	510	453	12.5
10	860	788	9.1	844	694	21.5

C) Critical point adjustment (ε_c, a_c)

	T = 0°C			T = 150°C		
λ	calc.	expt.	% diff.	calc.	expt.	% diff.
5	387	317	22.0	377	285	32.6
10	638	497	28.3	629	447	40.7
20	1020	740	37.8	1013	656	54.3
27.4	1282	882	45.3	1273	764	66.7

The modified Lennard-Jones adjustment brings theory and experiment into closest agreement this time. The Michels a_L and ϵ_L follow closely behind, whereas the agreement is worst for the critical a_c and ϵ_c. Significantly again, the discrepancy is largest at the higher temperatures with the hard core potential of interaction, confirming the suspicion that the form of the potential is inadequate.

B) Comparison of the Radial Distribution Function

It would be desirable to have a radial distribution function near one atmosphere to compare with the Eisenstein-Gingrich(11) experimental determination of this function by means of x-rays. However, as Figure III shows, solutions have not been obtained for small enough volumes. The solution at $p^* = .074$ was the last one which permitted the calculation of a liquid volume. The p^* corresponding to one atmosphere can be calculated once a choice of ϵ and a is made. This p^* is very small for any reasonable choice of parameters. For example, for a_L and ϵ_L, $p^* = .003$ corresponds to one atmosphere.

In order to have a radial distribution function at one atmosphere, it was decided to extrapolate to the λ value which corresponds to $p^* = .003$. This value of λ could not be determined from a power series extrapolation of the dome of the two-phase region to low p^* values, since the points of the dome do not form a smooth curve. The alternative procedure adopted was to make the ratio of the critical volume to the normal liquid volume the same in the theoretical and experimental equations of state. This yields $\lambda_0 = 13.128$ for the liquid at one atmosphere. As Figure III shows, this value does not disagree with a reasonable extrapolation of the dome.

ψ_0, ψ_1, and ψ_2 at this value of λ_0 were then obtained at each value of x by separate analytic extrapolations with a cubic polynomial in λ_0. This polynomial was so determined that it had the correct value of the ψ functions at $\lambda = 5$, 10, 20, and 27.4. The extrapolation formula was checked for ψ_0 at $\lambda = 33$ and proved to be in error by a maximum amount of about 10%. The extrapolation of ψ_0 at $x = 1.00$ then allowed the λ value to be determined as 37.297. For this value of λ the hard sphere integral equation is above its eigenvalue, 34.8(18). The functions ψ_0, ψ_1, and ψ_2 are recorded in Table XIII, and it can be seen that succeeding peaks in the ψ functions are not decreasing very fast, indicative of a high λ value and possibly non-integrability of the radial distribution function.

It then became necessary to determine the $\beta\varepsilon$ value which would correspond to the one atmosphere isotherm. By adopting several $\beta\varepsilon$ values and forming the corresponding radial distribution function, a radial distribution function was found which gave $p^* = .003$ when substituted in the equation of state (72). The appropriate value of $\beta\varepsilon$ was .843. Table XIII gives the radial distribution function for the value of $\beta\varepsilon = .850$, which is near enough to the correct one.

TABLE XIII

The extrapolated functions ψ which determine the radial distribution function as a function of x for the λ_0 value of 13.13 in the Born and Green equation and the corresponding radial distribution function for $\beta\varepsilon$ = .85.

$\psi(x) = x \log g(x)$, $x \geq 1$.

$\psi(x) = \psi_0(x) + (\beta\varepsilon)\psi_1(x) + (\beta\varepsilon)^2\psi_2(x)$

x	ψ_0	ψ_1	ψ_2	g
1.00	1.044	-1.015	.021	1.217
1.04	1.045	-.284	.013	2.185
1.08	1.043	.059	.009	2.769
1.12	1.012	.212	.004	2.907
1.16	.949	.242	-.014	2.683
1.20	.878	.207	-.024	2.373
1.24	.775	.151	-.035	2.030
1.28	.639	.088	-.035	1.713
1.32	.469	.037	-.044	1.427
1.36	.292	-.018	-.042	1.198
1.40	.100	-.078	-.042	1.002
1.44	-.094	-.114	-.043	.857
1.48	-.292	-.146	-.031	.744
1.52	-.490	-.153	-.026	.657
1.56	-.642	-.187	-.009	.596
1.60	-.805	-.165	-.002	.553
1.64	-.930	-.168	.018	.524
1.68	-1.024	-.142	.041	.515
1.72	-1.083	-.120	.061	.516

TABLE XIII (cont.)

x	ψ_0	ψ_1	ψ_2	g
1.76	-1.103	-.083	.081	.532
1.80	-1.060	-.066	.094	.559
1.84	-.962	-.064	.095	.597
1.88	-.833	-.035	.107	.660
1.92	-.647	-.028	.118	.737
1.96	-.412	-.021	.139	.845
2.00	-.131	-.015	.144	.980
2.04	.177	-.007	.109	1.130
2.08	.419	.083	.071	1.297
2.12	.615	.166	.038	1.447
2.16	.740	.211	.022	1.542
2.20	.820	.209	.006	1.577
2.24	.853	.179	-.024	1.552
2.28	.848	.112	-.068	1.480
2.32	.783	.049	-.098	1.384
2.36	.684	-.016	-.119	1.281
2.40	.568	-.078	-.127	1.186
2.44	.393	-.116	-.152	1.077
2.48	.251	-.183	-.167	.990
2.52	.063	-.213	-.177	.907
2.56	-.103	-.231	-.168	.848
2.60	-.272	-.249	-.135	.800
2.64	-.417	-.239	-.059	.778

TABLE XIII (cont.)

x	ψ_0	ψ_1	ψ_2	g
2.68	-.554	-.207	.005	.763
2.72	-.644	-.174	.053	.758
2.76	-.724	-.134	.111	.760
2.80	-.753	-.088	.143	.772
2.84	-.756	-.036	.154	.788
2.88	-.715	.022	.154	.816
2.92	-.640	.078	.154	.853
2.96	-.545	.135	.148	.897
3.00	-.406	.173	.128	.946
3.04	-.257	.222	.128	1.008
3.08	-.095	.259	.114	1.069
3.12	.064	.277	.091	1.124
3.16	.199	.302	.071	1.174
3.20	.336	.283	.050	1.211
3.24	.453	.242	.024	1.232
3.28	.530	.202	.005	1.240
3.32	.568	.149	-.024	1.226
3.36	.586	.085	-.061	1.200
3.40	.565	.012	-.096	1.160
3.44	.524	-.067	-.125	1.116
3.48	.443	-.127	-.142	1.069
3.52	.372	-.203	-.149	1.026
3.56	.242	-.244	-.147	.980
3.60	.161	-.304	-.139	.946

TABLE XIII (cont.)

x	ψ_0	ψ_1	ψ_2	g
3.64	.023	-.301	-.121	.916
3.68	-.073	-.325	-.116	.889
3.72	-.186	-.298	-.084	.874
3.76	-.261	-.302	-.039	.865
3.80	-.347	-.242	.005	.865
3.84	-.401	-.191	.042	.870
3.88	-.446	-.117	.087	.883
3.92	-.443	-.066	.126	.902
3.96	-.422	.002	.152	.925
4.00	-.399	.073	.163	.947
4.04	-.343	.127	.159	.971
4.08	-.279	.190	.155	.999
4.12	-.203	.241	.142	1.026
4.16	-.124	.278	.121	1.049
4.20	-.039	.305	.095	1.071
4.24	.047	.311	.072	1.089
4.28	.140	.281	.047	1.101
4.32	.208	.257	.022	1.108
4.36	.266	.222	-.009	1.108
4.40	.301	.176	-.037	1.101
4.44	.318	.092	-.064	1.082
4.48	.322	.043	-.109	1.064
4.52	.302	-.012	-.128	1.045
4.56	.279	-.082	-.151	1.021

TABLE XIII (cont.)

x	ψ_0	ψ_1	ψ_2	g
4.60	.240	-.124	-.146	1.006
4.64	.182	-.166	-.144	.986
4.68	.133	-.209	-.144	.969
4.72	.073	-.244	-.123	.954
4.76	.005	-.254	-.106	.941
4.80	-.055	-.252	-.071	.935
4.84	-.109	-.236	-.038	.933
4.88	-.144	-.224	-.017	.931
4.92	-.183	-.182	.008	.935
4.96	-.210	-.135	.041	.942
5.00	-.219	-.084	.082	.955
5.04	-.217	-.053	.111	.965
5.08	-.204	-.005	.126	.977
5.12	-.178	.036	.132	.990
5.16	-.151	.090	.135	1.004
5.20	-.118	.132	.127	1.017
5.24	-.071	.163	.116	1.029
5.28	-.039	.186	.098	1.037
5.32	-.006	.212	.087	1.046
5.36	.033	.209	.066	1.049
5.40	.066	.202	.043	1.051
5.44	.099	.184	.016	1.050
5.48	.120	.155	-.019	1.044
5.52	.130	.120	-.048	1.036

TABLE XIII(cont.)

x	ψ_0	ψ_1	ψ_2	g
5.56	.142	.079	-.077	1.028
5.60	.142	.040	-.095	1.019
5.64	.128	-.008	-.112	1.007
5.68	.116	-.043	-.124	.998
5.72	.093	-.076	-.134	.988
5.76	.070	-.080	-.115	.986
5.80	.060	-.123	-.109	.979
5.84	.031	-.144	-.091	.973
5.88	-.004	-.142	-.068	.971
5.92	-.025	-.146	-.039	.971
5.96	-.041	-.151	-.018	.970
6.00	-.064	-.134	.000	.971
6.04	-.082	-.111	.029	.975
6.08	-.088	-.079	.053	.981
6.12	-.085	-.064	.070	.985
6.16	-.085	-.035	.088	.992
6.20	-.080	.000	.093	.998
6.24	-.074	.022	.099	1.003
6.28	-.070	.045	.091	1.005
6.32	-.053	.060	.085	1.009
6.36	-.041	.090	.080	1.015
6.40	-.023	.093	.062	1.016
6.44	-.006	.105	.045	1.018
6.48	.006	.117	.035	1.020

TABLE XIII(cont.)

x	ψ_0	ψ_1	ψ_2	g
6.52	.023	.111	.012	1.019
6.56	.035	.097	-.006	1.017
6.60	.041	.085	-.023	1.015
6.64	.053	.062	-.041	1.011
6.68	.053	.045	-.058	1.007
6.72	.053	.027	-.064	1.004
6.76	.053	.015	-.070	1.002
6.80	.047	-.008	-.070	.999
6.84	.041	-.039	-.070	.994
6.88	.029	-.043	-.064	.992
6.92	.023	-.049	-.053	.992
6.96	.012	-.060	-.047	.990
7.00	-.006	-.060	-.035	.988
7.04	-.006	-.064	-.018	.990
7.08	-.006	-.076	-.006	.989
7.12	-.012	-.070	.006	.991
7.16	-.018	-.064	.023	.992
7.20	-.023	-.047	.035	.995
7.24	-.029	-.035	.041	.996
7.28	-.029	-.029	.047	.997
7.32	-.029	-.018	.053	.999
7.36	-.029	.000	.053	1.001
7.40	-.029	.012	.047	1.002
7.44	-.023	.023	.041	1.003

TABLE XIII (cont.)

x	ψ_0	ψ_1	ψ_2	g
7.48	-.018	.029	.035	1.004
7.52	-.012	.035	.029	1.005
7.56	-.006	.041	.023	1.006
7.60	.000	.041	.012	1.006
7.64	.006	.041	.000	1.005
7.68	.012	.041	-.006	1.006
7.72	.012	.035	-.018	1.004
7.76	.012	.029	-.023	1.003
7.80	.012	.023	-.023	1.002
7.84	.012	.018	-.035	1.000
7.88	.018	.012	-.035	1.000

The value of $\beta\varepsilon$ of .843 seems badly off. If the isotherms in the two phase region, Figure III, were to be extrapolated to this low p*, a value of around 1.00 would result. This discrepancy can not be due to the fact that the λ value of 37.297 is higher than the eigenvalue of the hard sphere integral equation, since an extrapolation of the radial distribution function to the eigenvalue itself, 34.8, would make the $\beta\varepsilon$ value at normal conditions even lower. It must be concluded that no great reliance can be placed on the extrapolation, since the rate of change of the Ψ functions is determined from the lower λ values. Near the eigenvalue one might expect a very much faster change in the distribution functions than the previous values at lower λ would indicate. We thus have limited our experimental comparison with thermodynamic data to the higher pressures where the radial distribution functions have been computed.

Figure IV compares this extrapolated radial distribution function with experimental radial distribution functions near one atmosphere(11). The value of the characteristic distance, a, was so adjusted that the first peaks coincide; that is, a = 3.274 Å. The agreement is fair if the scattering of the experimental data and the extrapolation used are taken into account.

All these radial distribution functions for fluids with intermolecular potentials of the Lennard-Jones type (42) exhibit their first and largest peak at the minimum of this potential near x = 1.15. As x increases, the curve goes through oscillations of diminishing amplitude. Succeeding peaks represent next nearest and further neighboring molecules, since g(x) is so defined that $\frac{N}{V}$ g(x) specifies the local molecular density at a distance x from a specified molecule. At large distances the function approaches unity, indicating no correlation at all. For $x < 1$, g(x) is zero since the hard-sphere core of the molecule at the center excludes a second molecule. It is also characteristic that the peaks are sharper for lower temperatures (higher $\beta\varepsilon$) and smaller molar volumes (higher λ). Figure I illustrates the first point, while Figure II illustrates the second. Finally, above some value of λ no integrable solution is obtainable. This point is identified with a change of state. As the parameter λ changes from values corresponding to a gas to those corresponding to a liquid, no abrupt change can be observed in the radial distribution function because, as was pointed out, the restraint of homogeneous density was put on .

In conclusion it can be said that the theory developed represents the experimental equation of state and internal energy of argon moderately well over a wide range of volume and temperature. It is hoped that this agreement will be even better once the exact radial distribution functions are used. Future plans to complete this project would include improving the radial distribution functions, at the values of λ where approximate radial distribution functions are now available, by the methods suggested in section III (page 17, this thesis), and completion of the solution at

$\lambda = 33$. This last value should yield a vapor pressure near one atmosphere. Depending on how well the experimental comparison then works out, it might prove worthwhile to investigate the effect of a different expression for the repulsive potential of interaction. Once the exact radial distribution functions are known for the modified Lennard-Jones potential, it should be easy to get the exact solutions with the complete Lennard-Jones potential. The radial distribution functions available ought to make very good first approximations in any of the procedures discussed in Section III (page 17, this thesis) and Appendix B-1.

Figure 4. A comparison of the extrapolated radial distribution function ($\rho^* = .003$, $\beta\varepsilon = .85$) with experimental radial distribution functions.

O (1.8 atm., 91.8°K)

X (.8 atm., 84.4°K)

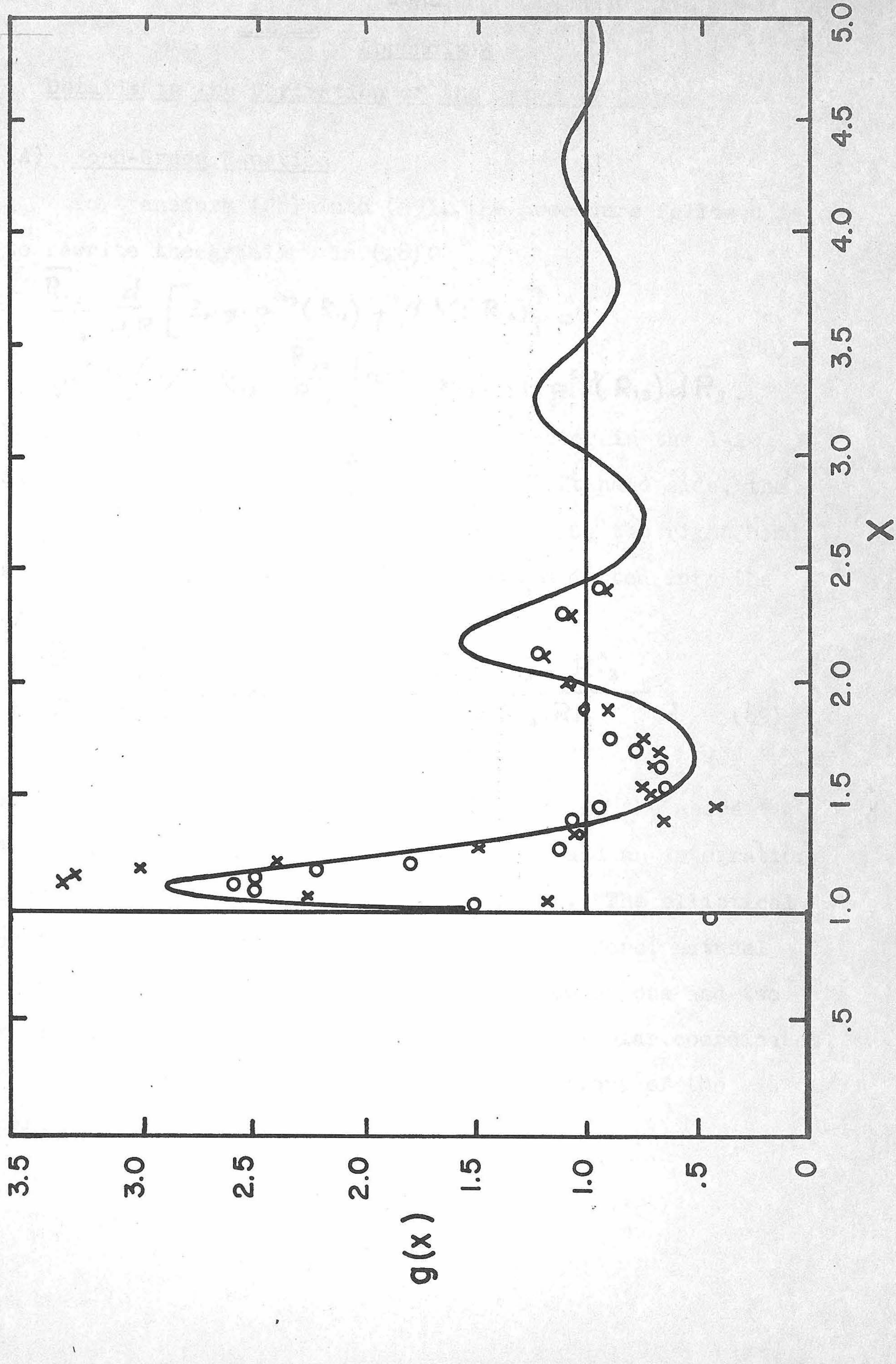
g(x)
3.5
3.0
2.5
2.0
1.5
1.0
.5
0
X
.5
1.0
1.5
2.0
2.5
3.0
3.5
4.0
4.5
5.0

Appendix A

Details in the Derivation of the Integral Equations

(A) Born-Green Equation

To transform (28) into (29), the procedure followed is to rewrite the gradient in (28):

$$\frac{\vec{R}_{12}}{R_{12}} \frac{d}{dR_1}\left[\log g^{(2)}(R_{12}) + \beta V(R_{12})\right] = \beta \rho^{(1)} \int V'(R_{13}) \frac{\vec{R}_{13}}{R_{13}} \left[g^{(2)}(R_{23}) - 1\right] g^{(2)}(R_{13})\, d\vec{R}_3 . \tag{88}$$

Equation (88) is dotted into the unit vector in the 1-2 direction, that is, into $\frac{\vec{R}_{12}}{R_{12}}$. On the left hand side, the unit vector dotted into itself is unity. On the right hand side the unit vector in the 1-2 direction dotted into the one in the 1-3 direction is:

$$\frac{\vec{R}_{12}}{R_{12}} \cdot \frac{\vec{R}_{13}}{R_{13}} = \cos(213) = \frac{R_{12}^2 + R_{13}^2 - R_{23}^2}{2 R_{12} R_{13}} , \tag{89}$$

where the law of cosines has been applied. In the above integral, molecules one and two are fixed and an integration over a movable molecule three is performed. The elliptical or the bipolar coordinate systems are, therefore, natural choices. In elliptical coordinates, molecules one and two would be at the foci of the ellipse. For bipolar coordinates, the following drawing illustrates the positions of the molecules:

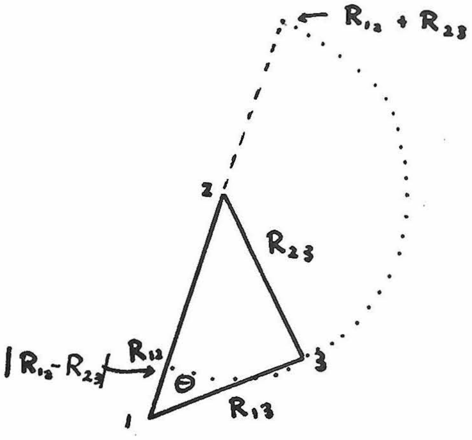

The volume element for this system of coordinates, which is used here, is equal to:

$$d\vec{R}_3 = 2\pi \frac{R_{13}R_{23}}{R_{12}} dR_{13}\, dR_{23}. \tag{90}$$

Thus

$$\frac{d}{dR_{12}}\left[\log g^{(2)}(R_{12}) + \beta V(R_{12})\right] = \frac{\pi\beta\rho^{(1)}}{R_{12}^2}\int_0^\infty dR_{23}\, R_{23}\left[g^{(2)}(R_{23})-1\right]\int_{|R_{12}-R_{23}|}^{R_{12}+R_{23}} d\vec{R}_{13}\, g^{(2)}(R_{13})\, V'(R_{13})\left[R_{12}^2+R_{13}^2-R_{23}^2\right]. \tag{91}$$

To transform this into (29) the definitions of $g^{(2)}(x)$ and $V(x)$ must be extended.

$$g^{(2)}(-R_{13}) = g^{(2)}(R_{13})$$
$$V(-R_{13}) = V(R_{13}). \tag{92}$$

The effect of this extension is an odd integrand in (91) for the integration over R_{13} and R_{23}. To proceed, the following change of limits is carried out:

$$\int_{|R_{12}-R_{23}|}^{R_{12}+R_{23}} = \int_{|R_{12}-R_{23}|}^{\infty} + \int_{\infty}^{R_{12}+R_{23}} = \int_{|R_{12}-R_{23}|}^{\infty} - \int_{R_{12}+R_{23}}^{\infty}. \tag{93}$$

Finally, an integration over R_{12} is necessary, so that the left hand side becomes: $\log g^{(2)}(R_{12}) + \beta V(R_{12})$, provided the limits of integration are chosen as infinity and R_{12}. At infinity the left hand side vanishes since $g^{(2)}$ is unity and V is zero. This integration over R_{12} can actually be carried out on the right hand side if the order of integration is interchanged between R_{13} and R_{12}.

$$\log g^{(2)}(R_{12}) + \beta V(R_{12}) =$$
$$\pi \beta \rho^{(1)} \int_0^\infty dR_{23}\, R_{23} \left[g^{(2)}(R_{23}) - 1\right] \int_\infty^{R_{12}} dR_{12} \left\{ \int_{|R_{12}-R_{23}|}^\infty dR_{13}\, g^{(2)}(R_{13}) \right. \tag{94}$$
$$\left. V'(R_{13}) \left[\frac{R_{12}^2 + R_{13}^2 - R_{23}^2}{R_{12}^2}\right] - \int_{R_{12}+R_{23}}^\infty dR_{13}\, g^{(2)}(R_{13})\, V'(R_{13}) \left[\frac{R_{12}^2 + R_{13}^2 - R_{23}^2}{R_{12}^2}\right] \right\}.$$

The following drawing illustrates the area of integration, so that by interchanging the order of integration:

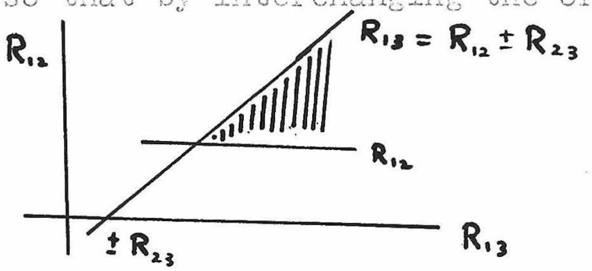

$$\log g^{(2)}(R_{12}) + \beta V(R_{12}) =$$
$$\pi \beta \rho^{(1)} \int_0^\infty dR_{23}\, R_{23} \left[g^{(2)}(R_{23}) - 1\right] \left\{ - \int_{|R_{12}-R_{23}|}^\infty dR_{13} \right.$$
$$g^{(2)}(R_{13})\, V'(R_{13}) \int_{R_{12}}^{R_{13}+R_{23}} dR_{12}\, \frac{R_{12}^2 + R_{13}^2 - R_{23}^2}{R_{12}^2} \; +$$
$$\left. + \int_{R_{12}+R_{23}}^\infty dR_{13}\, g^{(2)}(R_{13})\, V'(R_{13}) \int_{R_{12}}^{R_{13}-R_{23}} dR_{12}\, \frac{R_{12}^2 + R_{13}^2 - R_{23}^2}{R_{12}^2} \right\}. \tag{95}$$

Taking advantage of the parity (92) allows the combination of two integrals in (95). Thus by changing the variable R_{23} to $-R_{23}$ in one of the integrals

$$\log g^{(2)}(R_{12}) + \beta V(R_{12}) = -\pi\beta\rho^{(1)}\int_{-\infty}^{\infty} dR_{23}$$

$$R_{23}\left[g^{(2)}(R_{23})-1\right]\int_{|R_{12}-R_{23}|}^{\infty} dR_{13}\, g^{(2)}(R_{13})V'(R_{13})\int_{R_{12}}^{R_{12}+R_{23}} \frac{R_{12}^2+R_{13}^2-R_{23}^2}{R_{12}^2}\, dR_{12}. \quad (96)$$

The integration over R_{12} is carried out next. The resulting equation is identical with (29) if R_{23} is identified as r , R_{12} as R , and finally R_{13} as y .

(B) <u>Kirkwood Equation</u>

Starting with (36), a change to bipolar coordinates, as illustrated previously, is called for in order to obtain (37). This is followed by an integration over the coupling parameter between the limits zero and ξ . At $\xi = 0$, the left hand side vanishes, since, if there is no coupling between molecule one and the rest of the molecules, there can be no correlation; that is, $g^{(2)}$ is one and of course the potential of interaction is zero. Thus

$$\log g^{(2)}(R_{12},\xi) + \beta\xi V(R_{12}) =$$

$$-\frac{2\pi\beta\rho^{(1)}}{R_{12}}\int_0^{\xi}\int_0^{\infty} d\xi\, dR_{23}\left[g^{(2)}(R_{23})-1\right]R_{23}\int_{|R_{12}-R_{23}|}^{|R_{12}+R_{23}|} dR_{13}\, R_{13}V(R_{13})\,g^{(2)}(R_{13},\xi). \quad (97)$$

A change of limits analogous to the one illustrated in (93) results in:

$$\log g^{(2)}(R,\xi) + \beta\xi V(R) =$$

$$-\frac{2\pi\beta\rho^{(1)}}{R}\int_0^{\infty} dr\left[g^{(2)}(r)-1\right] r\int_0^{\xi} d\xi\left[\int_{|R-r|}^{\infty} ds\, s\, V(s)\,g^{(2)}(s,\xi) - \int_{R+r}^{\infty} ds\, s\, V(s)\,g^{(2)}(s,\xi)\right], \quad (98)$$

where R_{12} has been called R , $R_{13} = y$, and $R_{23} = r$. (37) is obtained from (98) if the variable r is changed to -r in one of the integrals. The two integrals can then be combined due to the parity conditions (92).

Appendix B-1

Other Methods Tried

A solution of the non-linear integral equation (40) was first attempted with the potential (42). Since no mathematical theory was known to attack the problem, the simple numerical device of a direct iterative procedure was first tried. Values of the two parameters were chosen appropriate to the liquid state. The process of direct iteration starts with a trial radial distribution function, $g^{(0)}_{(R)}(x)$. The kernel is calculated with it, and the convolution is performed so as to obtain $g^{(0)}_{L}(x)$, the radial distribution function on the left side. This $g^{(0)}_{L}(x)$ is now substituted in the right hand side of (40) as $g^{(1)}_{R}$, to obtain $g^{(1)}_{L}(x)$ on the left hand side. This process is repeated till the solution is found; that is, till the function substituted on the right hand side reproduces itself on the left hand side. Unfortunately, however, this procedure diverges for values of the parameters significant to the liquid state. If the first trial distribution function is very nearly the true solution, it might be surmised that such a procedure should converge. None of the initial trials substituted (i.e.: $g = 1$; $g = e^{-\beta\varepsilon\gamma_1(x)}$; the radial distribution function used by Kirkwood and Buff(7); or the experimental radial distribution function(11)) proved to be within the region of convergence. It became thus evident that the radial distribution function occurs in a very sensitive way in the right hand side of (40).

The only hope for convergence of a direct iterative procedure, therefore, lies in rearranging the equation in such a fashion that the right hand side is relatively insensitive to the radial distribution function. Such a possibility arises if one recalls the convolution theorem of Fourier analysis, which converts (40) to:

$$F(k) = \frac{\lambda_0}{4} Y(k)\, G(k)\,. \qquad (99)$$

The Fourier transforms are defined as follows:

$$F(k) = \int_{-\infty}^{\infty} e^{-ikt}\, t\left[\log g(t) + \beta\varepsilon\, \gamma(t)\right] dt \qquad (100)$$

$$\therefore Y(k) = \int_{-\infty}^{\infty} e^{-ikt}\left[t\,(g(t)-1)\right] dt \qquad (101)$$

$$G(k) = \int_{-\infty}^{\infty} e^{-ikt}\, K(t)\, dt. \qquad (103)$$

These Fourier transforms were calculated with the aid of I.B.M. equipment and the file of punched cards used for electron diffraction procedures. Direct iteration amounts to

$$F^{(n+1)}(k) = \frac{\lambda_0}{4} Y^{(n)}(k)\, G^{(n)}(k). \tag{104}$$

That is, a trial g(t) is used to evaluate t $[g(t)-1]$, [illegible] K(t), and their respective transforms. By (104), F(k) can be calculated. The cycle is repeated after an inverse transform of F(k) yields a new trial g(t). This procedure failed to converge. Direct iteration also failed for (105), (107), and (108), three other forms of (99) derived below:

$$Y^{(n+1)}(k) = \frac{4\, F^{(n)}(k)}{\lambda_0\, G^{(n)}(k)} \tag{105}$$

$$F(k) - Y(k) = \frac{\lambda_0}{4} Y(k) G(k) - Y(k) \tag{106}$$

$$\therefore Y^{(n+1)}(k) = \frac{Y^{(n)}(k) - F^{(n)}(k)}{1 - \frac{\lambda_0}{4} G^{(n)}(k)}. \tag{107}$$

Multiplying by $\frac{\lambda_0}{4}$G(k)

$$F^{(n+1)}(k) = \frac{Y^{(n)}(k) - F^{(n)}(k)}{1 - \frac{\lambda_0}{4} G^{(n)}(k)} \left[\frac{\lambda_0}{4} G^{(n)}(k)\right]. \tag{108}$$

(105) was expected to be less sensitive to $g^{(0)}$ than (104). The sensitivity in (107) and (108) lies in the denominator.

It approaches zero for certain values of k and for values of λ_0 significant to liquids. Indeed, for the case of a hard sphere liquid, Kirkwood(18) has shown that the denominator vanishes for values of λ_0 slightly higher than those corresponding to the liquid state. This means that a non-integrable radial distribution function is obtained. The smallest value of λ_0 at any value of k for which $1-\frac{\lambda_0}{4}G(k)= 0$ is then interpreted as a transition point.

A new attack on the problem had to be devised and the method of steepest descents looked most promising. At first this method was set up in its most general form. Let us define

$$D^{(n)}(x) = g_L^{(n)}(x) - g_R^{(n)}(x), \tag{109}$$

the difference in the radial distribution function between left and right hand side of (40)´ as the result of one direct iteration with the initial trial $g_R^{(n)}$. The object then is to introduce a new radial distribution function $g_R^{(m)}(x)$ so as to make the total absolute difference decrease most rapidly; that is,

$$\chi^{(m)} = \int_0^\infty D^{(m)^2}(x)\, dx \tag{110}$$

should become as small as possible. The method of steepest descents states that $g_R^{(m)}$ differs from $g_R^{(n)}$ by an amount proportional to the slope of $\chi^{(n)}$:

$$g_R^{(m)}(x) = g_R^{(n)}(x) + \gamma \frac{\partial \chi^{(n)}}{\partial g_R^{(n)}(x)}, \tag{111}$$

where γ is some appropriate constant. If $\chi^{(n)}$ were a monotonic function of $g_R^{(n)}(x)$, this method should converge. However, to calculate the above derivative proved to be a very cumbersome procedure. Furthermore, to find the best value of γ would essentially be a trial and error operation. To be precise, even γ should be a function of x if the descent is to be truly the steepest.

Since it is not possible to set up the method of steepest descents entirely rigorously anyway, procedures were sought which might be adaptable to I.B.M. machines. We must introduce at least one parameter which can be adjusted so as to decrease χ. The more parameters are introduced, the more complicated the procedure becomes, but the more rapidly will the solution be approached per cycle. The speed of convergence is not as essential as simplicity if the procedure is to be put on I.B.M. machines. Thus a one parameter system was first explored as follows:

$$\begin{aligned} g_R^{(n)}(x) &= \alpha^{(n)} g_L^{(n)} + (1-\alpha^{(n)})\, g_R^{(n)}(x) \\ \chi^{(n)} &= \int_0^\infty \left[g_L^{(n)}(x) - g_R^{(n)}(x)\right]^2 dx . \end{aligned} \tag{112}$$

If $g_R^{(n+1)} = g_L^{(n)}$, $\chi^{(n)}$ can be rewritten as

$$\begin{aligned} \chi^{(n)} = \int_0^\infty \left[D^{(n)}(x)\right]^2 dx + \alpha^{(n)2}\int_0^\infty \left[D^{(n+1)}(x) - D^{(n)}(x)\right]^2 dx - \\ - 2\alpha^{(n)}\int_0^\infty D^{(n)}(x)\left[D^{(n+1)}(x) - D^{(n)}(x)\right] dx . \end{aligned} \tag{113}$$

The value of $\alpha^{(n)}$ which minimizes $\chi^{(n)}$ is found to be:

$$\alpha^{(n)} = \frac{\int_0^\infty D^{(n)}(x)\left[D^{(n+1)}(x) - D^{(n)}(x)\right] dx}{\int_0^\infty \left[D^{(n+1)}(x) - D^{(n)}(x)\right]^2 dx} . \tag{114}$$

It can be shown that this method converges except in some singular cases. If this optimum value of $\alpha^{(n)}$ is substituted into the expression for $\chi^{(m)}$ we get, substituting $\chi^{(n)}$,

$$\chi^{(m)} = \chi^{(n)} - \frac{\left\{\int_0^\infty D^{(n)}(x)\left[D^{(n+1)}(x) - D^{(n)}(x)\right]dx\right\}^2}{\int_0^\infty \left[D^{(n+1)}(x) - D^{(n)}(x)\right]^2 dx} . \tag{115}$$

Since the last term in (115) is positive,

$$0 \leq \chi^{(m)} \leq \chi^{(n)} . \tag{116}$$

This means that the distribution function has been improved. It must be recognized that $g_L^{(m)}$, the iterate of $g_R^{(m)}$, is only approximately equal to:

$$\alpha^{(n)} g_L^{(n+1)} + (1-\alpha^{(n)})\, g_L^{(n)} . \tag{117}$$

This is the method of solution actually employed. However, it proved possible to simplify the scheme even further by not having to calculate an α value.

The above scheme is almost identical with the one developed in the paper given in Appendix (D). The method given there might however be improved by not using the entire inhomogeneous term as the first trial. Such a starting function might prove too crude or possibly make the convergence too slow. If no suitable initial guess can be found, the sure way to solve this linear integral equation (Appendix D, equation (32)) is to use the method of Fourier transforms (99).

Appendix B-2

I.B.M. Procedure

(A) Introduction

Utilizing the expansion (44) in powers of $\beta\varepsilon$, it is to be noted that only three basic operations are required to calculate all terms in the series for $\Psi(x)$. It proved possible to adapt I.B.M. machines to all three. However, there still remain a number of operations simple and easy enough to carry out on desk calculators, although they could have been mechanized also. Whether to do a problem on the desk calculator or the I.B.M. machines was dictated mainly by considerations of how tedious the calculation was and how often it had to be performed. Thus, for example, in the inhomogeneous part of the integral equation (58) convolutions have to be carried out, besides such trivial operations as multiplying a function by a constant and adding up all the various functions. All the simple operations including the preparation of the two functions making up the convolution are best done on desk machines, since the punching of the I.B.M. cards and the subsequent integration to get the kernel on I.B.M. machines would consume almost as much time as the entire hand operation. However, the convolution itself is very tedious and occurs repeatedly in the inhomogeneous parts of the integral equations. It therefore paid to work it out on I.B.M. machines.

Once knowing the inhomogeneous part, the iterative procedure described previously (69,70) can be started. Since one cycle of this iteration lasts roughly half an hour, it would have been awkward and very inefficient to stop the machines so often and make some hand calculations before proceeding to the next cycle. Thus the entire operation from $\Psi_r^{(n)}(x)$ to $\Psi_r^{(n+1)}(x)$ was wired up for the machines. This wiring, due to the limited number of operations that these machines can perform at any time, was split into two parts. The first part involves convoluting the hard sphere kernel. This kernel function never changes; but it is convoluted with a function which changes from iteration to iteration. Due to the simple nature of this kernel, this convolution could be done by a more efficient method than the convolution occurring in the inhomogeneous part. The second part of the iterative procedure consists of algebraic operations to obtain the next trial function.

(B) Convolution Needed for Inhomogeneous Part

The details of the actual wiring for the plugboards which perform the above calculations are included in Appendix B-3. It seems worthwhile, however, to describe briefly the principles involved in setting up the wiring diagrams. The convolution in the inhomogeneous part of the integral equation is of the form:

$$\int_{-\infty}^{\infty} K(s-x)\, E(s)\, ds = \int_{-\infty}^{\infty} K(t)\, E(x+t)\, dt. \qquad (118)$$

Both K (s-x) and E(s) are prepared by desk calculators and punched out on I.B.M. cards at an interval of .04 in the reduced units. This choice of spacing depends on the desire to have the distribution function at such close points. Also, with this interval, the trapezoidal rule of integration is accurate enough in the above convolution. As an additional factor, the hard sphere distribution function, which is involved in the higher terms in the expansion, had already been evaluated at this interval. The .04 interval was chosen in the hard sphere radial distribution function for the same reasons plus the fact that the Fourier analysis cards used there were convenient for such a spacing.

The machine takes these functions, K(t) and E(s), and for each value of x, at .04 intervals, carries out the integration indicated in (118). This convolution or integration has to be performed only for $x \geq 1$, since the distribution function, due to the hard sphere core, is zero inside one. We proceed by reproducing one function, let us say the kernel, as many times as there are values of x for which one needs the convolution. Then, to perform the integration for any one value of x, the two functions are multiplied at corresponding values of the argument, the product is printed on the cards containing the kernel, and finally the products are summed. This is essentially the procedure followed except that it proved possible to economize by doing four values of x simultaneously. Thus, the cards containing the kernel have that function punched on them four times in the following fashion:

TABLE XIV

Representative I.B.M. cards in the convolution of the inhomogeneous part.

Card #	First Field	Second Field	Third Field	Fourth Field	Fifth Field
1	t	K(t)			
2	t+.04	K(t+.04)	K(t)		
3	t+.08	K(t+.08)	K(t+.04)	K(t)	
4	t+.12	K(t+.12)	K(t+.08)	K(t+.04)	K(t)
5	t+.16	K(t+.16)	K(t+.12)	K(t+.08)	K(t+.04)

etc.,

where t starts at that part of the negative t axis where the kernel vanishes. The above operation, called spreading, ends when the kernel becomes negligibly small at the positive t axis. This spreading is accomplished by gang punching K(t) on the neighboring cards as indicated above by arrows. It is this set of kernel cards, called a deck, which is reproduced many times. It is labeled each time by a succeeding deck number starting with deck number one. This identification mark allows the machine to know with which value of E(s) the kernel has to be multiplied. That is, the corresponding argument of E(s) is obtained by adding [0.16(Deck #-1)+1] to the values in the first field. Thus, for deck number one, one is added to the entry in the first field. So, in the second field, the convolution (118) is performed for x = 1.00;

in the third field, the one for x#= 1.04; in the fourth, the one for x = 1.08; and in the fifth, the one for x = 1.12. In the second deck, according to the above formula, 1.16 is added on to the first field in order to find the argument of E(s), so that the second field will integrate for x = 1.16; and so on, till all the desired values of x are covered. The argument of E(s) obtained by the above formula is punched into the cards containing the kernel as they are prepared. The one set of cards punched with E(s) is next matched up with this number by the collator for all decks of the kernel cards simultaneously. That is, each E(s) card is sorted with all the kernel cards in all the decks containing the identification s. The 604 calculator then carries out four multiplications per card and punches the four products into the kernel cards. A sort on the deck number and a run through the tabulabor and summary punch yields the final result by printing and punching four sums at the end of each deck.

(C) Iteration

The convolutions occurring in the iterative procedure with the hard-sphere kernel could be handled in a way similar to the one just described. However, the above method is wasteful of both time and cards. An effort to improve it was successful because of the simple nature of the kernel. The advantage the hard-sphere kernel offers is that, by partial integrations, the convolution, L(x), can be reduced to the formation of integrals of the function, l(s), to be convoluted with the kernel. l(s) is of the form $g.\psi_r^{(n)}$. The partial integrations are carried out as follows:

$$L(x) = \int_{-\infty}^{\infty} \left[(x-s)^2 - 1 \right] \ell(s)\, ds, \tag{119}$$

where x-s is restricted to $|x-s| < 1$.

Therefore

$$L(x) = \int_{x-1}^{x+1} \left[(x-s)^2 - 1 \right] \ell(s)\, ds. \tag{120}$$

Integrating by parts yields:

$$L(x) = \left[(x-s)^2 - 1 \right] I\ell(s) \Big|_{x-1}^{x+1} + 2\int_{x-1}^{x+1} (x-s)\, I\ell(s)\, ds, \tag{121}$$

where

$$I\ell(s) = \int^{s} \ell(w)\, dw.$$

The first term vanishes at the limits, so:

$$L(x) = 2\int_{x-1}^{x+1} (x-s)\, I\ell(s)\, ds. \tag{122}$$

Again integrating by parts yields:

$$\begin{aligned} L(x) &= 2(x-s) I^2\ell(s) \Big|_{x-1}^{x+1} + 2\int_{x-1}^{x+1} I^2\ell(s)\, ds \\ &= -2\, I^2\ell(x+1) - 2 I^2\ell(x-1) + \\ &\quad + 2 I^3\ell(x+1) - 2 I^3\ell(x-1), \end{aligned} \tag{123}$$

where

$$\begin{aligned} I^2\ell(s) &= \int^{s} dv \int^{v} \ell(w)\, dw; \\ I^3\ell(s) &= \int^{s} dz \int^{z} dv \int^{v} \ell(w)\, dw. \end{aligned} \tag{124}$$

The evaluation of these multiple integrals is much more adaptable to I.B.M. machines than the direct procedure for the convolution, as can be seen from the following integration rules. Let us define the following operators:

$$E\ell(x) = \ell(x-1),$$

$$\Delta\ell(x) = (1-E)\ell(x) = \ell(x) - \ell(x-1),$$

$$\sum\ell(x) = \frac{1}{\Delta}\ell(x) = \frac{1}{1-E}\ell(x) = \tag{125}$$

$$(1+E+E^2+\dots)\ell(x) = \ell(x) + \ell(x-1) + \cdots,$$

$$D\ell(x) = \frac{d}{dx}\ell(x)$$

$$I\ell(x) = \int_{-\infty}^{x}\ell(\omega)\,d\omega.$$

Using the well known symbolic equation

$$E = e^{-D} = 1 - \Delta \tag{126}$$

or

$$-D = \log(1-\Delta)$$

and expanding the logarithm,

$$D = \Delta + \frac{\Delta^2}{2} + \frac{\Delta^3}{3} + \cdots \tag{127}$$

we get

$$I = \frac{1}{\Delta\left[1 + \frac{\Delta}{2} + \frac{\Delta^2}{3} + \cdots\right]} . \tag{128}$$

Carrying out the division, results in:

$$I = \sum\left[1 - \frac{\Delta}{2} - \frac{\Delta^2}{12} - \frac{\Delta^3}{24} - \frac{19\Delta^4}{720} + \cdots\right]. \tag{129}$$

By squaring the above,

$$I^2 = \sum^2 \left[1 - \Delta + \frac{\Delta^2}{12} + 0 - \frac{\Delta^4}{240} + \cdots \right]$$
$$\doteq \sum^2 E + \frac{1}{12} - \frac{\Delta^2}{240} . \tag{130}$$

By cubing I,

$$I^3 = \sum^3 \left[1 - \frac{3}{2}\Delta + \frac{\Delta^2}{2} + 0 + \frac{\Delta^4}{240} + \cdots \right]$$
$$\doteq \sum^3 \left[(1-\Delta)\left(1 - \frac{\Delta}{2}\right) \right] + \frac{\Delta}{240} = \sum^3 \frac{E(1+E)}{2} + \frac{\Delta}{240} . \tag{131}$$

Thus

$$I^2 l(x) = h^2 \left[\sum \sum^{x-h} l(x) + \frac{l(x)}{12} \right] + O(\Delta^2 l(x));$$
$$I^3 l(x) = \frac{h^3}{2} \left[\sum \sum \sum^{x-h} l(x) + \sum \sum \sum^{x-2h} l(x) \right] + O(\Delta l(x)), \tag{132}$$

where h is the interval. By (129), I becomes, accurate up to second differences:

$$I = \sum - \frac{1}{2} - \frac{\Delta}{12} - \frac{\Delta^2}{24} \cdots = \sum - \frac{1}{2} - \frac{1-E}{12} - \frac{(1-E)^2}{24} ;$$
$$I l(x) = h \left[\sum^{x} l(x) + \frac{-15 l(x) + 4 l(x-h) - l(x-2h)}{24} \right] . \tag{133}$$

I^2 is evaluated by neglecting terms in the second differences and I^3 by neglecting terms in the first differences in l(x). The formula for I itself is not needed explicitly except for values of x less than one. Because of the factor $g_0(x)$, the function l(x) goes discontinuously to zero at x = 1, and stays zero till x = 0. Thus, for x = 1, the formula for I^2 simply reduces to adding the integral of a constant.

$$I^2 l(x=1-nh) = I^2 l(x=1) + nh\, I l(x=1), \tag{134}$$

where n is the integral number of intervals of h away from x = 1. For I^3 the above is integrated again, so that:

$$I^3 l(x=1-nh) = I^3 l(x=1) + nh\, I^2 l(x=1) + + n^2h^2\, I l(x=1). \tag{135}$$

It is quite essential for numerical reasons to start integrating from the largest value of x towards x = 0. If we commence at x = 0, L(x) would be inaccurate for large x, since the difference of large quantities would have to be taken in the triple integral (124). Slight numerical errors would thus be greatly magnified. These can creep in not only due to the neglect of higher differences in (132), but also due to the discontinuity at x = 1, if the integration were started at x = 0. To take into account numerically the discontinuity occurring at x = 1, the formula for Il(x) (133) is used for two points below x = 1 in (134). Subsequent to these two points, l(x-h) and l(x-2h) are zero, and Il(x) is a constant.

It turns out that a choice of an interval in reduced units of .02 is extremely convenient. The reason for this is that with this interval the coefficient in front of the I^2 term (132) becomes 4 x 10^{-4} while the one in front of the I^3 term becomes 4 x 10^{-6}. Thus one can add I^2 and I^3 terms by merely an adjustment of the decimal point. Thus all inhomogeneous parts calculated at a .04 interval in x were interpolated to an interval in x of .02. The brief table below is intended to make clear how the multiple integrals were evaluated. The procedure starts with the maximum value of x for which l(x) does not vanish.

TABLE XV

Formation of Multiple Integrals

l(x)	x	Σ	$\Sigma\Sigma$	$\Sigma\Sigma\Sigma$
a	$x_{max,}$	a	a	a
b	$x_{max,}-.02$	$a+b$	$2a+b$	$3a+b$
c	$x_{max.}-.04$	$a+b+c$	$3a+2b+c$	$6a+3b+c$

Therefore by (132) and (133):

$$I\ell(x_{max.}-.04) = .02\left[a+b+c+\frac{-15c+4b-a}{24}\right]$$

$$I^2\ell(x_{max.}-.04) = (.02)^2\left[(2a+b)+\frac{c}{12}\right]$$

$$I^3\ell(x_{max.}-.04) = (.02)^3\,\frac{1}{2}\left[(3a+b)+a\right].$$

The operations to form $2I^2$ and $2I^3$ were wired up on a plugboard with 58 program cycles out of a maximum possible 60. The actual wiring diagram is given in Appendix B-3.

Due to the fact that almost all of the possible program cycles had been used up above, the iterative procedure had to be transferred to an additional plugboard. Again, the wiring diagram is attached in Appendix B-3 and the details are briefly described below. Before going into that, however, an intermediate step is necessary to form L(x). The previous calculation ended up so that on each card, (that is, for a given value of x), $2I^2\ell(x)$ and $2I^3\ell(x)$ was punched. It is necessary also to punch into each card the multiple integrals one unit removed in x in both the positive and negative direction in order to form L(x) (123). This is accomplished by a "backwards" sort on the units position followed by another sort on the tenths position. This brings adjacent to each card with a given value of x, the ones containing x-1 and x+1.

TABLE XVI

Illustration of Sorting Procedure

x originally	x first sort	x second sort
4.00	4.00	4.00
3.98	3.90	3.00
3.96	3.80	2.00
3.92	⋮	1.00
3.90	0.00	0.00
3.88	3.92	3.02
3.86	3.82	2.02
⋮	3.72	1.02
0.00	⋮	0.02
		3.04
		⋮

The 604 I.B.M. machine then allows one to punch the numbers on adjacent cards onto the one in the middle (see arrows). Those cards with zero in the hundredths position are then punched with unnecessary information, but these cards are not used in subsequent steps. The cards immediately following the cards with a zero in the hundredths position have nothing punched into them from this previous card; that is, this operation is suppressed. A sort on the hundredths position itself restores the cards to their normal sequence in x. On these cards, besides the various multiple integrals, $m_r(x)$ is punched as well as the known functions $g_0(x)$, $\varphi_0(x)$, and $\varphi_r^{(n)}(x)$, so that all the data for the operation to form $\varphi_r^{(n+1)}(x)$ are present (59). The difficulty now encountered is that not enough space is left on the cards to permit the calculations. A method had to be devised to transfer some of the information and the result of the calculation to another card.

This procedure involves the collator, which intersperses two blank cards between each pair of printed cards. Let us now consider the representative trio:

Blank card 1

Punched card A

Blank card 2 .

When this trio is sent through the 604 machine, each card goes through three cycles in the following order: a first reading station, a punch station, and a second reading station. When card A is at the first reading station and card one is at the punch station, the functions x, $\varphi_r^{(n)}(x)$, $\varphi_0(x)$, and $m_r(x)$ are transferred to card 1 from card A. At this time the machine combines the multiple integrals read from card A and forms L(x). That value is saved in the machines. During the next cycle when card 1 is at the second reading station, card A at the punch station, and card 2 at the first reading station, the digit emitter emits the values of $\varphi_r^{(n)}(1)$, λ, and the appropriate value of α. All the calculations to form $\varphi_r^{(n+1)}(x)$ are made during this cycle. The necessary values are read from card 1. Nothing is punched during this cycle, but in the third cycle, when card 2 is at the punch station and card A at the second read station, the answers are printed into card 2. In this same cycle, card 2 receives from card A the values of x, $g_0(x)$, $\varphi_0(x)$, and $m_r(x)$ and has them punched in. It is card 2 now which becomes card A in the next iteration after the new multiple integrals have also been punched in it.

For the iterations with the higher values of λ, a value of α around .1 was cautiously chosen to start out with. If convergence proceeded too slowly the values of α was increased to around .2 in steps. Somewhere between 10 and 20 cycles were needed before the solution was within the desired accuracy. The number of cycles increased with λ, and also depended somewhat on the choice of the initial trial. The initial distribution function, $g^{(0)}(x)$, was usually arbitrarily taken as what appeared to be then the best possible solution.

For example, half the inhomogeneous part was used successfully. Or, if the equation had already been solved for some other λ value, that solution, multiplied by a constant, was introduced as the initial trial. It usually proved worthwhile to do a few rough convolution cycles on a desk calculator to improve the solution somewhat before letting I.B.M. machines start with the iteration procedure.

Appendix B-3

Wiring Diagrams for I.B.M. Machine Calculations

APPLICATION ______ PROBLEM ______

NOTES	PROGRAM SUPPRESS	PROGRAM NUMBER	FACTOR STORAGE ASSIGNMENT 6 4 8 6 1	2	8-6 3	4	MULT. QUOT.	COUNTER	GENERAL STORAGE ASSIGNMENT 6- 6-6 1	2	6-6 3	4	PROGRAM NUMBER
X-40 NX-40		R	$\lvert k_1 \rvert$ x.xx	$\lvert k_2 \rvert$ xx.xxx	$\lvert k_3 \rvert$ x.xx	$\lvert k_4 \rvert$ xx.xxx	ψ x.xxx	▨					R
		1			RO	RO		RI 1					1
		2			RI	RI		RO 5					2
		3			RO	RO		RI 5 neg.					3
		4						R+R RO 1		RI			4
		5	RO	RO				RI 1					5
		6	RI	RI				RO 5					6
		7	RO	RO				RI 5 neg.					7
		8						R+R RO 1				RI	8
Multiply: Plus if Minus if	k_4 pos. k_4 neg.	9						x.xxxxxx		RO			9
1/2 adj.		10						RI 2 5					10
		11						R+R RO 3		RI			11
Multiply: Plus if Minus if	k_2 pos. k_2 neg.	12						x.xxxxxx				RO	12
1/2 adj.		13						RI 2 5					13
		14						R+R RO 3				RI	14
Multiply: Plus if Minus if	k_3 pos. k_3 neg.	15			RO	RO		x.xxxxxx					15
1/2 adj.		16						RI 2 5					16
		17						R+R RO 3	RI		RI		17
Multiply: Plus if Minus if	k_1 pos. k_1 neg.	18	RO	RO				x.xxxxxx					18
1/2 adj.		19						RI 2 5					19
		20											20
		P					▨	R+R k_1 ψ	RO k_3 ψ	RO k_4 ψ	RO k_3 ψ	RO k_2 ψ	P

APPLICATION ______________________ PROBLEM ______

NOTES	PROGRAM SUPPRESS	PROGRAM NUMBER	FACTOR STORAGE ASSIGNMENT 1	FACTOR STORAGE ASSIGNMENT 2	FACTOR STORAGE ASSIGNMENT 3	FACTOR STORAGE ASSIGNMENT 4	MULT QUOT	COUNTER	GENERAL STORAGE ASSIGNMENT 1	GENERAL STORAGE ASSIGNMENT 2	GENERAL STORAGE ASSIGNMENT 3	GENERAL STORAGE ASSIGNMENT 4	PROGRAM NUMBER
				ϕ/24(1.020) xxxx			ϕ/24(1.04) xxxx						
	No. 12 Col.79	R		G₀(x) xxxx			ψ(x) xxxx						
	Suppress X-77	1							RI	RI	RI	RI	1
Balance test		2				RI		RO 1					2
		3				RO		RI 1 neg.					3
	Suppress if counter and MQ have same sign	4					RO	RI 1 neg.					4
	Suppress if counter and MQ have opposite sign	5					RO	RI 1					5
		6					RI	RO 6					6
		7					RO	RI 6 neg.					7
	Same suppression as Prog. 5	8	RO		RO			RI 1 neg.					8
	Same suppression as Prog. 4	9	RO		RO			RI 1					9
	Same suppression as Prog. 5	10	RI		RI			R+R RO 1					10
	Same suppression as Prog. 4	11	RO		RO			RI 1					11
		12			RI		RO						12
DE "4"		13					RI 4						13
Multiply		14		RO				4 ϕ/24 (1.02) xxxxx					14
DE "5"		15					RI 5						15
Multiply neg.		16						-5 ϕ/24 (1.00) xxxxx				RO	16
		17						-10ϕ/24(1.00) RI 2 neg.				RO	17
		18	RO	RI	RO								18
		19	RI		RI			R+R RO 1					19
		20		RO				RI 6					20

APPLICATION ______ PROBLEM ______

NOTES	PROGRAM SUPPRESS	PROGRAM NUMBER	FACTOR STORAGE ASSIGNMENT 8-6 (6 4) 1	2	3	4	MULT QUOT.	COUNTER	GENERAL STORAGE ASSIGNMENT 6-6 1	2	3	4	PROGRAM NUMBER
		R											R
		21				RO		RI 1					21
		22					RI					RI	22
		23						RI 1 neg.				RO	23
		24						RI 1 neg.				RO	24
		25				RI		RO 1					25
		26						RO 6				RI	26
		27						RI 1			RO		27
		28						RI 4	RO	RO			28
		29						RO 1			RI		29
		30						RO 4	RI	RI			30
		31						RI 6				RO	31
		32				RO		RI 1					32
		33	RO		RO			RI 1					33
		34				RI		RO 1					34
		35						RO 6				RI	35
		36						RI 1			RO		36
		37						RI 4	RO	RO			37
		38						RO 1			RI		38
		39						R+R RO 4	RI	RI			39
Multiply		40		RO				$G_0\psi(x)=\phi(x)$ xxxxxxx					40
		P											P

APPLICATION ______________________ PROBLEM ______

NOTES	PROGRAM SUPPRESS	PROGRAM NUMBER	FACTOR STORAGE ASSIGNMENT				MULT. QUOT.	COUNTER	GENERAL STORAGE ASSIGNMENT				PROGRAM NUMBER
			6 4 1	2	8-6 3	4			1	2	6-6 3	4	
		R											R
1/2 adj.		41						RI 2 5					41
		42					RI	R+R RO 3					42
		43					RO	RI 1					43
		44	RO		RO			RI 1					44
		45	RI		RI			R+R RO 1					45
DE "2"		46						RI 2 2					46
DE "4"		47						RI 1 4					47
		48		RI				R+R RO 1					48
		49					RO	RI 2					49
Divide		50		RO			Φ/24 (x) xxxxx						50
		51						R+R					51
		52					RO	RI 1					52
1/2 adj.		53						RI 1 5					53
		54					RI	R+R RO 2					54
		55				RO		RI 1					55
		56						RI 6				RO	56
		57					RO	RI 1					57
		58					RO	RI 1					58
		59					RO					RI	59
		60											60
		P						RO $2I^2$ xxxxxxxx	RO $2I^3$ xx	RO $2I^3$ xxxxx	RO $2I^3$ x	RO Φ/24(x) xxxx	

APPLICATION ______________ PROBLEM ______________

NOTES	PROGRAM SUPPRESS	PROGRAM NUMBER	FACTOR STORAGE ASSIGNMENT 1 (8 6)	FACTOR STORAGE ASSIGNMENT 2	FACTOR STORAGE ASSIGNMENT 3 (8 6)	FACTOR STORAGE ASSIGNMENT 4	MULT. QUOT.	COUNTER	GENERAL STORAGE ASSIGNMENT 1 (6 4 8 6)	GENERAL STORAGE ASSIGNMENT 2	GENERAL STORAGE ASSIGNMENT 3 (6 6)	GENERAL STORAGE ASSIGNMENT 4	PROGRAM NUMBER
			$2I^2(x-1.00)$ xxx	xxxxx	$2I^3(x-1)$ xxx	xxxxx	$2I^2(x+1)$ xxxxx		$2I^2(x+1)$ xxx		$2I^3(x+1)$ xxx	xxxxx	
	X-77 1 cycle later	R	Iter no. n xx	$\lvert\psi^n(x)\rvert$ .xxxx	$\lvert m(x)\rvert$ x.x	$\lvert\psi_o(x)\rvert$ xx.xxx	$\psi^n(1.00)$ .xxxx		$\lambda/5$ x.xx				R
		1	RO	RO				RI 1 neg.					1
		2			RO	RO		RI 1					2
		3					RO	RI 1 neg.					3
		4						RI 6 neg.	RO				4
		5						RI 1 neg.			RO	RO	5
		6						R+R RO 1			RI	RI	6
		7											7
		8					RO			RI			8
		9					RI		RO				9
Multiply		10						.xxxxxxxxxx			RO	RO	10
1/2 adj.		11						RI 3 5					11
		12						R+R RO 4			RI	RI	12
		13					RI			RO			13
		14			RO	RO		RI 1					14
		15			RI	RI		RO 4					15
		16						RO 1	RI				16
Multiply ± as sign ψ_o		17						.xxxxxx	RO				17
RI ± as sign m(x)		18			RO	RO		RI 5					18
		19						RI 1			RO	RO	19
		20			RI	RI		RO 1					20
		P											P

APPLICATION ____ PROBLEM ____

NOTES	PROGRAM SUPPRESS	PROGRAM NUMBER	FACTOR STORAGE ASSIGNMENT 1 (8 6)	FACTOR STORAGE ASSIGNMENT 2	FACTOR STORAGE ASSIGNMENT 3 (8·6)	FACTOR STORAGE ASSIGNMENT 4	MULT QUOT.	COUNTER	GENERAL STORAGE ASSIGNMENT 1 (6-4 8 6)	GENERAL STORAGE ASSIGNMENT 2	GENERAL STORAGE ASSIGNMENT 3 (6·6)	GENERAL STORAGE ASSIGNMENT 4	PROGRAM NUMBER
		R											R
1/2 adj.		21						RI 3 5					21
		22					RI	R+R RO 4					22
		23	RO	RO				RI 1					23
		24	RI	RI				RO 6					24
		25						R+R RO 1		RI			25
RI ± as sign of $\psi^{n}(x)$		26						RI 1 neg.		RO			26
Balance test		27					RO	RI 1					27
Balance test for selector PU		28						R+R RO 1	RI				28
DE "a"		29					RI a						29
Multiply		30			RO	RO		$a\psi'(x)^{n+1}$ x.xxxxxxx					30
DE "b"		31					RI 4 b						31
Multiply I as sign $\psi^{n}(x)$		32						$b\psi^{n}(x)$ x.xx xxooo		RO			32
DE "(a + b)"		33			RI 3	RI 3 x							33
		34											34
		35											35
		36											36
Divide		37			RO	RO	$\psi^{n+1}(x)$ .xxxxx						37
		38						R+R					38
		39					RO	RI 1					39
1/2 adj.		40						RI 1 5					40
		P											P

APPLICATION

PROBLEM

NOTES	PROGRAM SUPPRESS	PROGRAM NUMBER	FACTOR STORAGE ASSIGNMENT 1	FACTOR STORAGE ASSIGNMENT 2	FACTOR STORAGE ASSIGNMENT 3	FACTOR STORAGE ASSIGNMENT 4	MULT QUOT	COUNTER	GENERAL STORAGE ASSIGNMENT 1	GENERAL STORAGE ASSIGNMENT 2	GENERAL STORAGE ASSIGNMENT 3	GENERAL STORAGE ASSIGNMENT 4	PROGRAM NUMBER
		41						R+R RO 2		RI			41
		42	RO	RO				RI 1					42
DE "1"		43						RI 1 1					43
		44	RI	RI				R+R RO 1					44
Suppress on minus balance		45						RI 1	RO				45
Suppress on plus balance		46						RI 1 neg.	RO				46
		47						R+R RO 1	RI				47
		48						RI 6			RO	RO	48
Balance test		49											49
Suppress on plus balance		50	RO	RO				RI 1 neg.					50
Suppress on minus balance		51	RO	RO				RI 1					51
Suppress on plus balance		52						RI 3 neg.	RO				52
Suppress on minus balance		53						RI 3	RO				53
		54											54
		55											55
		56											56
		57											57
		58											58
		59											59
		60											60
								R+R .xxxxxxx.xxxxx conv. ⋮ Δ ⋮ iter. no. (n+1)		RO .xxxx $\psi^{n+1}(x)$			

Notes to Wiring Diagrams for I.B.M. Machine Calculations

R.O. means read out.

R.I. means read in.

R.R. means read out and reset.

D.E. means digit emit.

M.Q. means multiplier quotient

P.U. means pick-up.

Additional notes to (2).

Programs 2-22 inclusive are suppressed if No. 12 punch col. 79 ($x \neq .98$). Lead card ($x - .80$) read zero into F.S, 1-3 R and R counter.

Additional notes to (3).

Programs 1-6 inclusive suppressed No. X-77. Programs 8-53 inclusive suppressed except first cycle after X-77.

Appendix C

Comparison of the Born-Green and Kirkwood Theories

In Section II, derivations were given for the Born-Green (29,30) and Kirkwood(37,38) integral equations, differing in the way in which the superposition approximation is introduced. To find out how the radial distribution functions differ when the Lennard-Jones potential is used, a solution to the Kirkwood equation was worked out. The added complication of the coupling parameter was eliminated as in the hard-sphere case. Again the formula for the chemical potential, which Kirkwood's theory alone obtains, is used to relate λ to the reduced volume (see equation 16, Appendix D):

$$g(1,\lambda)\int_0^{\lambda} g(1,\lambda')^{-\frac{1}{2}}\,d\lambda' = \frac{4\pi N a^3}{V} = \lambda_0 . \tag{136}$$

To preserve this relation, and the methods of solution of the integral equation used in the Born-Green case, the potential again had to be broken up into a hard-sphere core joined to the Lennard-Jones potential. Then, an expansion in $\beta\varepsilon\xi$ is essential.

In order to permit separate coupling of the hard-sphere core and the Lennard-Jones potential, two coupling parameters, $\xi^{(0)}$ and $\xi^{(1)}$, are introduced. (37) and (38) then become the following:

$$\Psi(x, \xi^{(0)}, \xi^{(1)}) = -\beta\varepsilon\,\xi^{(1)}\,x\,\gamma_1(x) + \frac{\lambda_0}{4}\int_{-\infty}^{\infty} K(x-s, \xi^{(0)}, \xi^{(1)})\,s\left[g(s)-1\right]ds; \tag{137}$$

$$g(x, \xi^{(0)}, \xi^{(1)}) = e^{+\left[\beta\varepsilon(-\xi^{(0)})\gamma_0(x) + \Psi(x, \xi^{(0)}, \xi^{(1)})/x\right]}; \tag{138}$$

$$\begin{aligned} K(t, \xi^{(0)}, \xi^{(1)}) = {} & -2\beta\varepsilon\int_{|t|}^{\infty} ds \int_0^{\xi^{(0)}} d\xi^{(0)}\, s\, \gamma_0(s)\, g_0(s, \xi^{(0)}, 0) - \\ & -2\beta\varepsilon\int_{|t|}^{\infty} ds \int_0^{\xi^{(1)}} d\xi^{(1)}\, s\, \gamma_1(s)\, g(s, \xi^{(0)}, \xi^{(1)}). \end{aligned} \tag{139}$$

The path of integration has been chosen so that first the hard sphere potential is coupled in by itself, and then the Lennard-Jones potential is added on. In other words:

$$K(t, \xi^{(0)}, \xi^{(1)}) = \int_0^{\xi^{(0)}} \left(\frac{\partial K}{\partial \xi^{(0)}}\right)_{\xi^{(1)}=0} d\xi^{(0)} + \int_0^{\xi^{(1)}} \left(\frac{\partial K}{\partial \xi^{(1)}}\right)_{\xi^{(0)}=\xi^{(0)}} d\xi^{(1)}. \tag{140}$$

Rewriting the first term in (139), $K_H(t, \xi^{(0)}, 0)$, by introducing the definition of $g_0(s, \xi^{(0)}, 0)$, yields:

$$K_H(t, \xi^{(0)}, 0) = -2\beta\varepsilon\int_{|t|}^{\infty} ds \int_0^{\xi^{(0)}} d\xi^{(0)}\, s\, \gamma_0(s)\, e^{-\beta\varepsilon\xi^{(0)}\gamma_0(s)}\, e^{\frac{\Psi_0(s, \xi^{(0)}, 0)}{s}} \quad \text{for } |t| \leq 1. \tag{141}$$

This is equal to:

$$K_H(t, \xi^{(0)}, 0) = -2\beta\varepsilon\int_{|t|}^{1} ds \int_0^{\xi^{(0)}} d\xi^{(0)}\, s\, \gamma_0(s)\, e^{-\beta\varepsilon\xi^{(0)}\gamma_0(s)}\, e^{\frac{\Psi_0(s, \xi^{(0)}, 0)}{s}}, \tag{142}$$

since for $s \geq 1$ the integrand is zero due to the $\gamma_0(s)$ factor. Furthermore

$$\lim_{\xi^{(0)} \to 0} e^{-\beta\varepsilon\xi^{(0)}\gamma_0(s)} = 1 \tag{143}$$

because, for physical reasons, a coupling constant of zero implies no potential of interaction and therefore no correlation. For any other $\xi^{(0)}$,

$$e^{-\beta\varepsilon\xi^{(0)}\gamma_0(s)} = 0 \quad \text{if } s \lessgtr 1. \tag{144}$$

The introduction of

$$u = e^{-\beta\varepsilon\xi^{(0)}\gamma_0(s)} - 1 \tag{145}$$

changes (142) into

$$K_H(t, \xi^{(0)}, 0) = 2\int_{|t|}^{1} ds \int_{0}^{-1} du \, s \, e^{\psi_0(s, \xi^{(0)}, 0)/s}, \quad |t| < 1. \tag{146}$$

When $\xi^{(0)} = 0$, $K_H(t, \xi^{(0)}, 0)$ is trivially equal to zero, (142), due to the limits of integration. For any other value of the coupling parameter the kernel and ψ_0 are independent of $\xi^{(0)}$ (144). Therefore, arbitrarily calling $\xi^{(0)} = 1$ and integrating over u results in:

$$K_H(t, 1, 0) = -2\int_{|t|}^{1} ds \, s \, e^{\psi_0(s, 1, 0)/s} \tag{147}$$

Following the procedure developed in a previous paper(18), $e^{\psi_0(s, 1, 0)/s}$ is taken out of the integral by replacing it by its average value in the interval of integration, $\langle e^{\psi_0/s}\rangle$:

$$K_H(t, 1, 0) = -2\langle g_0\rangle \int_{|t|}^{1} s \, ds = \langle g_0\rangle K_0(t). \tag{148}$$

It is this $\langle g_0 \rangle$ which is evaluated through the theory of the chemical potential.

As for the second term in the kernel, $K_L(t, \xi^{(0)}, \xi^{(1)})$, (139), the expansion of g in powers of $\beta\varepsilon\xi^{(1)}$ is substituted. First, however, the $\xi^{(0)}$ independence already found is introduced:

$$g(s, \xi^{(0)}, \xi^{(1)}) = g(s, 1, \xi^{(1)}) = g(s, \xi^{(1)}), \tag{149}$$

where we have left out, as we will henceforth, the coupling constants whenever they are fully coupled. This has been done also implicitly in the Born-Green equation. If

$$\psi(s, \xi^{(1)}) = \psi_0(s) + (\beta\varepsilon\xi^{(1)})\psi_1(s) + (\beta\varepsilon\xi^{(1)})^2\psi_2(s) + \cdots, \tag{150}$$

then

$$g(s, \xi^{(1)}) = e^{\psi(s, \xi^{(1)})/s} = g_0(s)\left[1 + \beta\varepsilon\xi^{(1)}\frac{\psi_1(s)}{s} + \cdots\right]. \tag{151}$$

So that:

$$K(t, \xi^{(1)}) = \langle g_0 \rangle K_0(t) + K_L(t, \xi^{(1)});$$

$$K_L(t, \xi^{(1)}) = (\beta\varepsilon\xi^{(1)})K_1(t) + (\beta\varepsilon\xi^{(1)})^2 K_2(t) \cdots, \tag{152}$$

$$K_1(t) = -2\int_{+\cancel{\infty}|t|}^{\infty} g_0(s)\, s\, \gamma_1(s)\, ds,$$

$$K_2(t) = -\int_{+\cancel{\infty}|t|}^{\infty} g_0(s)\, \psi_1(s)\, \gamma_1(s)\, ds. \tag{153}$$

Attention should be drawn to the hard sphere part of the kernel, where $\langle g_0 \rangle$ is independent of $\beta\varepsilon\,\xi^{(1)}$. Thus, this term need not be expanded, while in the Born-Green integral equation, $g^{(1)}$ had to be expressed by a series.

It is possible now to restrict ourselves to $\xi^{(1)} = 1$, the physically occurring potential, so that we can also expand the $g(s)$ in the integral equation (137) in powers of $\beta\varepsilon$ and collect equal powers of $\beta\varepsilon$. The equation for the terms in $(\beta\varepsilon)^0$ reads:

$$\Psi_0(x) = \frac{\lambda_0}{4}\langle g_0\rangle \int_{-\infty}^{\infty} K_0(x-s)\, s\left[g_0(s) - 1\right] ds. \tag{154}$$

This equation was solved in the paper previously published(13) (Appendix D). The terms in $(\beta\varepsilon)'$ combine to give the integral equation:

$$\Psi_1(x) = -x\,\gamma_1(x) + \frac{\lambda_0}{4}\int_{-\infty}^{\infty} K_1(x-s)\, s\left[g_0(s) - 1\right] ds + \tag{155}$$
$$+ \frac{\lambda_0}{4}\langle g_0\rangle \int_{-\infty}^{\infty} K_0(x-s)\, g_0(s)\, \Psi_1(s)\, ds.$$

This equation, as well as the equations for higher powers in $\beta\varepsilon$, is again of the form:

$$\Psi_r(x) = m_r(x) + \frac{\lambda_0}{4}\langle g_0\rangle \int_{-\infty}^{\infty} K_0(x-s)\, g_0(s)\, \Psi_r(s)\, ds, \tag{156}$$

so that the same method of solution as for (59) can be employed.

(155) was solved under the condition that $\lambda_0\langle g_0\rangle = 20$. Ψ_2 and higher terms were not calculated. Actually, in

order to deal with smaller quantities, the difference between the Born-Green and the Kirkwood integral equations was studied. This difference equation is again an integral equation of the same type as (156). The accuracy with which the solution was calculated is that direct iterates of $\psi_1(x)$ agree within ± .003. The results are recorded in Table XIX, and a comparison of the radial distribution functions using only the first two terms in the expansion of $\psi(x)$ is plotted in graph V. This comparison is made at $\beta\varepsilon = .60$ and $\lambda_0 = 10.00$ for the Kirkwood radial distribution function (corresponds to $\lambda = 20$) and $\lambda_0 = 10.28$ for the Born-Green case (corresponds to $\lambda = 27.4$). The agreement is remarkable and would even be better for $\beta\varepsilon = .80$ and 1.00. For still higher $\beta\varepsilon$ and for $\beta\varepsilon$ lower than .60, the agreement is less exact since in the region of $\beta\varepsilon$ between .60 and 1.00 there is a compensation of the $\psi_0(x)$ and $\psi_1(x)$ terms.

The region between $\beta\varepsilon = .60$ and 1.00, however, is the one important to the liquid state. Since the radial distribution functions do not differ greatly there, we can expect close agreement between the two theories in the calculated properties. The confirmation of this is given below in Tables XVII and XVIII where p* and the excess internal energy, respectively, are compared, at almost equal reduced volume.

TABLE XVII

Reduced Pressure

$\beta\varepsilon$	$\lambda_0 = 10.00$ Kirkwood	$\lambda_0 = 10.28$ Born-Green
.6	1.833	2.091
.8	.218	.169
1.0	-.751	-.993

TABLE XVIII

Excess Internal Energy

$\beta\varepsilon$	$\lambda_0 = 10.00$ Kirkwood	$\lambda_0 = 10.28$ Born-Green
.6	5.881	6.181
.8	5.986	6.232
1.0	6.102	6.280

Figure 5. A comparison of the radial distribution functions, correct to Ψ_1 , for the Kirkwood and Born-Green integral equations.

$\lambda_0 = 10.00$ $\beta\varepsilon = .60$ — Kirkwood

$\lambda_0 = 10.28$ $\beta\varepsilon = .60$ ---- Born-Green

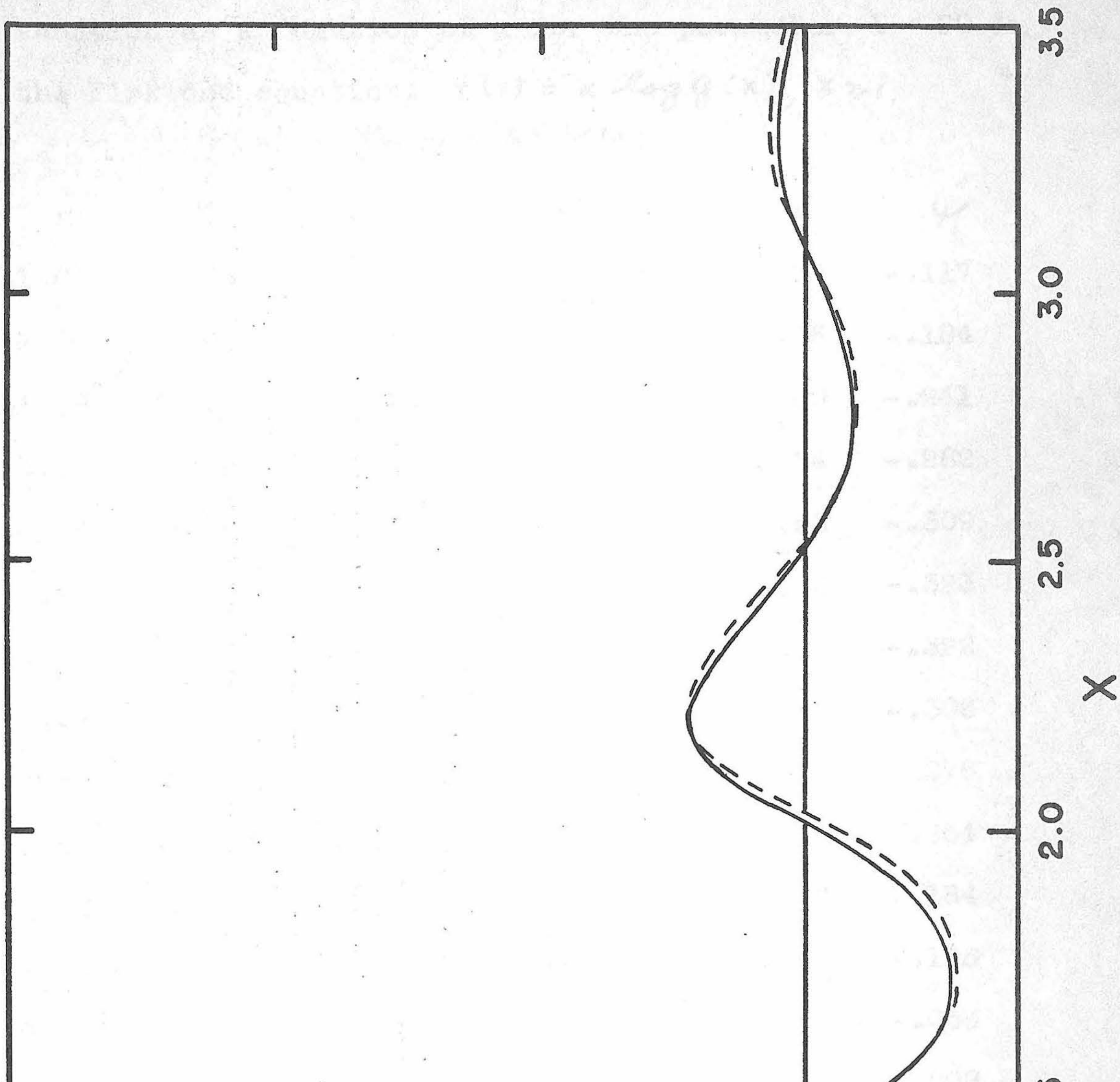
g(x)
2.0
1.5
1.0
.6
X
1.0
1.5
2.0
2.5
3.0
3.5

TABLE XIX

The function ψ_1 which determines the radial distribution function as a function of x for the parameter $\lambda = 20$ in the Kirkwood equation; $\psi(x) = x \log g(x)$, $x \geq 1$.

$$\psi(x) = \psi_0(x) + \beta\varepsilon\,\psi_1(x)$$

x	ψ_1	x	ψ_1	x	ψ_1
1.00	-.788	1.76	-.371	2.52	-.117
1.04	-.091	1.80	-.321	2.56	-.184
1.08	.241	1.84	-.256	2.60	-.241
1.12	.363	1.88	-.181	2.64	-.282
1.16	.374	1.92	-.093	2.68	-.309
1.20	.324	1.96	.008	2.72	-.323
1.24	.242	2.00	.118	2.76	-.322
1.28	.147	2.04	.244	2.80	-.306
1.32	.046	2.08	.356	2.84	-.276
1.36	-.052	2.12	.431	2.88	-.234
1.40	-.141	2.16	.465	2.92	-.184
1.44	-.220	2.20	.465	2.96	-.125
1.48	-.290	2.24	.434	3.00	-.058
1.52	-.345	2.28	.380	3.04	.008
1.56	-.387	2.32	.307	3.08	.071
1.60	-.416	2.36	.223	3.12	.127
1.64	-.428	2.40	.135	3.16	.172
1.68	-.425	2.44	.043	3.20	.206
1.72	-.407	2.48	-.039	3.24	.227

TABLE XIX (cont.)

x	ψ_1	x	ψ_1	x	ψ_1
3.28	.233	4.28	.071	5.28	.004
3.32	.224	4.32	.082	5.32	.012
3.36	.208	4.36	.087	5.36	.018
3.40	.179	4.40	.088	5.40	.023
3.44	.146	4.44	.085	5.44	.026
3.48	.106	4.48	.079	5.48	.028
3.52	.066	4.52	.068	5.52	.028
3.56	.023	4.56	.056	5.56	.028
3.60	-.016	4.60	.040	5.60	.025
3.64	-.055	4.64	.024	5.64	.021
3.68	-.084	4.68	.009	5.68	.019
3.72	-.112	4.72	-.005	5.72	.014
3.76	-.128	4.76	-.020	5.76	.008
3.80	-.139	4.80	-.032	5.80	.002
3.84	-.142	4.84	-.041	5.84	-.002
3.88	-.140	4.88	-.046	5.88	-.006
3.92	-.130	4.92	-.051	5.92	-.009
3.96	-.113	4.96	-.051	5.96	-.011
4.00	-.094	5.00	-.050	6.00	-.013
4.04	-.069	5.04	-.046	6.04	-.014
4.08	-.044	5.08	-.039	6.08	-.016
4.12	-.017	5.12	-.031	6.12	-.014
4.16	.008	5.16	-.022	6.16	-.014
4.20	.032	5.20	-.014	6.20	-.012
4.24	.052	5.24	-.005	6.24	-.010

TABLE XIX (cont.)

x	ψ_1	x	ψ_1	x	ψ_1
6.28	-.008	6.56	.006	6.84	.004
6.32	-.005	6.60	.006	6.88	.002
6.36	-.003	6.64	.006	6.92	.001
6.40	.000	6.68	.006	6.96	.000
6.44	.002	6.72	.005	7.00	-.002
6.48	.003	6.76	.006	7.04	-.004
6.52	.004	6.80	.005		

Appendix D

Reprint of the paper: "Radial Distribution Functions and the Equation of State of a Fluid Composed of Rigid Spherical Molecules", by J. G. Kirkwood, E. K. Maun and B. J. Alder, J. Chem. Phys. 18, 1040, (1950).

Reprinted from THE JOURNAL OF CHEMICAL PHYSICS, Vol. 18, No. 8, 1040–1047, August, 1950
Printed in U. S. A.

Radial Distribution Functions and the Equation of State of a Fluid Composed of Rigid Spherical Molecules*

JOHN G. KIRKWOOD, EUGENE K. MAUN, AND BERNI J. ALDER
Gates and Crellin Laboratories of Chemistry, Pasadena, California

(Received March 20, 1950)

The integral equation for the radial distribution function of a fluid of rigid spherical molecules has been integrated numerically in the Kirkwood approximation and in the Born-Green approximation over a wide range of densities. The distribution functions so obtained have been used to calculate the equation of state and excess entropy of the fluid. The results are compared with those obtained by means of the free volume theory of the liquid state.

I.

IN the statistical-mechanical theory of liquids composed of molecules possessing a potential of intermolecular force of the form,

$$V_N = \sum_{i<k=1}^{N} V(R_{ik}), \tag{1}$$

the average density $\rho^{(2)}(\mathbf{R}_1, \mathbf{R}_2)$ in the configuration space of molecular pairs plays a central role. In the fluid states of aggregation, gas or liquid, it is possible to define a function $g(R_{12})$, called the radial distribution function, by the relation,

$$\begin{aligned} \rho^{(2)} &= [\rho^{(1)}]^2 g(R_{12}), \\ \rho^{(1)} &= N/v, \end{aligned} \tag{2}$$

where the average number density $\rho^{(1)}$ in singlet space is uniform and equal to the reciprocal of the volume per molecule, and R_{12} is the scalar distance in the relative configuration space of a representative molecular pair. As is well known, the radial distribution function may be determined experimentally by the x-ray scattering technique.[1]

The thermodynamic functions of a liquid are related to the potential of intermolecular force $V(R)$ and the radial distribution function by the theories of Kirkwood,[2] Born and Green,[3] Mayer,[4] and Yvon,[5] which are basically equivalent although differing in certain details. The equation of state is given by

$$\frac{pv}{NkT} = 1 - \frac{2\pi N}{3vkT}\int_0^\infty R^3 \frac{dV}{dR} g(R)dR, \tag{3}$$

the internal energy by

$$\frac{E}{NkT} = \frac{3}{2} + \frac{2\pi N}{vkT}\int_0^\infty R^2 V(R) g(R) dR, \tag{4}$$

and the chemical potential by

$$\begin{aligned} \frac{\mu}{NkT} &= \log p + \frac{\mu^E}{NkT} + \frac{\mu^*(T)}{NkT}; \quad \mu^*(T) = \lim_{p\to 0}[\mu - NkT\log p] \\ \mu^E &= \frac{4\pi N^2}{v}\int_0^1\int_0^\infty R^2 V(R) g(R,\xi) dR d\xi \\ &\qquad - NkT \log\frac{pv}{NkT}, \end{aligned} \tag{5}$$

---

* This work was carried out under Task Order XIII of Contract N6onr-244 between the ONR and the California Institute of Technology.

[1] F. Zernike and J. A. Prins, Zeits. f. Physik **41**, 184 (1927); P. Debye and H. Menke, Physik. Zeits. **31**, 797 (1930); B. E. Warren, J. App. Phys. **8**, 645 (1937); A. Eisenstein and N. S. Gingrich, Phys. Rev. **62**, 261 (1942).

[2] J. G. Kirkwood, J. Chem. Phys. **3**, 300 (1935).

[3] M. Born and H. S. Green, Proc. Roy. Soc. **A188**, 10 (1946).

[4] J. E. Mayer, J. Chem. Phys. **15**, 187 (1947).

[5] J. Yvon, *Actualités Scientifiques et Industrielles* (Hermann et Cie, Paris, 1935), p. 203. Because of its relative inaccessibility, the pioneering work of Yvon has been largely overlooked by other investigators.

where $g(R, \xi)$ is the radial distribution function for a pair of molecules, one of which, i, is partially coupled to those of the rest of the fluid, corresponding to a potential of intermolecular force,

$$V_N(\xi)=V_{N-1}+\xi\sum_{k=1}^{N} V(R_{ik}). \tag{6}$$

$\mu^*(T)$ is the ideal gas reference value of the chemical potential, depending on temperature alone.

Systems of integro-differential equations for the average densities in the configuration space of subsets of n molecules of a liquid have been developed in equivalent forms by Kirkwood,[2] Born and Green,[3] Mayer,[4] and Yvon.[5] In general, one has

$$\begin{gathered}\rho^{(n)}=\frac{N!}{(N-n)!}\frac{1}{v^n}e^{-\beta W^{(n)}}\\ \beta=1/(kT),\end{gathered} \tag{7}$$

where $W^{(n)}$ is the potential of average force acting on the molecular subset n, the resultant of their direct interaction and their average interactions with the other $N-n$ molecules of the liquid. When $W^{(3)}(123)$ is approximated by

$$W^{(3)}(123)=W^{(2)}(12)+W^{(2)}(13)+W^{(2)}(23), \tag{8}$$

where 1, 2, 3 denote the coordinates of a molecular triplet, the several sets of integro-differential equations may be closed to give an integral equation for the pair function and thus for the radial distribution function. This approximation, superposition of mean forces between pairs in a set of triplets may be regarded as analogous to the Hartree approximation in quantum mechanics, applied to the density $\rho^{(3)}$ in the space of triplets as the product of the densities $\rho^{(2)}$ for the sets in the space of molecular pairs. As has been shown by one of us,[6] the corresponding Hartree-like approximation in singlet space leads to the free-volume theory of liquids.

The resulting integral equation for the radial distribution function for a pair of molecules, one of which is partially coupled to other molecules of the fluid according to the potential of Eq. (6), takes the form

$$\begin{aligned}\log g(R, \xi)&=-\beta\xi V(R)\\ &+\frac{\pi N}{vR}\int_0^\infty[K(R-r, \xi)-K(R+r, \xi)]r[g(r)-1]dr,\\ K(t, \xi)&=-2\beta\int_0^\xi\int_{|t|}^\infty sV(s)g(s, \xi)dsd\xi;\quad \mathrm{K}\\ K(t, \xi)&=\beta\xi\int_{|t|}^\infty(s^2-t^2)\frac{dV}{ds}g(s, \xi)ds;\quad \mathrm{BGY}\end{aligned} \tag{9}$$

where now as henceforth $g(r)$ denotes $g(r, 1)$, with $\xi=1$. The kernel designated by K refers to the Kirkwood theory and that designated by BGY refers to the Born-Green-Yvon theory. Although the original sets of integro-differential equations in the two theories are exact, the superposition approximation, Eq. (8), leads to the two different kernels of Eq. (9). The numerical discrepancies, reflecting the influence of the superposition approximation are not great and will be discussed later. Since the essentials of the derivation of Eqs. (9) have been given elsewhere[2,3,7] they will not be reproduced here.

The potential of intermolecular force $V(R)$ is conveniently expressed in the form,

$$\begin{gathered}V(R)=\epsilon\gamma(x),\\ x=R/a,\end{gathered} \tag{10}$$

where ϵ is an energy and a is a length characteristic of the molecules. Thus for a Lennard-Jones potential, we have

$$\gamma(x)=(1/x^n)-(1/x^6) \tag{11}$$

where n is an exponent in the neighborhood of 12 and a and ∞ are the two values of R for which $V(R)$ vanishes. For rigid spheres,

$$\begin{aligned}\lim_{\epsilon\to\infty}e^{-\beta\epsilon\gamma(x)}&=0;\quad 0\leqslant x\leqslant 1,\\ &=1;\quad x>1,\end{aligned} \tag{12}$$

where a is the diameter of the spheres. If we define a function $\psi(x)$ by the relation

$$\begin{aligned}g(x, \xi)&=e^{-\beta\xi\epsilon\gamma(x)+[\psi(x, \xi)/x]},\\ g(-x)&=g(x),\\ \gamma(-x)&=\gamma(x),\\ \psi(-x)&=-\psi(x),\end{aligned} \tag{13}$$

and extend the definitions of $g(x)$ and $\gamma(x)$ to the negative real axis by means of the last three of Eqs. (13), the integral equation, Eq. (9), becomes

$$\begin{aligned}\psi(x, \xi)&=\frac{\lambda_0}{4}\int_{-\infty}^\infty K(x-s, \xi)s[g(s)-1]ds\\ \lambda_0&=(4\pi Na^3)/v\\ K(t, \xi)&=-2\beta\epsilon\int_{|t|}^\infty\int_0^\xi s\gamma(s)g(s, \xi)d\xi ds;\quad \mathrm{K}\\ K(t, \xi)&=\xi\beta\epsilon\int_{|t|}^\infty(s^2-t^2)\frac{d\gamma(s)}{ds}g(s, \xi)ds;\quad \mathrm{BGY}.\end{aligned} \tag{14}$$

The solution of Eq. (14) with the Lennard-Jones potential, Eq. (11), by numerical methods with the use of International Business Machine equipment is at present under investigation. Since direct iterative operation on a sequence of trial functions $g(s)$ with the integral

---

[6] J. G. Kirkwood, J. Chem. Phys. **18**, 380 (1950).

[7] J. G. Kirkwood and E. M. Boggs, J. Chem. Phys. **10**, 394 (1942).

operator $\int_{-\infty}^{\infty} dsK(x-s)$ in general fails to give convergent results for values of λ_0 appropriate to liquid densities, other methods are being developed, which depend on starting with a relatively good zero approximation to $g(s)$. In order to obtain a set of trial functions for the zero approximation base, as well as for their intrinsic interest, we have undertaken the integration of Eq. (14) for fluids composed of rigid spheres.

For rigid spheres, Eq. (14) becomes,

$$\begin{aligned} \psi(x) &= \frac{\lambda}{4}\int_{-\infty}^{\infty} K_0(x-s)s[g(s)-1]ds \\ g(s) &= e^{\psi(s)/s} \quad |s|\geqslant 1 \\ &= 0 \quad |s|<1 \\ K_0(t) &= t^2-1 \quad |t|\leqslant 1 \\ &= 0 \quad |t|>1 \end{aligned} \tag{15}$$

where $\psi(x)$ denotes $\psi(x, 1)$. The parameter λ is related to the density in different ways according to the Kirkwood theory and the Born-Green theory (see Appendix).

$$\begin{aligned} [g_1(\lambda)]^{-\frac{1}{2}}\int_0^{\lambda}[g_1(\lambda')]^{-\frac{1}{2}}d\lambda' &= 4\pi\sqrt{2}v_0/v; \quad \mathrm{K} \\ [g_1(\lambda)]^{-1}\lambda &= 4\pi\sqrt{2}(v_0/v); \quad \mathrm{BG} \\ v_0 &= Na^3/\sqrt{2}, \end{aligned} \tag{16}$$

where v_0 is the close-packed volume of the system of spheres and $g_1(\lambda)$ denotes $g(1+\epsilon, \lambda)$ as $\epsilon\rightarrow+0$. The two systems of integro-differential equations underlying the Kirkwood and the Born and Green theories are equivalent and exact. However, the superposition approximation in the space of triplets leads to different equations in the space of pairs. The discrepancy reflected in Eq. (16) is thus a measure of the error produced by this approximation.

Equation (15), linearized with respect to the function $\psi(x)$, assumes the form,

$$\begin{aligned} \psi(x) = \frac{\lambda}{4}\int_{-\infty}^{\infty} K_0(x-s)[A\{|s|-1\}\psi(s) \\ -[1-A\{|s|-1\}]s]ds, \\ A\{t\} = 1 \quad t\geqslant 0, \\ = 0 \quad t<0, \end{aligned} \tag{17}$$

where $A(t)$ is the unit step-function. Equation (17) has been given approximate analytical solutions by Kirkwood and Boggs[7] for several values of λ. The present numerical solutions of the non-linear equation, Eq. (15), cover a wider range of the parameter λ than those of Kirkwood and Boggs. For the same values of λ in the linear approximation, they are found to agree with the analytical solutions for large values of x and to correct the latter in the neighborhood of the first peak of the radial distribution function.

II.

We shall now describe the methods employed in the numerical solution of Eq. (15), which we write in the form

$$\begin{aligned} \psi(x) &= \frac{\lambda}{4}\int_{-\infty}^{\infty} K_0(x-s)\varphi(s)ds \\ \varphi(x) &= x[g(x)-1] \\ g(x) &= A(|x|-1)e^{\psi(x)/x}. \end{aligned} \tag{18}$$

The resolvent kernel $k(t)$ of $K_0(t)$ may be expressed in the form[8]

$$\begin{aligned} k(t) &= -\frac{\lambda}{\pi}\int_0^{\infty}\frac{G(u)}{1-\lambda G(u)}\cos ut du \\ G(u) &= \frac{1}{4}\int_{-\infty}^{\infty}K_0(t)e^{iut}dt = \frac{u\cos u-\sin u}{u^3}. \end{aligned} \tag{19}$$

By the method of Fourier transforms, we obtain from Eq. (18)

$$\begin{aligned} \psi(x) &= -\int_{-\infty}^{\infty}k(x-s)f(s)ds \\ f(x) &= \varphi(x)-\psi(x) \end{aligned} \tag{20}$$

from which $\psi(x)$ may be determined for $x>1$ when $f(x)$ is known. An alternative form of Eq. (20) is

$$f(x) = \varphi(x)+\int_{-\infty}^{\infty}k(x-s)f(s)ds. \tag{21}$$

In the linear approximation,

$$\begin{aligned} &\varphi_0(x) = A\{|x|-1\}\psi_0(x)-[1-A\{|x|-1\}]x \\ &f_0(x) = 0; \quad x>1 \\ &\varphi_0(x) = -x; \quad x\leqslant 1 \end{aligned} \tag{22}$$

and Eqs. (20) and (21) become

$$\begin{aligned} f_0(x) &= -x+\int_{-1}^{+1}k(x-s)f_0(s)ds; \quad x<1 \\ \psi_0(x) &= -\int_{-1}^{+1}k(x-s)f_0(s)ds; \quad x>1. \end{aligned} \tag{23}$$

The first of Eqs. (23) determines $f_0(x)$ and the second determines the linear approximation $\psi_0(x)$ for $x>1$. In this approximation the determination of $g(x)$ thus reduces to the solution of a linear integral equation for $f_0(x)$ on the finite interval $-1<x<+1$, with the resolvent kernel $k(t, \lambda)$.

The resolvent kernel $k(t, \lambda)$ was calculated for a suitable range of the parameter, $\lambda=5$, 10, 20, 27.4, with the use of IBM equipment and the file of punched cards of $\sin ut$ employed in these laboratories for electron

---

[8] E. C. Titchmarsh, *Introduction to the Theory of Fourier Integrals* (Oxford University Press, London, 1948), pp. 303–305.

TABLE I.[a] Radial distribution functions for several values of parameter λ. $x[g(x)-1]$ as a function of x.

$x \backslash \lambda$	5	10	20	27.4	33
1.00	0.45	0.80	1.36	1.66	1.85
1.08	0.39	0.66	1.08	1.36	1.62
1.16	0.32	0.53	0.83	1.04	1.25
1.24	0.26	0.40	0.59	0.73	0.87
1.32	0.20	0.29	0.37	0.44	0.47
1.40	0.15	0.18	0.18	0.16	0.11
1.48	0.09	0.09	0.01	−0.08	−0.19
1.56	0.05	0.01	−0.12	−0.26	−0.41
1.64	0.01	−0.05	−0.22	−0.39	−0.56
1.72	−0.02	−0.10	−0.29	−0.46	−0.64
1.80	−0.04	−0.13	−0.31	−0.48	−0.63
1.88	−0.05	−0.13	−0.28	−0.41	−0.52
1.96	−0.05	−0.10	−0.18	−0.25	−0.29
2.04	−0.03	−0.05	−0.03	0.02	0.10
2.12	−0.02	−0.01	0.09	0.24	0.44
2.20	0.00	0.02	0.16	0.34	0.63
2.28	0.00	0.04	0.18	0.38	0.65
2.36	0.01	0.04	0.17	0.32	0.52
2.44	0.01	0.04	0.13	0.22	0.30
2.52	0.01	0.03	0.07	0.09	0.06
2.60	0.01	0.02	0.01	−0.03	−0.16
2.68	0	0.01	−0.04	−0.13	−0.32
2.76		0.00	−0.07	−0.20	−0.42
2.84		−0.01	−0.09	−0.24	−0.45
2.92		−0.01	−0.09	−0.21	−0.38
3.00		−0.01	−0.07	−0.15	−0.25
3.08		−0.01	−0.04	−0.06	−0.03
3.16		−0.01	0.00	0.03	0.14
3.24		0	0.02	0.09	0.29
3.32			0.04	0.15	0.41
3.40			0.05	0.17	0.36
3.48			0.05	0.14	0.28
3.56			0.04	0.09	0.14
3.64			0.02	0.03	0.00
3.72			0.00	−0.02	−0.12
3.80			−0.01	−0.06	−0.23
3.88			−0.02	−0.10	−0.28
3.96			−0.02	−0.11	−0.26
4.04			−0.02	−0.08	−0.20
4.12			−0.02	−0.05	−0.11
4.20			−0.01	−0.02	0.00
4.28			0.00	0.02	0.11
4.36			0.00	0.04	0.18
4.44			0.01	0.06	0.24
4.52			0.01	0.07	0.22
4.60			0.01	0.06	0.15
4.68			0.01	0.03	0.08
4.76			0.01	0.01	−0.01
4.84			0	−0.01	−0.09
4.92				−0.03	−0.15
5.00				−0.03	−0.19
5.08				−0.03	−0.18
5.16				−0.03	−0.13
5.24				−0.02	−0.06
5.32				0.00	0.01
5.40				0.01	0.07
5.48				0.02	0.12
5.56				0.02	0.16
5.64				0.02	0.14
5.72				0.02	0.10
5.80				0.01	0.05
5.88				0.00	−0.01
5.96				0.00	−0.06
6.04				0.00	−0.10
6.12				0.00	−0.13
6.20				−0.01	−0.12
6.28				−0.01	−0.08
6.36				−0.01	−0.03
6.44				−0.01	0.01
6.52				0	0.05
6.60					0.08
6.68					0.09
6.76					0.08
6.84					0.05
6.92					0.02
7.00					0.00
7.08					−0.02
7.16					−0.07
7.24					−0.07
7.32					−0.06
7.40					−0.05
7.48					−0.02
7.56					0.00
7.64					0.02
7.72					0.03
7.80					0.04
7.88					0.04
7.96					0.03
8.04					0.02
8.12					0.01
8.20					−0.01
8.28					−0.02
8.36					−0.02
8.44					−0.02
8.52					−0.02
8.60					−0.01
8.68					−0.01
8.76					0.00
8.84					0.00
8.92					0.00
9.00					0.01
9.08					0.01
9.16					0.01
9.24					0.01
9.32					0.01
9.40					0.01
9.48					0

[a] The solutions $g(x)$ were checked by direct iteration in Eq. (15) at intervals of 0.04 in x. The input $g(x)$ checked with the output $g(x)$ to ± 0.005 for $\lambda=5$, 10, and 20, and to ± 0.02 for $\lambda=27.4$ and 33.

diffraction calculation.[9] For these calculations it was transformed by partial integration in the following manner,

$$k(t)=-\frac{\lambda}{\pi t}\int_0^\infty \frac{3uG(u)+\sin u}{u^2[1-\lambda G(u)]^2}\sin ut\,du. \tag{24}$$

Convolution operations with the kernel $k(x-s)$ involved in the solution of Eqs. (23) were then carried out on desk calculators.

Since, except for small values of λ, the kernel $k(t)$ possesses one or more eigenvalues less than unity,[10] solution of Eq. (23) by direct iteration fails to give convergent results (see Appendix). In order to overcome this difficulty, $k(t)$ is expressed in the form

$$k(t)=k_0(t)+k_1(t),$$
$$k_0(t)=A_0+A_1\cos\gamma_1 t+A_2\cos\gamma_2 t, \tag{25}$$

where the parameters A_0, A_1, A_2, γ_1, and γ_2 are chosen by trial to give $\int_0^2 k_1(t)^2dt$ a sufficiently small value to raise all of the eigenvalues of $k_1(t)$, which may be shown

---

[9] Shaffer, Schomaker, and Pauling, J. Chem. Phys. 14, 659 (1946).

[10] R. Courant and D. Hilbert, *Methoden der Mathematischen Physik* (Interscience Publishers, Inc., New York), Vol. I, pp. 104–110, 1943.

to be bounded below by $[2\int_0^2(2-t)k_1^2(t)dt]^{-\frac{1}{2}}$, above unity.[10] When this condition is fulfilled, $f_0(x)$ may be represented by the convergent sum

$$f_0(x)=\sum_{n=0}^{\infty} f_{0,n}(x), \tag{26}$$

where

$$f_{0,n}(x)=\sigma_{0,n}(x)+\int_{-1}^{+1} k_0(x-s)f_{0,n}(s)ds,$$

$$\sigma_{0,0}(x)=-x,$$

$$\sigma_{0,n}(x)=\int_{-1}^{+1} k_1(x-s)f_{0,n-1}(s)ds. \tag{27}$$

Since the approximate kernel $k_0(x-s)$ is chosen in degenerate form, the sequence of integral equations, Eq. (27), are solvable in closed form,

$$f_{0,n}(x)=\sigma_{0,n}(x)+2A_1M_{1,n}\sin\gamma_1 x+2A_2M_{2,n}\sin\gamma_2 x,$$

$$M_{1,n}=\int_0^1 f_{0,n}(s)\sin\gamma_1 s ds,$$

$$M_{2,n}=\int_0^1 f_{0,n}(s)\sin\gamma_2 s ds, \tag{28}$$

where the $M_{\alpha,n}$ are to be determined in each case by solving a set of two linear equations, following from their definition and the first of Eqs. (28). Several iterations, the number increasing with increasing values of λ, suffice to determine $f_0(x)$, which upon substitution in Eq. (23) yields the desired solution of the linearized problem.

In the non-linear case, $f(x)$ of Eqs. (20) and (21) no longer vanishes outside the interval $-1\leqslant x\leqslant +1$. Nevertheless, we write Eq. (21) in the form

$$f(x)=\sigma(x)+\int_{-1}^{+1} k(x-s)f(s)ds,$$

$$\sigma(x)=-x+\int_1^{\infty} k(x-s)f(s)ds$$
$$+\int_{-\infty}^{-1} k(x-s)f(s)ds \quad x\leqslant 1, \tag{29}$$

and consider the sequence of integral equations,

$$f_n(x)=\sigma_n(x)+\int_{-1}^{+1} k(x-s)f_n(s)ds \quad x\leqslant 1,$$

$$\sigma_n(x)=-x+\int_1^{\infty} k(x-s)f_{n-1}(s)ds$$
$$+\int_{-\infty}^{-1} k(x-s)f_{n-1}(s)ds,$$

$$f_n(x)=x[e^{[\psi_n(x)/x]}-1]-\psi_n(x) \quad x>1,$$

$$\psi_n(x)=-\int_{-1}^{+1} k(x-s)f_n(s)ds-\int_1^{\infty} k(x-s)f_{n-1}(s)ds$$
$$-\int_{-\infty}^{-1} k(x-s)f_{n-1}(s)ds. \tag{30}$$

Starting with the solution of Eq. (23) as $f_0(x)$ with $\sigma_0(x)=-x$, and solving each of the linear integral equations, Eq. (30), by the method employed in the solution of Eq. (23), we find that the sequence $\psi_n(x)$ converges to the solution $\psi(x)$ of the non-linear integral equation, Eq. (18). All solutions are finally tested by direct iteration with the kernel $K_0(x-s)$ of Eq. (18).

For large values of the parameter λ, convergence is slow by the method of solution described here. However, when a moderately good approximation $\psi^0(x)$ has been obtained by this method, it may be refined by the following iterative procedure. If we linearize Eq. (18) with respect to the error $\omega(x)$, equal to $\psi(x)-\psi^0(x)$, we find,

$$\psi(x)=\psi^0(x)+\omega(x),$$

$$\omega(x)=L\omega+O(\omega^2),$$

$$L\omega=\nu(x)+\frac{\lambda}{4}\int_{-\infty}^{\infty} K_0(x-s)A\{|s|-1\}$$
$$\times\exp\left[\frac{\psi^0(s)}{s}\right]\omega(s)ds$$

$$\nu(x)=\frac{\lambda}{4}\int_{-\infty}^{\infty} K_0(x-s)\varphi^0(s)ds-\psi^0(x) \tag{31}$$

where L is an inhomogeneous linear operator and $\nu(x)$ is the iterative defect of the trial function $\psi^0(x)$. Let us consider the sequence

$$\psi^{(n)}(x)=\psi^{(n-1)}(x)+\omega^{(n)}(x)$$

$$\omega^{(n)}(x)=L^{(n)}\omega^{(n)}$$

$$L^{(n)}\omega^{(n)}=\nu^{(n)}(x)+\frac{\lambda}{4}\int_{-\infty}^{\infty} K_0(x-s)A\{|s|-1\}$$
$$\times\exp\left[\frac{\psi^{(n-1)}(s)}{s}\right]\omega^{(n)}(s)ds$$

$$\nu^{(n)}(x)=\frac{\lambda}{4}\int_{-\infty}^{\infty} K_0(x-s)\varphi^{(n-1)}(s)ds-\psi^{n-1}(x), \tag{32}$$

where $\omega^{(n)}$ exactly satisfies the linear equation, $L^{(n)}\omega^{(n)}=\omega^{(n)}$, and $\psi^0(x)$ is the first member of the sequence $\psi^{(n)}$. We now define a sequence

$$\omega_0^{(n)}=\nu^{(n)}(x),$$

$$\omega_1^{(n)}=L^{(n)}\omega_0^{(n)},$$

$$\omega_2^{(n)}=L^{(n)}\omega_1^{(n)},$$

$$\omega_3^{(n)}=\alpha^{(n)}\omega_1^{(n)}+(1-\alpha^{(n)})\omega_0^{(n)},$$

$$\Delta_{kk'}^{(n)} = \int_{-\infty}^{\infty} \chi_k^{(n)} \chi_{k'}^{(n)} dx; \quad \chi_k^{(n)} = L^{(n)} \omega_k^{(n)} - \omega_k^{(n)}. \quad (33)$$

The value of α which minimizes $\Delta_{33}^{(n)}$ is given by

$$\alpha^{(n)} = (\Delta_{00}^{(n)} - \Delta_{01}^{(n)}) / (\Delta_{11}^{(n)} + \Delta_{00}^{(n)} - 2\Delta_{01}^{(n)})$$

$$\frac{\Delta_{33}^{(n)}}{\Delta_{00}^{(n)}} = 1 - \epsilon^{(n)} \quad \epsilon^{(n)} = \frac{1}{\Delta_{00}^{(n)}} \frac{[\Delta_{00}^{(n)} - \Delta_{01}^{(n)}]^2}{\Delta_{11}^{(n)} + \Delta_{00}^{(n)} - 2\Delta_{01}^{(n)}}. \quad (34)$$

The denominator in the expression for $\epsilon^{(n)}$ is positive by the Schwarz inequality. Thus $\epsilon^{(n)}$ is positive and we have,

$$0 \leqslant \Delta_{33}^{(n)} / \Delta_{11}^{(n)} \leqslant 1. \quad (35)$$

Repetition of this cycle will, except in singular cases, lead to a sequence $\omega_k^{(n)}(x)$ which converges in the mean to the solution $\omega^{(n)}(x)$ of the linear equation, $L^{(n)}\omega^{(n)} = \omega^{(n)}$, of Eq. (32). However, the most economical path to a solution of the non-linear problem is through the sequence

$$\psi_3^{(n)} = \psi_3^{(n-1)} + \omega_3^{(n)}, \quad (36)$$

where $\omega_3^{(n)}$ is given by Eqs. (33) and (34). Except in singular cases $\psi_3^{(n)}$ converges to the solution $\psi(x)$ of the non-linear equation Eq. (18).

III.

The methods described in Section II have been used to calculate $g(x, \lambda)$ for the fluid of rigid spheres for values of the parameter λ equal to 5, 10, 20, 27.4, and 33. The results of the calculations are presented in Table I and Fig. 1. In Fig. 2, the linear and non-linear solutions of Eq. (18) are compared for λ-27.4. It will be observed that they are appreciably different only in the neighborhood of $x=1$. A comparison of the linear solution for $\lambda=27.4$, with the approximate analytical solution of Kirkwood and Boggs,[7] shows the latter to be somewhat inaccurate in the neighborhood of $x=1$.

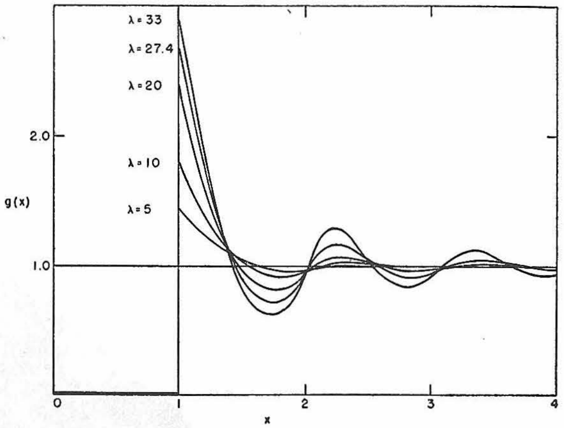

FIG. 1. Radial distribution functions for several values of the parameter λ.

All radial distribution functions exhibit their first peak at $x=1$, decreasing monotonically to the first minimum, which is followed by oscillations of diminishing amplitude resembling those of the experimentally determined radial distribution functions of real liquids.

From the values of $g_1(\lambda)$ obtained from the solutions presented in Table I, the densities corresponding to the family of distribution functions $g(x, \lambda)$ may be determined by means of Eq. (16) according to the Kirkwood theory and according to the Born and Green theory. The densities are presented as a function of λ for the two theories in Table II.

For values of λ equal to or exceeding 34.8, no solutions of Eq. (15) exist for which $x^2[g(x)-1]$ is integrable. This value of λ, corresponding to an expansion v/v_0 equal to 1.24 on the Kirkwood theory and 1.48 on the Born-Green theory evidently represents the limit of stability of a fluid phase of rigid spheres. For greater densities, a crystalline phase is the stable phase.[11] The transition between fluid and crystalline phases cannot be discussed quantitatively without an investigation of distribution functions in the crystalline phase itself. In the case of rigid spheres, it appears likely that the transition may be of second order rather than of first order, although at present this is no more than a surmise. It is also possible that the crystalline phase possesses some intrinsic disorder arising from the inability of rigid spheres to distinguish between next nearest neighbors and the likelihood of stacking errors leading to structures intermediate between the face-centered cubic and the hexagonal close-packed arrangements.

The equation of state, Eq. (3), becomes for rigid spheres,

$$\frac{pv}{NkT} - 1 = \frac{2\pi\sqrt{2}}{3} \frac{v_0}{v} g_1(\lambda), \quad (37)$$

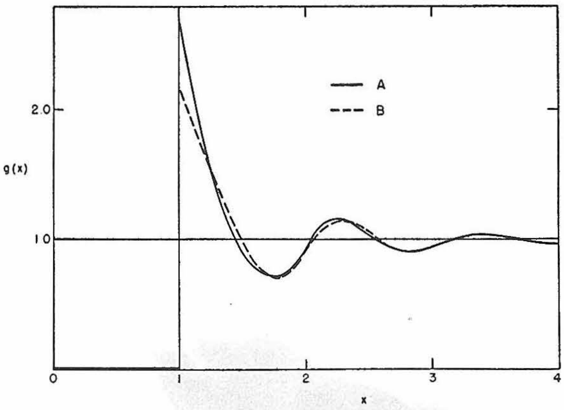

FIG. 2. Radial distribution functions for $\lambda=27.4$. A, solution of non-linear integral equation. B, solution of linear integral equation.

---

[11] J. G. Kirkwood and E. M. Boggs, J. Chem. Phys. 9, 514 (1941).

TABLE II. Fluid densities as function of λ.[a]

λ	$g_1(\lambda)$	v/v_0 (K)	v/v_0 (BG)
5	1.45	4.74	5.15
10	1.80	2.83	3.20
20	2.36	1.78	2.10
27.4	2.66	1.45	1.73
33	2.85	1.29	1.53
34.8	2.90	1.24	1.48

[a] v/v_0 = ratio of volume to close packed volume of spheres.

where $g_1(\lambda)$ is given as a function of density v/v_0 in Table II. In Table III, $pv/RT-1$ is presented as a function of v/v_0 for both the Kirkwood and the Born-Green theories. This function is also plotted in Fig. 3 together with the free volume[12] expression for rigid spheres,

$$\frac{pv}{RT}-1=\frac{1}{(v/v_0)^{\frac{1}{3}}-1}, \tag{38}$$

where v_0 is the close-packed volume of a face-centered cubic lattice rather than that of the simple cubic lattice originally used by Eyring and Hirschfelder.

The excess molal entropy, S^E, of a fluid phase is defined by the relation,

$$S=-R\log p+S^*(T)+S^E$$

$$S^E=\int_0^p\left[\frac{R}{p}-\left(\frac{\partial v}{\partial T}\right)_p\right]dp$$

$$S^*(T)=\lim_{p\to 0}[S+R\log p]. \tag{39}$$

For the fluid of rigid spheres,

$$\frac{S^E}{R}=\frac{-A^E}{RT}=-\frac{\mu^E}{RT}+\left[\frac{pv}{RT}-1\right],$$

$$\frac{S^E}{R}=\frac{2\pi\sqrt{2}}{3}\int_\infty^{v/v_0}\frac{g_1[\lambda(y)]}{y^2}dy+\log\left[1+\frac{2\pi\sqrt{2}}{3}\frac{v_0}{v}g_1\right],$$

$$y=v/v_0, \tag{40}$$

since the excess internal energy E^E vanishes. The excess entropy in the Born-Green approximation has been calculated by numerical integration, with the use of the second of Eqs. (40) and the values of $g_1(\lambda)$ as a function of v/v_0 presented in Table II. In the Kirkwood approximation, Eq. (5) and the first of Eqs. (40) yield the expression,

$$\frac{S^E}{R}=-\frac{\lambda}{3}+\frac{2\pi\sqrt{2}}{3}\frac{v_0}{v}g_1+\log\left[1+\frac{2\pi\sqrt{2}}{3}\frac{v_0}{v}g_1\right], \tag{41}$$

from which the excess entropy has been calculated with the aid of the data of Table II. The results of the two calculations are presented in Table IV.

It will be remarked that the agreement between the Kirkwood and the Born-Green approximations is moderately good both for the equation of state and for the entropy. In the case of the equation of state, the free volume theory yields a result which does not deviate greatly from either the Kirkwood or the Born-Green results, the departures becoming smaller as the density increases toward close-packing.

APPENDIX

1. The relation between the density Na^3/v and the parameter λ may be derived for the Kirkwood theory with the following thermodynamic equation, the equation of state, Eq. (37), and the expression for the chemical potential Eq. (34c) given by Kirkwood and Boggs,[7]

$$\frac{1}{RT}\left(\frac{\partial\mu}{\partial v}\right)_T=\frac{v}{RT}\left(\frac{\partial p}{\partial v}\right)_T, \tag{42}$$

$$\frac{\mu}{RT}=-\log v+\frac{\lambda}{3}+\frac{\mu^*(T)}{RT} \tag{34c}$$

$$\frac{p}{RT}=\frac{1}{v}+\frac{2\pi\sqrt{2}}{3}\frac{v_0}{v^2}g_1(\lambda), \tag{37}$$

where $g_1(\lambda)$ is $g(1+\epsilon)$ as $\epsilon\to+0$. By differentiating the last two equations with respect to v and equating their derivatives by the first expression, we get

$$-\frac{1}{v}+\frac{1}{3}\frac{d\lambda}{dv}=-\frac{1}{v}+\frac{2\pi\sqrt{2}}{3}v_0v\left[\frac{d}{dv}\left(\frac{g_1(\lambda)}{v^2}\right)\right]; \tag{43}$$

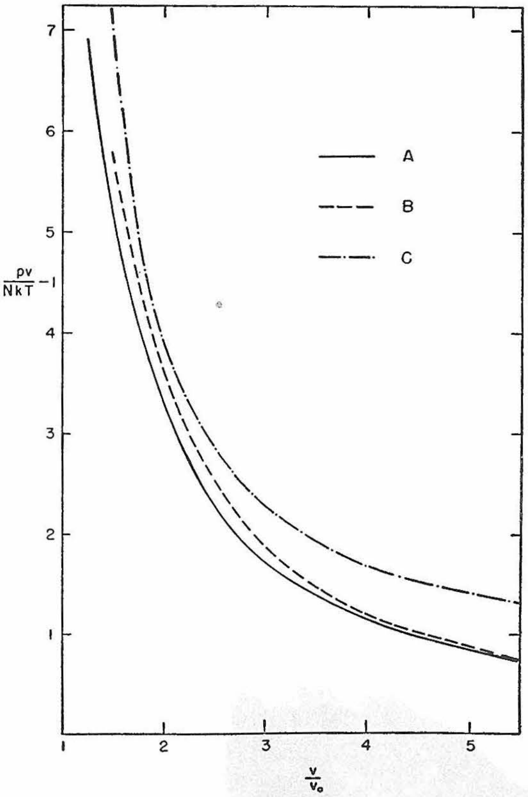

FIG. 3. Equation of state: $pv/RT-1$ as function of v/v_0. A, Kirkwood basis. B, Born and Green, C, free-volume theory. v = volume per mole, v_0 = volume per mole in close-packed arrangement.

---

[12] H. Eyring and J. O. Hirschfelder, J. Phys. Chem. 41, 249 (1937).

TABLE III. Equation of state of the fluid of rigid spheres.

v/v_0[a]	$pv/RT-1$ (K)	$pv/RT-1$ (BG)
8.38	0.44	0.44
4.74	0.91	0.93
3.48	1.39	1.46
2.83	1.89	2.04
2.42	2.40	2.65
2.15	2.91	3.21
1.94	3.43	3.75
1.78	3.93	4.33
1.64	4.44	4.96
1.53	4.95	5.54
1.44	5.46	
1.37	5.99	
1.30	6.50	
1.24	6.93	

[a] For values of the Kirkwood parameter $\lambda=2.5, 5.0, \cdots$, except for the last point, $\lambda=34.8$.

TABLE IV. Excess entropy of the fluid of rigid spheres as a function of density.

v/v_0	S^E/R (K)	S^E/R (BG)
8.38	−0.03	−0.03
4.74	−0.12	−0.11
3.48	−0.24	−0.23
2.83	−0.39	−0.37
2.42	−0.55	−0.56
2.15	−0.73	−0.76
1.94	−0.92	−1.00
1.78	−1.14	−1.23
1.64	−1.37	−1.49
1.53	−1.60	−1.77
1.44	−1.84	
1.37	−2.07	
1.30	−2.32	
1.24	−2.60	

hence, introducing $z=v/[g_1(\lambda)]^{\frac{1}{3}}$,

$$\frac{d\lambda}{[g_1(\lambda)]^{\frac{1}{3}}}=-4\pi Na^3\frac{dz}{z^2};\quad Na^3=\sqrt{2}v_0, \tag{44}$$

and integration with the limits (λ, v) and $(\lambda=0, v=\infty)$ yields Eq. (16, K).

2. The divergence of a direct iteration attempt to solve Eq. (23) may be seen by considering

$$f(x)=\sigma(x)+\int_a^b k(x,s)f(s)ds,$$

$$f^{(n)}(x)=\sigma(x)+\int_a^b k(x,s)f^{(n-1)}(s)ds; \tag{45}$$

hence, by subtraction,

$$\Delta f^{(n)}=f-f^{(n)}=\int_a^b k(x,s)\Delta f^{(n-1)}(s)ds, \tag{46}$$

where $f(x)$ is the exact solution of the linear integral equation whose inhomogeneous part is $\sigma(x)$, $f^{(n-1)}(x)$ is a trial solution, and $f^{(n)}(x)$ the iterate of the trial solution. Using a representation for the real symmetric kernel $k(x, s)$ in terms of its orthonormal set of eigenfunctions χ_i and its eigenvalues λ_i, and expanding $\Delta f^{(n-1)}$ in the form,

$$k(x,s)=\Sigma_i\frac{\chi_i(x)\chi_i(s)}{\lambda_i},$$

$$\Delta f^{(n-1)}(s)=\Sigma_j a_j^{(n-1)}\chi_j(s), \tag{47}$$

leads by substitution into Eq. (46) to

$$\Delta f^{(n)}(x)=\Sigma_j\frac{a_j^{(n-1)}\chi_j(x)}{\lambda_j}=\Sigma_j a_j^{(n)}\chi_j(x),$$

$$a_j^{(n)}=\frac{a_j^{(n-1)}}{\lambda_j}. \tag{48}$$

Thus $a_j^{(n-1)}$ is increased by $1/\lambda_j$ after each iteration, hence divergence occurs if for any $|\lambda_j|<1$ $a_j^{(n-1)}\neq 0$, because then

$$\left|\frac{a_j^{(n)}}{a_j^{(n-1)}}\right|>1$$

and $\Delta f^{(n)}$ increases in magnitude with each iteration.

Appendix E

Inte-rpolation Formulae

The empirical equation of state valid for $\lambda \geq 5$ which results from the radial distribution function correct to Ψ_2 :

(A) With linear isometrics, $p^* = aT^* + b$

$$a = \frac{.101306}{v^*} + \frac{11.025}{v^{*2}} - \frac{27.447}{v^{*3}} + \frac{45.691}{v^{*4}} - \frac{22.484}{v^{*5}} \qquad (157)$$

$$b = -\frac{7.0393}{v^{*2}} + \frac{5.2986}{v^{*3}} - \frac{19.285}{v^{*4}} + \frac{15.861}{v^{*5}} .$$

(B) With quadratic isometrics, $p^* = aT^{*2} + bT^* + c$

$$a = -\frac{.1892}{v^{*2}} - \frac{.2788}{v^{*3}} + \frac{.6806}{v^{*4}} - \frac{.3716}{v^{*6}}$$

$$b = \frac{.1013}{v^*} + \frac{11.1551}{v^{*2}} - \frac{21.9676}{v^{*3}} + \frac{27.4701}{v^{*4}} - \frac{9.6530}{v^{*6}} \qquad (158)$$

$$c = -\frac{8.0782}{v^{*2}} + \frac{2.7487}{v^{*3}} - \frac{7.3144}{v^{*4}} + \frac{4.0070}{v^{*6}} .$$

The following equation of state is valid for $\lambda \leq 5$ and for $.60 \leq \beta\varepsilon \leq 1.0$:

$$p^* = \frac{T^*}{v^*} + \frac{b}{v^{*2}} + \frac{c}{v^{*3}} + \frac{d}{v^{*4}} \qquad (159)$$

$$b = -18.403T^* + 18.190\, T^{*2} - 4.937\, T^{*3}$$

$$c = -41.925 + 61.449\, T^* - 20.295\, T^{*2}$$

$$d = 182.536 - 251.766T^* + 84.665\, T^{*2}.$$

The excess internal energy fitted empirically as a function of volume and temperature :

$$\frac{E^E}{N\varepsilon} = e_0 + e_1(\beta\varepsilon) + e_2(\beta\varepsilon)^2 \qquad (160)$$

$$e_0 = -.44710\,\lambda_0 - .017277\,\lambda_0^2 + .0005912\,\lambda_0^3 - .0000197\,\lambda_0^4$$

$$e_1 = -.12393 - .064711\,\lambda_0 + .011858\,\lambda_0^2 - .0007322\,\lambda_0^3$$

$$e_2 = .21407 - .62844\,\lambda_0^{\frac{1}{2}} + .24619\,\lambda_0 - .006406\,\lambda_0^2 .$$

The equation of state valid for $\lambda \leq 5$ and for $\beta\varepsilon \leq 0.40$:

$$p^* = \frac{T^*}{v^*} + \frac{a}{v^{*2}} + \frac{b}{v^{*3}} \tag{161}$$

$$a = 2.212\,T^* - 6.442$$

$$b = 3.177\,T^* - 2.520 .$$

REFERENCES

1. J. G. Kirkwood, J. Chem. Phys. 3, 300, (1935).
2. M. Born and H. S. Green, Proc. Roy. Soc., A 188, 10 (1946).
3. J. E. Mayer, J. Chem. Phys. 15, 187, (1947).
4. J. Yvon, Actualités Scientifiques et Industrielles (Hermann et Cie., Paris, 1935), vol. 203.
5. J. E. Lennard-Jones, Physica, 4, 941 (1937).
6. J. G. Kirkwood, J. Chem. Phys., 14, 180 (1946).
7. J. G. Kirkwood, F.P. Buff, and M. S. Green, J. Chem. Phys. 17, 988 (1949).
8. P. Debye and H. Mencke, Phys. Zeit., 31, 797 (1930).
9. F. Zernicke and J. A. Prins, Zeit. f. Physik, 41, 184 (1927).
10. B. E. Warren, J. App. Phys., 8, 645 (1937).
11. A. Eisenstein and N. S. Gingrich, Phys. Rev., 62, 261 (1942).
12. J. G. Kirkwood, J. Chem. Phys., 18, 380, (1950).
13. J. G. Kirkwood, E. K. Maun, and B. J. Alder, J. Chem. Phys., 18, 1040 (1950).
14. International Critical Tables (MacGraw-Hill Book Co., New York, 1928), Vol. III, p. 203.
15. R. B. Bird, E. L. Spotz and J. O. Hirschfelder, J. Chem. Phys., 18, 1395 (1950).
16. A. Michels, H. Wijker, and H. Wijker, Physica, 15, 627 (1949).
17. A. Michels, R. J. Lunbeck and G. J. Wolkers, Physica, 15, 689 (1949).
18. J. G. Kirkwood and E. M. Boggs, J. Chem. Phys., 10, 394 (1942).

PART II

A STATISTICAL MECHANICAL THEORY OF THE COEFFICIENT OF THERMAL CONDUCTIVITY OF MONATOMIC LIQUIDS

A STATISTICAL MECHANICAL THEORY OF THE COEFFICIENT OF THERMAL CONDUCTIVITY OF MONATOMIC LIQUIDS

INTRODUCTION

The general objective of statistical mechanics is to express macroscopic properties in terms of molecular variables. With this aim in mind for the coefficient of heat conductivity, a procedure very much like the one for the coefficient of viscosity$^{(1)}$ may be followed. The equations of hydrodynamics provide the phenomenological relations for the desired transport process. These are: the equation of continuity,

$$\nabla \cdot (\rho \vec{u}) + \frac{\partial \rho}{\partial t} = 0 \; ; \tag{1}$$

the equation of motion,

$$\rho \frac{\partial \vec{u}}{\partial t} = \vec{X} + \nabla \cdot \underset{\sim}{\sigma} \; ; \tag{2}$$

and in addition the equation of energy transport which contains the heat current density, $\vec{q}$, explicitly:

$$\frac{\partial E}{\partial t} + \nabla \cdot \left[E\vec{u} + \vec{q} - \vec{u} \cdot \underset{\sim}{\sigma} \right] = 0 , \tag{3}$$

where ρ is the density, $\vec{u}$ is the particle velocity, $\vec{X}$ is the external force, $\underset{\sim}{\sigma}$ is the stress tensor, and E is the internal energy density. Finally a supplementary relation defines the thermal conductivity, $\varkappa$, as the proportionality factor between the heat current density and the temperature gradient:

$$\vec{q} = -\varkappa \nabla T. \tag{3a}$$

These hydrodynamic equations have been derived by means of classical statistical mechanics and the proper terms have been put into correspondence$^{(2)}$ so that expressions result for the heat current density and the stress tensor, in terms of molecular variables, which are the molecular distribution function and the intermolecular force. Just as in the formula for the stress tensor, two types of terms arise in the one for the heat current density. One of these is due to momentum transport and corresponds to the familiar expression in the kinetic theory of gases. The other term, contributed by the intermolecular forces, is expressed as a quadrature of the potential of intermolecular force and of the density and current density in the configuration space of pairs of molecules.

The probability densities involved in the expressions for the density and current density are, however, perturbed from their equilibrium value due to hydrodynamic flow resulting from the temperature gradient. One would have to solve the Liouville equation after integrating it over the phase space of N-n molecules in a system of N molecules and after time smoothing in order to obtain an explicit expression for the probability density in n-space. This problem, however, is not unlike the one which presents itself in the solution for the equilibrium distribution function where a chain of integro-differential equations has to be solved, each of which relates a probability density in a given space to the one in the next higher space. This chain was broken there by the so called superposition approximation(3), a generalization of which has been introduced in the present case by Born and Green(4) to accomplish the same end. Alternate steps taken to close the set of equations are those explained in SMT I(5) where the theory of Brownian motion is utilized to get the differential equation for the probability distribution function in the phase space of sets of one, two, and three molecules of the liquid. The Born and Green approach differs from Kirkwood's only in the representation of the dissipative mechanism which in the latter case is essentially contained in the phenomenological friction constant. This friction constant enters explicitly since the Langevin equation of motion has to be brought in to describe the movements of a Brownian particle in an environment in statistical equilibrium. The Langevin equation however has been derived through statistical mechanics and thereby an expression for the friction constant results. It has not as yet been possible to calculate accurately the value of the constant.

To close the set of equations for the probability density therefore Kirkwood assumes local statistical equilibrium in order to introduce the above Brownian motion theory. The resulting differential equation, which is a generalization of the Fokker-Planck equation, then allows the construction of the perturbed probability density to be substituted in the expression for the heat current density. The probability density is the steady state solution with the proper boundary conditions where only linear terms in the gradient of the temperature will be kept in the differential equations.

GENERAL PRELIMINARIES

In statistical mechanics, macroscopic observables are set into correspondence with average values determined by probability densities $\bar{f}^{(n)}(\vec{p},\vec{q};t)$ in the phase space $(\vec{p},\vec{q})$ of a subset of n molecules in a system of N molecules. Here

$$\bar{f}^{(n)}(\vec{p},\vec{q};t) = \iint \bar{f}^{(N)}(\vec{p},\vec{q},\vec{P},\vec{Q};t)\,d\vec{P}\,d\vec{Q}, \tag{4}$$

and

$$\bar{f}^{(N)}(\vec{p},\vec{q},\vec{P},\vec{Q};t) = \frac{1}{\mathcal{T}}\int_0^{\mathcal{T}} f^{(N)}(\vec{p},\vec{q},\vec{P},\vec{Q};t+s)\,ds; \tag{5}$$

$(\vec{P},\vec{Q})$ is the phase space of the N-n remaining molecules. The time smoothing interval $\mathcal{T}$ is determined by the process of measurement; that is, $\mathcal{T}$ should be long relative to the microscopic fluctuations but short compared to the macroscopic time resolution, so that observables in the liquid effectively do not depend on $\mathcal{T}$. For the representation of average values of functions of the configuration coordinates ($\vec{q}$) only, the number density $\rho^{(n)}(\vec{q};t)$ is convenient:

$$\rho^{(n)}(\vec{q};t) = \frac{N!}{(N-n)!}\int \bar{f}^{(n)}(\vec{p},\vec{q};t)\,d\vec{p}. \tag{6}$$

In the singlet configuration space, ($\vec{r}$), this expression reduces to the ordinary mass density, $\rho(\vec{r};t)$, and occurs in the current density, $\vec{j}^{(1)}(\vec{r};t)$, of the macroscopic equations of hydrodynamics:

$$\rho(\vec{r};t) = m\,\rho^{(1)}(\vec{r};t) = m\,N\int \bar{f}^{(1)}(\vec{r},\vec{p};t)\,d\vec{p} \tag{7}$$

$$\vec{j}^{(1)}(\vec{r};t) = \vec{u}\,\rho^{(1)}(\vec{r};t) = N\int \frac{\vec{p}}{m}\,\bar{f}^{(1)}(\vec{r},\vec{p};t)\,d\vec{p}, \tag{8}$$

where m is the mass of the molecules. Similarly, $\rho^{(2)}(\vec{R}_1,\vec{R}_2;t)$, the pair density, and $\vec{j}_1^{(2)}(\vec{R}_1,\vec{R}_2;t)$, the particle current density in pair space projected on the singlet space of molecule 1, are given in the configuration space $(\vec{R}_1,\vec{R}_2)$ by:

$$\rho^{(2)}(\vec{R}_1,\vec{R}_2;t) = N^2\iint \bar{f}^{(2)}(\vec{R}_1,\vec{R}_2,\vec{p}_1,\vec{p}_2;t)\,d\vec{p}_1\,d\vec{p}_2 \tag{8a}$$

$$\vec{j}_1^{(2)}(\vec{R}_1,\vec{R}_2;t) = N^2\iint \frac{\vec{p}_1}{m}\,\bar{f}^{(2)}(\vec{R}_1,\vec{R}_2,\vec{p}_1,\vec{p}_2;t)\,d\vec{p}_1\,d\vec{p}_2. \tag{9}$$

In a system of molecules for which the intermolecular potential V_N can be represented in the form

$$V_N = \sum_{\substack{i<k\\=1}}^{N} V(R_{ik}) \tag{10}$$

where V (R) is a fuction of the distance R_{ik} between the ith and kth molecules, this pair number density plays a particularly important role. However, it is more convenient to deal with the pair correlation function $g^{(2)}(\vec{r},\vec{R};t)$

defined, for a fluid with identical particles, by

$$\rho^{(2)}(\vec{R}_1, \vec{R}_2; t) = \rho^{(2)}(\vec{r}, \vec{r}+\vec{R}; t) = \rho^{(1)}(\vec{R}_1; t)\,\rho^{(1)}(\vec{R}_2; t)\, g^{(2)}(\vec{r}, \vec{R}; t). \tag{11}$$

In the bulk liquid this function, $g^{(2)}(\vec{r},\vec{R};t)$, is insensitive to $\vec{r}$, the macroscopic location, but sensitive to $\vec{R} = \vec{R}_2 - \vec{R}_1 = \vec{R}_{12}$, the relative coordinate between molecules. Now a liquid with a potential of the form (10) has, at equilibrium and in the absence of external forces, a correlation function $g_0^{(2)}(\vec{R})$.

$$g_0^{(2)}(\vec{R}) = \exp.\left\{-\frac{1}{kT}\left[W^{(2)}(\vec{R}) - W_1^{(1)} - W_2^{(1)}\right]\right\}, \tag{12}$$

where $W^{(2)}(\vec{R})$ and $W^{(1)}$ are the potentials of mean force in pair and singlet space. As has been shown in part I of this thesis, $g_0^{(2)}(\vec{R})$ is a solution of an integral equation. The negative gradient with respect to molecule one, for example, of the potential of mean force is then the equilibrium average force on molecule one in a set of n molecules, $\overset{\circ}{\langle} \vec{F}_1 \rangle^{(n)}$;

$$\overset{\circ}{\langle} \vec{F}_1 \rangle^{(2)} = -\nabla_{\vec{R}_1} W^{(2)}(\vec{R}). \tag{13}$$

Therefore, taking the logarithmic gradient of (12) with respect to molecules one and two results in:

$$ {}^{\circ}\langle \vec{F}_1 \rangle^{(2)} - {}^{\circ}\langle \vec{F}_1 \rangle^{(1)} = kT \nabla_{\vec{R}_1} \log g_0^{(2)}(\vec{R}) \tag{14} $$

$$ {}^{\circ}\langle \vec{F}_2 \rangle^{(2)} - {}^{\circ}\langle \vec{F}_2 \rangle^{(1)} = kT \nabla_{\vec{R}_2} \log g_0^{(2)}(\vec{R}). \tag{15} $$

The time dependent distribution functions, as was pointed out, satisfy partial differential equations of the type derived by Chandrasekhar on the basis of the phenomenological theory of Brownian motion. For the momentum part of the heat current density of a liquid in a steady state under a temperature gradient, only the singlet equation for $\bar{f}^{(1)}(\vec{r}, \vec{p}; t)$ is necessary:

$$ \frac{\partial \bar{f}^{(1)}}{\partial t} + \frac{\vec{P}}{m} \cdot \nabla_{\vec{R}} \bar{f}^{(1)} + \nabla_{\vec{P}} \cdot \vec{F}^{(1)} \bar{f}^{(1)} = \xi \nabla_{\vec{P}} \cdot \left[\vec{\pi} \bar{f}^{(1)} + kT \nabla_{\vec{P}} \bar{f}^{(1)} \right], \tag{16} $$

where $\vec{\pi} = \frac{\vec{P}}{m} - \vec{u}$, $\vec{F}^{(1)} = {}^{\circ}\langle \vec{F} \rangle^{(1)} + \vec{F}^{+}$, and ξ is the friction constant. $\vec{F}^{+}$ is the perturb~~at~~ing force on a molecule situated at $\vec{R}$. For the intermolecular force contribution to the heat current density, the pair equation for $\bar{f}^{(2)}(\vec{P}_1, \vec{R}_1, \vec{P}_2, \vec{R}_2; t)$ has to be employed:

$$ \frac{\partial \bar{f}^{(2)}}{\partial t} + \frac{\vec{P}_1}{m} \cdot \nabla_{\vec{R}_1} \bar{f}^{(2)} + \frac{\vec{P}_2}{m} \cdot \nabla_{\vec{R}_2} \bar{f}^{(2)} + \nabla_{\vec{P}_1} \cdot \vec{F}_1^{(2)} \bar{f}^{(2)} + \nabla_{\vec{P}_2} \cdot \vec{F}_2^{(2)} \bar{f}^{(2)} = $$

$$ \nabla_{\vec{P}_1} \cdot \underset{\sim}{\vec{\xi}_1}^{(2)} \cdot \left[\vec{\pi}_1 \bar{f}^{(2)} + kT \nabla_{\vec{P}_1} \bar{f}^{(2)} \right] + \nabla_{\vec{P}_2} \cdot \underset{\sim}{\vec{\xi}_2}^{(2)} \cdot \left[\vec{\pi}_2 \bar{f}^{(2)} + kT \nabla_{\vec{P}_2} \bar{f}^{(2)} \right], \tag{17} $$

where $\underset{\sim}{\xi}^{(2)}$ is a friction tensor in the six dimensional space of pairs, $\vec{F}_1^{(2)} = \langle \vec{F}_1 \rangle^{(2)} + \vec{F}_1^{(2)\dagger}$, and $\vec{F}_1^{(2)\dagger}$ is the perturb~~at~~ing force acting on molecule 1 of the fixed pair 1 and 2. Due to the potential (10) assumed, only the probability densities in the phase space of singlet and pair molecules are significant.

The solutions of these differential equations for the probability densities have to be substituted into the equation for the heat current densities obtained through the statistical mechanical theory of the equations of hydrodynamics. The procedure in the derivation of the macroscopic equations of hydrodynamics is to utilize the statistical mechanical expressions for ρ, $\vec{j}$, and for all the other quantities which have obvious statistical mechanical analogues. The time derivative of these quantities can also be calculated through statistical mechanics by means of the Liouville equation. The equation of continuity (1) then falls out immediately by expressing the conservation of particles in terms of these expressions. In the equation of motion (2), obvious statistical mechanical expressions are available for all terms except the stress tensor. The correspondence here is obtained by difference after the remaining term has been changed into the form of the gradient of a quantity to be identified with the stress tensor. In a similar fashion, the heat current density, in terms of microscopic variables for a single component, single phase system with a potential of the type (10) can be formed from the energy transport Eq. (3). Let us write

$$\vec{q} = \vec{q}_K + \vec{q}_v \tag{18}$$

Here,

$$\vec{q}_K(\vec{r};t) = N\int d\vec{p}\,\frac{m}{2}\left|\frac{\vec{p}}{m}-\vec{u}\right|^2\left[\frac{\vec{p}}{m}-\vec{u}\right]\bar{f}^{(1)}(\vec{p},\vec{r};t); \tag{19}$$

$\vec{q}_K$ can easily be seen to represent the transport of thermal kinetic energy. The expression can be simplified by substituting $\vec{\pi}$ for $\left[\frac{\vec{p}}{m}-\vec{u}\right]$:

$$\vec{q}_K = \frac{Nm}{2}\int d\vec{p}\,|\vec{\pi}|^2\,\vec{\pi}\,\bar{f}^{(1)}. \tag{20}$$

Also*,

$$\vec{q}_v(r;t) = \frac{1}{2}\int\left[V(R)\underset{\sim}{1} - \frac{\vec{R}\vec{R}}{R}V'(R)\right]\cdot \left[\vec{j}_1^{(2)}(\vec{r},\vec{r}+\vec{R};t) - \vec{u}(\vec{r};t)\rho^{(2)}(\vec{r},\vec{r}+\vec{R};t)\right]d\vec{R}. \tag{21}$$

The expression for $\vec{q}_v$ is interpreted physically by noting that the term involving $V(R)$ represents the current density of potential energy due to macroscopically imperceptible random motion, whereas the term involving $V'(R)$ is connected with the work that has to be done for this random motion to occur. It is the term $\vec{q}_v$ which is dominant in liquids.

---

* Gradients with respect to $\vec{r}$ have been neglected in (21) since the quantities involved, $\rho^{(2)}$ and $\vec{j}_1^{(2)}$ are relatively slow functions of this variable.

MOMENTUM CONTRIBUTION TO THE HEAT CURRENT DENSITY

The momentum contribution to the heat current density, $\vec{q}_K$, will be evaluated by multiplying the $\bar{f}^{(1)}$ Fokker-Planck equation (16) by $|\vec{\pi}|^2\vec{\pi}$ and integrating over momentum space, according to (20). However, to interpret the rest of the terms of the integrated Fokker-Planck equation, we need the relations in which (16) is multiplied by $\underset{\sim}{1}$ and $\vec{p}$ and then integrated over momentum space.

So let us first integrate (16) over momentum space. Here, as henceforth, we will frequently use Green's theorem in both configuration space and momentum space. Whenever Green's theorem is used, the integrated part will vanish, since the probability distribution functions fall off sufficiently rapidly for large momenta or distances. Thus, only the first two terms of (16) remain upon integration over momentum space:

$$\frac{\partial \rho^{(1)}}{\partial t} + \nabla_{\vec{R}} \cdot \bar{j}^{(1)} = 0. \qquad (22)$$

This is the equation of continuity where the definitions (7) and (8) have been introduced.

Multiplication of (16) by $\frac{\bar{P}}{m}$ and integration over $\vec{p}$ yields the following equation:

$$\frac{\partial \bar{j}^{(1)}}{N\partial t} + \nabla_{\vec{R}} \cdot \int d\vec{p}\, \frac{\bar{P}}{m}\frac{\bar{P}}{m}\bar{f}^{(1)} - \frac{\vec{F}^{(1)}\rho^{(1)}}{Nm} = 0. \qquad (23)$$

The right hand side vanishes because subsequent to the use of Green's theorem the identity

$$\int d\vec{p}\left[\frac{\vec{P}}{m}-\vec{u}\right]\bar{f}^{(1)}=\int d\vec{p}\;\vec{\pi}\,\bar{f}^{(1)}=0 \tag{24}$$

occurs. (See (7) and (8)). The second term in (23) can be rewritten in terms of macroscopic variables so that an expression for $\vec{F}^{(1)}$ results. Consider the following identity:

$$\begin{aligned}\int d\vec{p}\left[\frac{\vec{P}}{m}-\vec{u}\right]\left[\frac{\vec{P}}{m}-\vec{u}\right]\bar{f}^{(1)}&=\int d\vec{p}\,\frac{\vec{P}}{m}\frac{\vec{P}}{m}\bar{f}^{(1)}-\int d\vec{p}\,\frac{\vec{P}}{m}\vec{u}\,\bar{f}^{(1)}\\&\quad-\int d\vec{p}\;\vec{u}\,\frac{\vec{P}}{m}\bar{f}^{(1)}+\int d\vec{p}\;\vec{u}\,\vec{u}\,\bar{f}^{(1)}.\end{aligned} \tag{25}$$

By (7) and (8) the last three terms can be combined. Furthermore, $(\frac{m}{2})$ times the left hand side is approximated as the kinetic energy density in one degree of freedom; that is,

$$\frac{m}{2}\int d\vec{p}\left[\frac{\vec{P}}{m}-\vec{u}\right]\left[\frac{\vec{P}}{m}-\vec{u}\right]\bar{f}^{(1)}=\frac{kT\rho^{(1)}}{2N}\,\underset{\sim}{1}. \tag{26}$$

The total kinetic energy density is then:

$$\frac{m}{2}\int d\vec{p}\left|\frac{\vec{P}}{m}-\vec{u}\right|^{2}\bar{f}^{(1)}=\frac{3kT\rho^{(1)}}{2N}. \tag{27}$$

Thus (25) becomes

$$\frac{2}{m}\,\frac{kT\rho^{(1)}}{2N}\,\underset{\sim}{1}=\int d\vec{p}\,\frac{\vec{P}}{m}\frac{\vec{P}}{m}\bar{f}^{(1)}-\frac{\vec{u}\,\vec{u}\,\rho^{(1)}}{N}, \tag{28}$$

which, when substituted into (23), yields

$$\frac{\partial\vec{j}^{(1)}}{\partial t}+\frac{\nabla_{\vec{R}}\cdot\left[kT\rho^{(1)}\,\underset{\sim}{1}\right]}{m}+\nabla_{\vec{R}}\cdot\left[\vec{u}\,\vec{u}\,\rho^{(1)}\right]-\frac{\vec{F}^{(1)}\rho^{(1)}}{m}=0. \tag{29}$$

Now, using (8) and then (22),

$$\begin{aligned}\frac{\partial\vec{j}^{(1)}}{\partial t}+\nabla_{\vec{R}}\cdot\left[\vec{u}\,\vec{u}\,\rho^{(1)}\right]&=\frac{\partial\left[\rho^{(1)}\vec{u}\right]}{\partial t}+\vec{u}\,\nabla_{\vec{R}}\cdot\left[\rho^{(1)}\vec{u}\right]\\&\quad+\rho^{(1)}\vec{u}\cdot\nabla_{\vec{R}}\,\vec{u}\\&=\frac{\partial\left[\rho^{(1)}\vec{u}\right]}{\partial t}-\vec{u}\,\frac{\partial\rho^{(1)}}{\partial t}+\rho^{(1)}\vec{u}\cdot\nabla_{\vec{R}}\,\vec{u}\end{aligned} \tag{30}$$

$$= \rho^{(1)} \left[\frac{\partial \vec{u}}{\partial t} + \vec{u} \cdot \nabla_{\vec{R}} \vec{u} \right] \cong 0. \qquad (31)$$

The term in the brackets in (31), being the substantial derivative of the velocity, is of second order in the velocity. Within this approximation, (29) becomes:

$$\bar{F}^{(1)} = \frac{1}{\rho^{(1)}} \nabla_{\vec{R}} \left[kT \rho^{(1)} \right]. \qquad (32)$$

We are now ready to multiply (16) by $|\vec{\pi}|^2 \vec{\pi}$ and integrate over $\vec{p}$. Introducing immediately the definition of $\vec{q}_K$, (20) and also using Green's theorem where the gradient with respect to momentum occurs in ~~the~~ (16), we obtain:

$$\frac{2}{Nm} \frac{\partial}{\partial t} \vec{q}_K + \int d\vec{p}\, |\vec{\pi}|^2 \vec{\pi} \frac{\vec{p}}{m} \cdot \nabla_{\vec{R}} \bar{f}^{(1)} -$$

$$- \frac{1}{m} \int d\vec{p} \left[|\vec{\pi}|^2 \vec{F}^{(1)} + 2 \vec{\pi} \vec{\pi} \cdot \vec{F}^{(1)} \right] \bar{f}^{(1)} = \qquad (33)$$

$$- \frac{\xi}{m} \int d\vec{p} \Big[|\vec{\pi}|^2 (\vec{\pi} \bar{f}^{(1)} + kT \nabla_p \bar{f}^{(1)}) \Big] + 2 \vec{\pi} \vec{\pi} \cdot (\vec{\pi} \bar{f}^{(1)} + kT \nabla_{\vec{p}} \bar{f}^{(1)}) \Big].$$

The right hand side can be rearranged by applying Green's theorem again to the integrals involving the gradient with respect to $\vec{p}$ and by collecting terms:

$$- \xi \left[3 \int d\vec{p}\, |\vec{\pi}|^2 \vec{\pi} \bar{f}^{(1)} - \frac{6kT}{m} \int d\vec{p}\, \vec{\pi} \bar{f}^{(1)} \right] = - \frac{6 \xi}{N m^2} \vec{q}_K, \qquad (34)$$

where the definition of $\vec{q}_K$ and (24) have been used in the last reduction. Now in the left hand side of (33), the second term is rewritten to avoid the unknown gradient of $\bar{f}^{(1)}$, and in the third term the expression for $\bar{F}^{(1)}$ found in (32) is substituted, so that:

$$\vec{q}_K = -\frac{m}{3\xi}\frac{\partial}{\partial t}\vec{q}_K - \frac{Nm^2}{6\xi}\Big[\nabla_{\vec{R}}\cdot\int d\vec{p}\,|\vec{\pi}|^2\vec{\pi}\,\frac{\vec{P}}{m}\bar{f}^{(1)} - \int d\vec{p}\,\bar{f}^{(1)}\frac{\vec{P}}{m}\cdot\nabla_{\vec{R}}|\vec{\pi}|^2\vec{\pi}\Big] + \frac{Nm}{6\xi\rho^{(1)}}\nabla_{\vec{R}}\left[kT\rho^{(1)}\right]\cdot\int d\vec{p}\left[|\vec{\pi}|^2\underset{\sim}{1} + 2\vec{\pi}\vec{\pi}\right]\bar{f}^{(1)}. \qquad (35)$$

We must now replace $\frac{\vec{P}}{m}$ by $\vec{\pi}$ in all integrands by adding and subtracting $\vec{u}$. The last term is already in that form and can be evaluated through (26) and (27).

$$\vec{q}_K = -\frac{m}{3\xi}\frac{\partial}{\partial t}\vec{q}_K - \frac{Nm^2}{6\xi}\Big[\nabla_{\vec{R}}\cdot\int d\vec{p}\,|\vec{\pi}|^2\vec{\pi}\vec{\pi}\bar{f}^{(1)} + \left[\nabla_{\vec{R}}\cdot\vec{u}\right]\int d\vec{p}\,|\vec{\pi}|^2\vec{\pi}\bar{f}^{(1)} + \vec{u}\cdot\nabla_{\vec{R}}\int d\vec{p}\,|\vec{\pi}|^2\vec{\pi}\bar{f}^{(1)} - \int d\vec{p}\,\bar{f}^{(1)}\vec{\pi}\cdot\left[\nabla_{\vec{R}}\cdot|\vec{\pi}|^2\right]\vec{\pi} - \vec{u}\cdot\int d\vec{p}\,\bar{f}^{(1)}\left[\nabla_{\vec{R}}\cdot|\vec{\pi}|^2\right]\vec{\pi}\Big] + \frac{5kT}{6\xi}\nabla_{\vec{R}}\left[kT\rho^{(1)}\right]. \qquad (36)$$

Carrying out the differentiation indicated for the last two terms in the bracket yields:

$$\vec{q}_K = \frac{m}{3\xi}\frac{\partial}{\partial t}\vec{q}_K - \frac{Nm^2}{6\xi}\Big[\nabla_{\vec{R}}\cdot\int d\vec{p}\,|\vec{\pi}|^2\vec{\pi}\vec{\pi}\bar{f}^{(1)} + \left[\nabla_{\vec{R}}\cdot\vec{u}\right]\int d\vec{p}\,|\vec{\pi}|^2\vec{\pi}\bar{f}^{(1)} + \vec{u}\cdot\nabla_{\vec{R}}\int d\vec{p}\,|\vec{\pi}|^2\vec{\pi}\bar{f}^{(1)} + \int d\vec{p}\,\bar{f}^{(1)}\vec{\pi}\cdot\nabla_{\vec{R}}\vec{u}\cdot\left[|\vec{\pi}|^2\underset{\sim}{1} + 2\vec{\pi}\vec{\pi}\right] + \vec{u}\cdot\nabla_{\vec{R}}\vec{u}\cdot\int d\vec{p}\,\bar{f}^{(1)}\left[|\vec{\pi}|^2\underset{\sim}{1} + 2\vec{\pi}\vec{\pi}\right]\Big] + \frac{5kT}{6\xi}\nabla_{\vec{R}}\left[kT\rho^{(1)}\right]. \qquad (37)$$

(20), (26), and (27) simplify the above to:

$$\vec{q}_K = \frac{5kT}{6\xi}\nabla_{\vec{R}}\left[kT\rho^{(1)}\right] - \frac{m}{3\xi}\Big[\frac{\partial}{\partial t}\vec{q}_K + \vec{u}\cdot\nabla_{\vec{R}}\vec{q}_K + \nabla_{\vec{R}}\cdot\vec{u}\,\vec{q}_K + \vec{q}_K\cdot\nabla_{\vec{R}}\vec{u}\Big] + \vec{u}\cdot\nabla_{\vec{R}}\vec{u}\left[\frac{5kT\rho^{(1)}m}{6\xi}\right] - \frac{Nm^2}{6\xi}\Big[\nabla_{\vec{R}}\cdot\int d\vec{p}\,|\vec{\pi}|^2\vec{\pi}\vec{\pi}\bar{f}^{(1)} + \int d\vec{p}\,\bar{f}^{(1)}\vec{\pi}\cdot\nabla_{R}\vec{u}\cdot\left[2\vec{\pi}\vec{\pi}\right]\Big]. \qquad (38)$$

Now let us drop second-order terms. Since $\frac{1}{\xi}$ is small and since $\vec{q}_K$ is of order $\frac{1}{\xi}$ (see leading term in (38)), the terms on the right hand side involving $\frac{\vec{q}_R}{\xi}$ are of the order $\frac{1}{\xi}$ and can be neglected. The term containing $\vec{u}\cdot\nabla_{\vec{R}}\,\vec{u}$ vanishes because it is a non-linear term, and because, under the condition of the problem only gradients in the temperature and none in the velocity are allowed. The last integral is also negligible because it involves the gradient of a velocity, and because it is of order $\frac{1}{\xi^2}$, as can be shown by multiplying the Fokker-Planck equation (16) by $\vec{\pi}\cdot[\nabla_R\vec{u}]\cdot\vec{\pi}\,\vec{\pi}$ and integrating over $\vec{p}$. The only remaining terms of (38) are thus:

$$\vec{q}_R = \frac{5kT}{6\xi}\nabla_{\vec{R}}\left[kT\rho^{(1)}\right] - \frac{Nm^2}{6\xi}\nabla_{\vec{R}}\cdot\int d\vec{p}\,|\vec{\pi}|^2\,\vec{\pi}\,\vec{\pi}\,\bar{f}^{(1)}. \tag{39}$$

The last term will be evaluated with the aid of (16). First let us rewrite (16), after dividing through by ξ:

$$\begin{aligned}\nabla_{\vec{p}}\cdot\left[\vec{\pi}\bar{f}^{(1)} + kT\nabla_{\vec{p}}\bar{f}^{(1)}\right] - \frac{1}{\xi}\frac{\partial \bar{f}^{(1)}}{\partial t} - \frac{1}{\xi}\frac{\vec{p}}{m}\cdot\nabla_{\vec{R}}\bar{f}^{(1)} - \\ - \frac{1}{\xi}\nabla_{\vec{p}}\cdot\vec{F}^{(1)}\bar{f}^{(1)} = 0.\end{aligned} \tag{16a}$$

Since the last three terms have the coefficient $\frac{1}{\xi}$ they give a contribution of order $\frac{1}{\xi^2}$ in (39), and so are negligible. Then multiplying (16a) by $|\vec{\pi}|^2\vec{\pi}\,\vec{\pi}$ and integrating over $\vec{p}$, we have:

$$\int d\vec{p}\,\vec{\pi}\,\vec{\pi}\,|\vec{\pi}|^2\,\nabla_{\vec{p}}\cdot\left[\vec{\pi}\bar{f}^{(1)} + kT\nabla_{\vec{p}}\bar{f}^{(1)}\right] = 0 \tag{40}$$

By Green's theorem this equals ~~to:~~

$$-\frac{2}{m}\int d\vec{p}\left[|\vec{\pi}|^2\,\vec{\pi}\,\underset{\sim}{1} + \vec{\pi}\,\vec{\pi}\,\vec{\pi}\right]\cdot\left[\vec{\pi}\bar{f}^{(1)} + kT\nabla_{\vec{p}}\bar{f}^{(1)}\right] = 0. \tag{41}$$

Applying Green's theorem again, we get:

$$2\int d\vec{p}\,\vec{\pi}\,\vec{\pi}\,|\vec{\pi}|^{2}\bar{f}^{(1)} = \frac{kT}{m}\int d\vec{p}\left[|\vec{\pi}|^{2}\underline{\underline{1}} + 5\,\vec{\pi}\,\vec{\pi}\right]\bar{f}^{(1)}. \tag{42}$$

By (26) and (27), we finally get:

$$\int d\vec{p}\,\vec{\pi}\,\vec{\pi}\,|\vec{\pi}|^{2}\bar{f}^{(1)} = \frac{4\left[kT\right]^{2}\rho^{(1)}\underline{\underline{1}}}{Nm^{2}}. \tag{43}$$

Substituting (43) into (39), and treating $\rho^{(1)}$ as a constant when taking the gradient:

$$\vec{q}_{k} = \frac{5k^{2}T\rho^{(1)}}{6\xi}\nabla T - \frac{4k^{2}\rho^{(1)}}{6\xi}2T\nabla T = -\frac{\rho^{(1)}k^{2}T\nabla T}{2\xi} \tag{44}$$

Thus, by the definitions (3a) and (18), the momentum contribution, $\varkappa_{k}$, to the coefficient of thermal conductivity is:

$$\varkappa_{k} = \frac{\rho^{(1)}k^{2}T}{2\xi} = \frac{N^{*}k^{2}T}{2\xi v}. \tag{45}$$

INTERMOLECULAR FORCE CONTRIBUTION TO THE HEAT CURRENT DENSITY

In order to evaluate $\vec{q}_v$, as (21) shows, the relative current density, $\vec{j}_1^{(2)} - \vec{u}_1 \rho^{(2)}$, has to be expressed by means of the Fokker-Planck equation (17) in pair space, because it involves the probability density in pair space. The procedure is thus quite similar to the one just completed. (17) is multiplied by various powers of $\vec{p}$ and integrated over momentum space till the desired relative current density is ferreted out. The only difference is that here six dimensional spaces are dealt with.

Consequently, multiplication of both sides of (17) by $\vec{P}_1$, followed by integration over momentum space of both particles, yields:

$$\frac{m}{N^2}\frac{\partial \vec{j}_1^{(2)}}{\partial t} + \nabla_{\vec{R}_1} \cdot \iint \frac{\vec{P}_1}{m}\vec{P}_1 \bar{f}^{(2)} d\vec{P}_1 \, d\vec{P}_2 - \frac{\vec{F}^{(2)}\rho^{(2)}}{N^2}$$
$$+ \nabla_{\vec{R}_2} \cdot \iint \frac{\vec{P}_2}{m}\vec{P}_1 \bar{f}^{(2)} d\vec{P}_1 \, d\vec{P}_2 = \tag{46}$$
$$- \vec{\underset{\sim}{\xi}}_1^{(2)} \cdot \iint \left[\vec{\pi}\bar{f}^{(2)} + kT\,\nabla_{\vec{P}_1}\bar{f}^{(2)}\right] d\vec{P}_1 \, d\vec{P}_2 = - \vec{\underset{\sim}{\xi}}_1^{(2)} \cdot \left[\frac{\vec{j}_1^{(2)}}{N^2} - \frac{\vec{u}_1\rho^{(2)}}{N^2}\right],$$

where Green's theorem and (8a) and (9) defining $\rho^{(2)}$ and $\vec{j}_1^{(2)}$ have been applied. As a simplification

$$\underset{\sim}{\xi}^{(2)} = \xi(T_1)\,\underset{\sim}{1}^{(1)} + \xi(T_2)\,\underset{\sim}{1}^{(2)} \tag{47}$$

has been assumed where ξ is the singlet friction constant. This assumption neglects the dependence of the friction tensor $\underset{\sim}{\xi}^{(2)}$ on the relative configuration of pairs and makes it~~s~~ momentum independent. Since the situation is symmetrical with respect to the two molecules, multiplication by $\vec{p}_2$ and integration over momentum space leads to an identical equation except that the roles of molecules one and two are interchanged. The right hand side of (46) is the desired quantity. To evaluate the left hand side in terms of known quantities, (17) has also to be integrated over momentum space yielding the continuity equation in pair space:

$$\frac{\partial \rho^{(2)}}{\partial t} + \nabla_{\vec{R}_1} \cdot \vec{j}_1^{(2)} + \nabla_{\vec{R}_2} \cdot \vec{j}_2^{(2)} = 0. \tag{48}$$

Furthermore, the second term on the left hand side of (46) is, as usual, obtained by multiplying (17) by $\vec{p}_1 \vec{p}_1$ and integrating over momentum space. By an argument similar to that following (16a), we can see that the contribution of the terms on the left hand side of (17) to the integral is of order $\frac{1}{\xi}$. Therefore, only the right hand terms of (17) are significant. Multiplying and integrating the right hand side and using Green's theorem once then results in:

$$-\underset{\sim}{\vec{\xi}}{}_1^{(2)} \cdot \iint \vec{p}_1 \left[\left(\frac{\vec{p}_1}{m} - \vec{u}_1 \right) \bar{f}^{(2)} + kT \, \nabla_{\vec{p}_1} \bar{f}^{(2)} \right] d\vec{p}_1 \, d\vec{p}_2 = 0. \tag{49}$$

Expanding and applying Green's theorem again leads to

$$\iint \vec{p}_1 \frac{\vec{p}_1}{m} \bar{f}^{(2)} \, d\vec{p}_1 \, d\vec{p}_2 = \frac{kT \rho^{(2)}}{N^2} \underset{\sim}{1} + \frac{m \vec{u}_1 \vec{j}_1^{(2)}}{N^2}. \tag{50}$$

In order to evaluate the third term of (46), we multiply the right hand side of (17) by $\vec{p}_1 \ \vec{p}_2$, integrate over momentum space, and apply Green's theorem:

$$\underset{\sim}{\vec{\xi}}{}_1^{(2)} \cdot \iint \vec{p}_2 \left[\left(\frac{\vec{p}_1}{m} - \vec{u}_1 \right) \bar{f}^{(2)} + kT \, \nabla_{\vec{p}_1} \bar{f}^{(2)} \right] d\vec{p}_1 \, d\vec{p}_2 + \qquad (51)$$

$$+ \underset{\sim}{\vec{\xi}}{}_2^{(2)} \cdot \iint \vec{p}_1 \left[\left(\frac{\vec{p}_2}{m} - \vec{u}_2 \right) \bar{f}^{(2)} + kT \, \nabla_{\vec{p}_2} \bar{f}^{(2)} \right] d\vec{p}_1 \, d\vec{p}_2 = 0.$$

Rewriting (51) by using Green's theorem again, we obtain:

$$\underset{\sim}{\vec{\xi}}{}_1^{(2)} \cdot \left[\iint \vec{p}_2 \, \vec{p}_1 \, \bar{f}^{(2)} \, d\vec{p}_1 \, d\vec{p}_2 - \frac{\vec{u}_1 \vec{j}_2^{(2)}}{N^2} \right] + \qquad (52)$$

$$+ \underset{\sim}{\vec{\xi}}{}_2^{(2)} \cdot \left[\iint \vec{p}_1 \, \vec{p}_2 \, \bar{f}^{(2)} \, d\vec{p}_1 \, d\vec{p}_2 - \frac{\vec{u}_2 \vec{j}_1^{(2)}}{N^2} \right] = 0.$$

Taking the gradients of (50) and (52), in order to substitute them into (46), and neglecting the $\vec{j}\vec{u}$ terms, since they are non-linear and involve the gradient of the velocity, yields:

$$\frac{m}{\xi} \frac{\partial \vec{j}_1^{(2)}}{\partial t} + \frac{1}{\xi} \nabla_{\vec{R}_1} \left[kT \rho^{(2)} \right] - \frac{\vec{F}_1^{(2)} \rho^{(2)}}{\xi} = - \left[\vec{j}_1^{(2)} - \vec{u}_1 \rho^{(2)} \right]. \qquad (53)$$

Since we are neglecting second order terms, the time derivative of the current density can also be struck out because $\vec{j}_1^{(2)}$ is of order $\frac{1}{\xi}$ itself and is combined with the $\frac{1}{\xi}$ coefficient in front of this term.

An equation similar to (53) exists for molecule two. These two equations are the differential equations for the pair probability distribution function. Before they can be solved they must be expressed in terms of a common function which has been chosen here for convenience as the correlation function defined in (11). Thus:

$$\nabla_{\vec{R}_1}\left[kT\rho^{(2)}(\vec{R}_1,\vec{R}_2;t)\right] =$$

$$\nabla_{\vec{R}_1}\left[kT\rho^{(1)}(\vec{R}_1;t)\rho^{(1)}(\vec{R}_2;t)\,g^{(2)}(\vec{R}_1,\vec{R}_2;t)\right] =$$

$$\rho^{(1)}(\vec{R}_2;t)\left\{g^{(2)}(\vec{R}_1,\vec{R}_2;t)\,\nabla_{\vec{R}_1}\left[kT\rho^{(1)}(\vec{R}_1;t)\right] + \right. \qquad (54)$$

$$\left. + \; kT\rho^{(1)}(\vec{R}_1;t)\,\nabla_{\vec{R}_1}g^{(2)}(\vec{R}_1,\vec{R}_2;t)\right\}.$$

Introducing (32) changes the above into

$$= \rho^{(1)}(\vec{R}_2;t)\rho^{(1)}(\vec{R}_1;t)\left[g^{(2)}(\vec{R}_1,\vec{R}_2;t)\,\vec{F}_1^{(1)} + kTg^{(2)}(\vec{R}_1,\vec{R}_2;t)\right]. \qquad (55)$$

Substitution of this into (53), with the additional simplification that the mean intermolecular force $\vec{F}$ is replaced by its equilibrium value ${}^{\circ}\langle\vec{F}\rangle$, results in :

$$\vec{j}_1^{(2)} - \vec{u}_1\rho^{(2)} =$$

$$- \frac{\rho^{(1)}\rho^{(1)}}{\xi}\left[{}^{\circ}\langle\vec{F}_1\rangle^{(1)}g^{(2)} + kT\nabla_{\vec{R}_1}g^{(2)} - {}^{\circ}\langle\vec{F}_1\rangle^{(2)}g^{(2)}\right]. \qquad (56)$$

By (14) therefore:

$$\vec{j}_1^{(2)} - \vec{u}_1\rho^{(2)} = -\frac{\rho^{(1)}\rho^{(1)}}{\xi}kT\left[\nabla_{\vec{R}_1}g^{(2)} - g^{(2)}\nabla_{\vec{R}_1}\log g_0^{(2)}\right]. \qquad (57)$$

It is to be noted that $g_0^{(2)}$, the equilibrium radial distribution function, in the above equation refers to the conditions at molecule one. $g_0^{(2)}$ differs from the time dependent distribution function $g^{(2)}$ by $g'^{(2)}$, the perturbation term, which alone depends on time:

$$g^{(2)} = g_0^{(2)} + g'^{(2)}. \qquad (58)$$

$g^{(2)}$, as has been pointed out, is a function of $\vec{R}_1$, $\vec{R}_2$, and time; of course, it is also a function of temperature and pressure. Now, under the existing temperature gradient, the temperatures at $\vec{R}_1$ and $\vec{R}_2$ are different so that really:

$$g^{(2)} = g^{(2)}(\vec{R}_1, \vec{R}_2, T(\vec{R}_1), T(\vec{R}_2), p; t). \qquad (59)$$

However, (58) necessitates the determination of a temperature at which the equilibrium radial distribution function is to be evaluated. The most natural choice is at the average temperature between $T(\vec{R}_1)$ and $T(\vec{R}_2)$.* Since in liquids $g^{(2)}$ is a function of the relative distance $|\vec{R}|$ only, we can write, if pressure is held constant throughout:

$$g^{(2)}(\vec{R}, T(\vec{R}_1), T(\vec{R}_2); t) =$$

$$g_0^{(2)}\left(\vec{R}, \frac{T(\vec{R}_1) + T(\vec{R}_2)}{2}\right) + g'^{(2)}(\vec{R}, T(\vec{R}_1), T(\vec{R}_2); t). \qquad (60)$$

Define

$$T = \frac{T(\vec{R}_1) + T(\vec{R}_2)}{2} \qquad (61)$$

and

$$\vec{r} = \frac{\vec{R}_1 + \vec{R}_2}{2} \qquad (62)$$

When taking the gradient of $g_0^{(2)}$ at $\vec{R}_1$ we have to correct for the fact that the temperature is not evaluated at that point,

---

* Defining $g^{(2)} = g^{(2)}[\vec{R}, T(\vec{R}_1)] + g'^{(2)}$ leads to unsymmetrical equations with respect to molecules one and two. The resulting differential equation for the probability density is different but the final result is, of course, the same. See Appendix I.

so that

$$\nabla_{\vec{R}_1} g_0^{(2)} = \nabla_{\vec{R}_1} g_0^{(2)}(\vec{R},T) + \frac{1}{2} \nabla T \frac{\partial g_0^{(2)}}{\partial T} + \cdots \quad . \tag{63}$$

Since

$$\vec{R} = \vec{R}_2 - \vec{R}_1 \, , \quad \text{and} \quad \nabla_{\vec{R}} = -\nabla_{\vec{R}_1} = \nabla_{\vec{R}_2} \tag{64}$$

the Taylor expansion keeping only linear terms gives

$$\nabla_{\vec{R}_1} g^{(2)} = -\nabla_{\vec{R}} g_0^{(2)}(\vec{R},T) - \nabla_{\vec{R}} g'^{(2)} + \frac{1}{2} \nabla T \left[\frac{\partial g_0^{(2)}}{\partial T} \right]_P . \tag{65}$$

The other term on the right hand side of (57), $\nabla_{\vec{R}_1} \log g_0^{(2)} \left[\vec{R}, T(\vec{R}_1)\right]$ involves $T(\vec{R}_1)$ only since it refer~~r~~s to the conditions at molecule one. It is written now as the difference of two quantities, as verifiable by a linear Taylor expansion, so that $g_0^{(2)}$ is expressed in terms of the same temperature throughout. Expanding $\log g_0^{(2)}$ about the temperature T leads to

$$\log g_0^{(2)} \left[\vec{R}, T(\vec{R}_1)\right] =$$

$$\log g_0^{(2)} \left[\vec{R}, T(\vec{r})\right] + \left[\frac{\partial \log g_0^{(2)} \left[\vec{R}, T(\vec{R}_1)\right]}{\partial T(\vec{R}_1)} \right]_{T(\vec{R}_1) = T(\vec{r}), P} \left[T(\vec{r}) - T(\vec{R}_1) \right] . \tag{66}$$

Similarly expanding $T(\vec{r})$ about $T(\vec{R}_1)$ yields

$$\begin{aligned} T(\vec{r}) &= T(\vec{R}_1) + \nabla T \cdot \left[\vec{R}_1 - \vec{r}\right] + \cdots \\ T(\vec{r}) - T(\vec{R}_1) &= -\frac{1}{2} \nabla T \cdot \vec{R} \, . \end{aligned} \tag{67}$$

Thus

$$-\nabla_{\vec{R}} \log g_0^{(2)} \left[\vec{R}, T(\vec{R}_1)\right] =$$

$$-\nabla_{\vec{R}} \left[\log g_0^{(2)}(\vec{R},T) - \frac{1}{2} (\vec{R} \cdot \nabla T) \left\{ \frac{\partial}{\partial T} \log g_0^{(2)}(\vec{R},T) \right\}_P \right] , \tag{68}$$

so that

$$\vec{j}_1^{(2)} - \vec{u}_1\rho^{(2)} = \frac{-\rho^{(1)}\rho^{(1)}}{\xi} kT\Bigg[-\nabla_{\vec{R}}\, g_0^{(2)} - \nabla_{\vec{R}}\, g'^{(2)} + \\ + \frac{1}{2}\nabla T\left[\frac{\partial g_0^{(2)}}{\partial T}\right]_P + \\ + \left[g_0^{(2)} + g'^{(2)}\right]\nabla_{\vec{R}}\left\{\log g_0^{(2)} - \frac{1}{2}(\vec{R}\cdot\nabla T)\left[\frac{\partial \log g_0^{(2)}}{\partial T}\right]_P\right\}\Bigg]. \tag{69}$$

Multiplying (69) out and cancelling the first term results in:

$$\vec{j}_1^{(2)} - \vec{u}_1\rho^{(2)} = \frac{-\rho^{(1)}\rho^{(1)}}{\xi} kT\Bigg[-\nabla_{\vec{R}}\, g'^{(2)} + \frac{1}{2}\nabla T\left[\frac{\partial g_0^{(2)}}{\partial T}\right]_P + \\ + g'^{(2)}\nabla_{\vec{R}}\log g_0^{(2)} - \\ - \frac{1}{2} g_0^{(2)}\nabla_{\vec{R}}\left\{(\vec{R}\cdot\nabla T)\left[\frac{\partial \log g_0^{(2)}}{\partial T}\right]_P\right\}\Bigg], \tag{70}$$

where the term $g'^{(2)}\nabla_{\vec{R}}(\vec{R}\cdot\nabla T)\left[\frac{\partial \log g_0^{(2)}}{\partial T}\right]_P$ has been neglected since it is of second order, involving the product of the perturbation and the temperature gradient. When the gradient is taken in the last term of (70), one term cancels out, so that

$$\vec{j}_1^{(2)} - \vec{u}_1\rho^{(2)} = \frac{-\rho^{(1)}\rho^{(1)}}{\xi(T_1)} kT\Bigg[-\nabla_{\vec{R}}\, g'^{(2)} + g'^{(2)}\nabla_{\vec{R}}\log g_0^{(2)} - \\ - \frac{1}{2} g_0^{(2)}(\vec{R}\cdot\nabla T)\nabla_{\vec{R}}\left[\frac{\partial \log g_0^{(2)}}{\partial T}\right]_P\Bigg]. \tag{71}$$

An exactly similar equation* holds in the space of molecule two except that some signs are reversed, due to (64):

$$\vec{j}_2^{(2)} - \vec{u}_2\rho^{(2)} = -\frac{\rho^{(1)}\rho^{(1)}}{\xi(T_2)} kT\Bigg[\nabla_{\vec{R}}\, g'^{(2)} - g'^{(2)}\nabla_{\vec{R}}\log g_0^{(2)} - \\ - \frac{1}{2} g_0^{(2)}(\vec{R}\cdot\nabla T)\nabla_{\vec{R}}\left[\frac{\partial \log g_0^{(2)}}{\partial T}\right]_P\Bigg]. \tag{72}$$

It would now be possible to evaluate the relative current density if the perturbation $g'^{(2)}$ were known. A differential

* $\xi(T_1)$ and $\xi(T_2)$ differ by terms of second order.

equation is obtained for this quantity if we express the left hand side of (71) or (72) in terms of the radial distribution function. To accomplish this it is necessary to take the divergence of both sides of (71) so that the continuity Eq(47) can be used to convert the current density into a probability density. It is more convenient to carry out this operation in the six dimensional space. After taking the divergence and adding the two equations, (71) and (72), the left hand side contains:

$$\nabla_{\vec{R}_1}\cdot\left[\vec{j}_1^{\,(2)} - \vec{u}_1\rho^{(2)}\right] + \nabla_{\vec{R}_2}\cdot\left[\vec{j}_2^{\,(2)} - \vec{u}_2\rho^{(2)}\right]. \tag{73}$$

(48) changes this into

$$\begin{aligned} &-\frac{\partial\rho^{(2)}}{\partial t} - \nabla_{\vec{R}_1}\cdot\left[\vec{u}_1\rho^{(2)}\right] - \nabla_{\vec{R}_2}\cdot\left[\vec{u}_2\rho^{(2)}\right] = \\ &\frac{\partial\left[\rho^{(1)}(\vec{R}_1;t)\,\rho^{(1)}(\vec{R}_2;t)\,g^{(2)}(\vec{R};t)\right]}{\partial t} - \\ &-\rho^{(1)}(\vec{R}_2;t)\,\nabla_{\vec{R}_1}\cdot\left[\vec{u}_1\rho^{(1)}(\vec{R}_1;t)\,g^{(2)}(\vec{R};t)\right] - \\ &-\rho^{(1)}(\vec{R}_1;t)\,\nabla_{\vec{R}_2}\cdot\left[\vec{u}_2\rho^{(1)}(\vec{R}_2;t)\,g^{(2)}(\vec{R};t)\right], \end{aligned} \tag{74}$$

where the definition of $g^{(2)}$, (11), has been introduced. The continuity equation (22) and (64) transform (74) to:

$$\begin{aligned} &-\rho^{(1)}\rho^{(1)}\left[\frac{\partial g^{(2)}}{\partial t} + \vec{u}_1\cdot\nabla_{\vec{R}_1} g^{(2)} + \vec{u}_2\cdot\nabla_{\vec{R}_2} g^{(2)}\right] = \\ &-\rho^{(1)}\rho^{(1)}\left[\frac{\partial g^{(2)}}{\partial t} + \left[\vec{u}_2 - \vec{u}_1\right]\cdot\nabla_{\vec{R}} g^{(2)}\right]. \end{aligned} \tag{75}$$

Since only the perturbation term depends on the time, and since a Taylor expansion can be made up to linear terms of

$\vec{u}(\vec{R}_2)$ about $\vec{u}(\vec{R}_1)$,

$$\vec{u}(\vec{R}_2) - \vec{u}(\vec{R}_1) = \vec{R} \cdot \nabla_{\vec{r}} \vec{u} \tag{76}$$

and since $\vec{R}_1$ is approximately equal to $\vec{r}$,

$$\vec{u}(\vec{R}_2) - \vec{u}(\vec{R}_1) = \vec{R} \cdot \nabla_{\vec{r}} \vec{u}, \tag{77}$$

(75) is transformed into:

$$\nabla_{\vec{R}_1} \cdot \left[\vec{j}_1^{\,(2)} - \vec{u}_1 \rho^{(2)}\right] + \nabla_{\vec{R}_2} \cdot \left[\vec{j}_2^{\,(2)} - \vec{u}_2 \rho^{(2)}\right] = \\ -\rho^{(1)}\rho^{(1)} \left[\frac{\partial g'^{(2)}}{\partial t} + \vec{R} \cdot \left[\nabla_{\vec{r}} \vec{u}\right] \cdot \vec{R} \, \frac{\partial g^{(2)}}{\partial R}\right]. \tag{78}$$

This last term, involving the gradient of the velocity, is important in the theory of the coefficient of viscosity. It is here zero since the physical conditions permit no velocity gradient. Finally by (71), (72), and (78):

$$\nabla_{\vec{R}} \cdot \left[-\left(\vec{j}_1^{\,(2)} - \vec{u}_1 \rho^{(2)}\right) + \left(\vec{j}_1^{\,(2)} - \vec{u}_2 \rho^{(2)}\right)\right] = \\ -\rho^{(1)}\rho^{(1)} \frac{\partial g'^{(2)}}{\partial t} = \nabla_{\vec{R}} \cdot \left[\frac{2\rho^{(1)}\rho^{(1)}}{\xi} kT \left\{-\nabla_{\vec{R}} g'^{(2)} + \right.\right. \\ \left.\left. + g'^{(2)} \nabla_{\vec{R}} \log g_0^{(2)}\right\}\right]. \tag{79}$$

This is the desired differential equation for the probability density expressed in terms of the perturbation.

The complete solution of this equation leads to the molecular interpretation of the relaxation time spectrum due to flow caused by a temperature gradient. For the determination of the coefficient of thermal conductivity it suffices to consider the steady state solutions. The boundary conditions subject to which this equation is to be solved are derived from the conditions imposed on the excess probability current density in pair space. The vanishing of the pair probability current and its divergence at the origin will certainly satisfy ~~that~~ the requirements that there be no source or sinks of pairs. The pair probability current and its divergence should also vanish at infinity because of the physical interpretation of the current. The particular solution of (79) $g'^{(2)} = 0$, satisfying these conditions can immediately be found by inspection. It obviously satisfies the boundary conditions that the relative current density and its divergence vanish at $\vec{R} = 0$ and $\vec{R} = \infty$. By (79),

$$\nabla\cdot\left[\vec{j}^{(2)} - \vec{u}\rho^{(2)}\right] = 0 \text{ at } \vec{R} = 0 \text{ and } \vec{R} = \infty \tag{80}$$

If $g'^{(2)} = 0$, the first and second terms on the right hand side of (71) vanish, leaving:

$$\vec{j}_1^{(2)} - \vec{u}_1\rho^{(2)} = \frac{kT^{*}\rho^{(1)2}}{2\xi}\, g_0^{(2)}(\vec{R}\cdot\nabla T)\,\nabla_{\vec{R}}\left[\frac{\partial \log g_0^{(2)}}{\partial T}\right]_P \tag{81}$$

At $\vec{R} = 0$, $g_0^{(2)}$ vanishes exponentially so that $\vec{j}_1^{(2)} - \vec{u}_1\rho^{(2)} = 0$. At $\vec{R} = \infty$, when $g_0^{(2)} = 1$, the boundary condition is also satisfied. Thus, by (21), for a spherically symmetric potential,

$$\vec{q}_V = \frac{kT\rho^{(1)2}}{4\xi}\int d\vec{R}\left[V - R\frac{dV}{dR}\right] g_0^{(2)}(\vec{R}\cdot\nabla T)\,\frac{\vec{R}}{R}\,\frac{d}{dR}\left[\frac{\partial \log g_0^{(2)}}{\partial T}\right]_P \tag{82}$$

Now let us use polar coordinates

$$d\vec{R} = R^2 \sin\Theta \, dR \, d\Theta \, d\varphi \qquad (83)$$

$$\frac{\vec{R}}{R} = \cos\Theta$$

and choose the z axis along the direction of ∇T,

$$\vec{R}\cdot\nabla T = \nabla T \, R \cos\Theta, \qquad (84)$$

Then the integration in (82) over φ can be carried out immediately, giving 2π, so that:

$$\vec{q}_v = \qquad (85)$$

$$\frac{\pi k T \rho^{(1)2}}{2\xi} \nabla T \int_0^\infty dR \left[V - R\frac{dV}{dR}\right] g_0^{(2)} R^3 \frac{d}{dR}\left[\frac{\partial \log g_0^{(2)}}{\partial T}\right]_P \int_0^\pi d\theta \sin\Theta \cos^2\Theta$$

Integration over Θ gives 2/3. Therefore the intermolecular contribution to the coefficient of thermal conductivity, which is the negative of the factor multiplying ∇T, becomes:

$$\varkappa_v = \frac{\pi k T^2 \rho^{(1)2}}{3\xi} \int_0^\infty dR \left[R\frac{dV}{dR} - V\right] R^3 g_0^{(2)} \frac{d}{dR}\left[\frac{\partial \log g_0^{(2)}}{\partial T}\right]_P. \qquad (86)$$

EVALUATION OF THE COEFFICIENT OF THERMAL CONDUCTIVITY

The expression for $\varkappa_v$ can be changed into various forms more convenient for calculation purposes. By so transforming this equation it has been possible to express some of the terms in $\varkappa_v$ by means of thermodynamic quantities. This is desirable since it decreases the reliance on the radial distribution function, which is not accurately known and which occurs in a rather sensitive way in the integrals.

We write

$$g_0^{(2)}\frac{d}{dR}\left[\frac{\partial \log g_0^{(2)}}{\partial T}\right]_p = g_0^{(2)}\left[\frac{1}{g_0^{(2)}}\frac{d}{dR}\left[\frac{\partial g_0^{(2)}}{\partial T}\right]_p - \frac{1}{[g_0^{(2)}]^2}\frac{dg_0^{(2)}}{dR}\left[\frac{\partial g_0^{(2)}}{\partial T}\right]_p\right]. \tag{87}$$

So (86) becomes by (87) and then by partial integration:

$$\varkappa_v = \frac{\pi k T \rho^{(1)2}}{3\xi}\int_0^\infty dR\left[R^4\frac{dV}{dR} - R^3V\right]\left[\frac{d}{dR}\left[\frac{\partial g_0^{(2)}}{\partial T}\right]_p - \frac{d\log g_0^{(2)}}{dR}\left[\frac{\partial g_0^{(2)}}{\partial T}\right]_p\right] \tag{88}$$

$$= -\frac{\pi k T \rho^{(1)2}}{3\xi}\left\{\frac{\partial}{\partial T}\int_0^\infty dR\left[3R^3\frac{dV}{dR} - 3R^2V + R^4\frac{d^2V}{dR^2}\right]g_0^{(2)} + \right.$$
$$\left. + \int_0^\infty dR\left[R^4\frac{dV}{dR} - R^3V\right]\frac{d\log g_0^{(2)}}{dR}\left[\frac{\partial g_0^{(2)}}{\partial T}\right]_p\right\}. \tag{89}$$

The first part of (89), $\varkappa_v^{(1)}$, is evaluated through thermodynamic data as follows.

Let V(R) be the Lennard-Jones potential:

$$V(R) = 4\varepsilon\left[\left(\frac{a}{R}\right)^{12} - \left(\frac{a}{R}\right)^{6}\right]. \tag{90}$$

Writing x for

$$x = \frac{R}{a}\,, \tag{91}$$

$\varkappa_v^{(1)}$ becomes:

$$\varkappa_v^{(1)} = \frac{\pi k T \rho^{(1)2}}{3\xi}\frac{\partial}{\partial T}\left[\int_0^\infty dx\,\frac{13\cdot 9}{x^{10}}\,g_0^{(2)} - \int_0^\infty dx\,\frac{7\cdot 3}{x^4}\,g_0^{(2)}\right]. \tag{92}$$

Consider now the equation of state and the equation for the internal energy as two simultaneous linear equations in the two unknown integrals. That is, the equation of state with the potential (90) becomes:

$$\begin{gathered}\int_0^\infty dx\; x^3\,\frac{dV}{dx}\,g_0^{(2)} = \\ -\int_0^\infty dx\,\frac{12}{x^{10}}\,g_0^{(2)} + \int_0^\infty dx\,\frac{6}{x^4}\,g_0^{(2)} = \left[\rho^{(1)}kT - p\right]\frac{3}{2\pi\rho^{(1)2}}\;;\end{gathered} \tag{93}$$

and similarly the thermal equation of state becomes:

$$\begin{gathered}\int_0^\infty dx\; x^2\,\frac{\cancel{d}V(x)}{\cancel{dx}}\,g_0^{(2)} = \\ \int_0^\infty dx\,\frac{g_0^{(2)}}{x^{10}} - \int_0^\infty dx\,\frac{g_0^{(2)}}{x^4} = \frac{\Delta E}{2\pi N\rho^{(1)}}\,,\end{gathered} \tag{94}$$

where $\Delta E = E - E_g$ is the difference between the actual internal energy and that of the perfect gas. Solving for these two integrals in (93) and (94) and substituting the result into (92) yields:

$$\varkappa_v^{(1)} = -\frac{\partial}{\partial T}\left[75\,\frac{\Delta E}{2\pi N\rho^{(1)}} + 16\left[\rho^{(1)}kT - p\right]\frac{3}{2\pi\rho^{(1)2}}\right]_p . \tag{95}$$

For a liquid p can be neglected compared to ρkT in $\rho kT - p$, since ρkT is the pressure that would exist if there were no forces between the molecules. Carrying out the differentiation with respect to T yields

$$\varkappa_v^{(1)} = 75\left[\frac{\frac{3}{2}R - C_p^{(\ell)}}{2\pi N\rho^{(1)}} - \frac{\Delta E}{2\pi N}\left(\frac{\partial v}{\partial T}\right)_p\right] - \frac{24}{\pi}\left[\frac{k}{\rho^{(1)}} + \frac{kT}{N}\left(\frac{\partial v}{\partial T}\right)_p\right], \tag{96}$$

where $C_p^{(\ell)}$ is defined as the heat capacity of the liquid at constant pressure. Introducing the thermal expansion coefficient $b = \frac{1}{v}\left(\frac{\partial v}{\partial T}\right)_p$, one obtains

$$\varkappa_v^{(1)} = \frac{1}{2\pi N\rho^{(1)}}\left[75\left(\tfrac{3}{2}R - C_p^{(\ell)} - \Delta E b\right) - 48\left(R + RTb\right)\right]. \tag{97}$$

By then adding on the remainder of the intermolecular contribution and also the kinetic contribution, (45), the thermal conductivity coefficient is evaluated by the following equation:

$$\varkappa = \frac{kT}{2\xi v}\left[R - 25\left(\tfrac{3}{2}R - C_p^{(\ell)} - \Delta E b\right) + 16\left(R + RTb\right)\right] - \frac{\pi kT\rho^{(1)2}}{3\xi}\int_0^\infty dR\left[R^4\frac{dV}{dR} - R^3 V\right]\frac{d\log g_0^{(2)}}{dR}\left[\frac{\partial g_0^{(2)}}{\partial T}\right]_p. \tag{98}$$

In the first term of (98), $\varkappa^{(1)}$, we introduce

$$\Delta H = H_\ell - H_g = E_\ell + (pv)_\ell - E_g - RT \cong \Delta E - RT, \tag{99}$$

because data are usually given in terms of H, the enthalpy, so that

$$\varkappa^{(1)} = \frac{kT}{2\xi v}\left[25\,C_p^{(e)} - \frac{41}{2}R + b(25\Delta H + 41\,RT)\right]. \qquad (100)$$

With the following data(6,7)

$T = 89^oK$

$P = 1.2$ atm

$\Delta H = -1543$ cal/mole

$b = .0042 / {}^oK$

$v = 28.96$ cc.

$C_p^{(e)} = 10.10$ cal/^{o}C

. (101)

$$\varkappa^{(1)} = \frac{1.68\times10^{-14}}{\xi} \quad \text{cal./ cm. sec. oK}$$

If the repulsive exponent were 11.4 in (90) instead of 12, $\varkappa^{(1)}$ becomes equal to

$$\varkappa^{(1)} = \frac{1.55\times10^{-14}}{\xi} \quad \text{cal.}/\text{cm. sec. }{}^oK. \qquad (102)$$

For the integrals in (98) it is necessary to know the radial distribution function and its derivatives with respect to distance and temperature. The first calculations were performed with a reasonable analytic approximation to the experimental radial distribution function found useful in the calculation for the coefficient of viscosity(1).

$$g_0^{(2)} = \left(\frac{a_1}{R}\right)^s \exp.\left[\left(\frac{a_m}{a_1}\right)^t - \left(\frac{a_m}{R}\right)^t\right] \qquad 0 \le R \le a_1 \qquad (103)$$

$$= 1 \qquad\qquad R > a_1 ,$$

where a_1 = 4.5 A° and t = 14

a_m = 3.554 and s = 7.007

The parameters a_1 and t were adjusted to fit the first peak of the experimental data of Eisenstein and Gingrich for the radial distribution function(8) and were found to be relatively temperature insensitive. The other two parameters a_m and s were then determined so that this radial distribution function, when substituted into the theoretical expression for the equation of state and the internal energy, reproduced the experimental data. Now to find the temperature derivative of this radial distribution function in accordance with the above findings, it is assumed that only a_m and s are temperature-dependent. To evaluate this dependence the above procedure is repeated, using the temperature derivatives of the expressions for the equation of state and internal energy. That is, the two parameters $\left(\frac{\partial a_m}{\partial T}\right)_p$ and $\left(\frac{\partial s}{\partial T}\right)_p$ are so adjusted by solving two linear simultaneous equations that they are consistent with the experimental data for the heat capacity and the compressibility. The two derivatives proved to be equal to:

$$\left(\frac{\partial a_m}{\partial T}\right)_p = 2.948\times10^{-4}\,;\quad \left(\frac{\partial s}{\partial T}\right)_p = -1.529\times10^{-2}. \qquad (104)$$

It is then possible by direct substitution to get

$$\int_0^\infty R^3 V \frac{\partial \log g_0^{(2)}}{\partial R}\left(\frac{\partial g_0^{(2)}}{\partial T}\right)_p dR = -1.316\times10^{-15}\ \text{ergs}\ \text{Å}^3$$

$$\int_0^\infty R^4 \frac{dV}{dR}\ \frac{\partial \log g_0^{(2)}}{\partial R}\left(\frac{\partial g_0^{(2)}}{\partial T}\right)_p dR = 6.308\times10^{-14}\ \text{ergs}\ \text{Å}^3. \qquad (105)$$

Thus

$$\varkappa = \frac{6.5\times 10^{-15}}{\xi}\ \text{cal.}/\text{cm. sec. °C.} \qquad (106)$$

It remains to give a numerical value for the friction constant which is determined from the very general formula(5)

$$\xi = \frac{\beta}{3}\int_0^{\tau}\left[\iint \vec{F}(t)\cdot\vec{F}(t+s)\,\overset{\circ}{f}{}^{(N)}\,d\vec{p}\,d\vec{Q}\right]ds. \qquad (107)$$

One crude way to evaluate this expression is to approximate ξ by

$$\xi = \frac{\beta\Theta}{3}\left[\iint \vec{F}(t)\cdot\vec{F}(t)\,\overset{\circ}{f}{}^{(N)}\,d\vec{P}\,d\vec{Q}\right], \qquad (108)$$

where the integration over s has been replaced by Θ, thus defining Θ as the correlation time. Since this correlation time is of the order of magnitude of the relaxation time, $\frac{m}{\xi}$, (108) becomes upon substitution:

$$\vec{F}(t) = -\nabla V_N$$

$$\xi^2 = \frac{\beta m}{3}\left[\int \nabla V_N\cdot\nabla V_N\, e^{-\beta V_N}\,d\vec{Q}\right] = \qquad (109)$$

$$\frac{\beta m}{3}\left[-\frac{1}{\beta}\int \nabla V_N\cdot\nabla e^{-\beta V_N}\,d\vec{Q}\right].$$

By Green's theorem

$$\xi = \frac{\beta m}{3}\left[\frac{4\pi\rho^{(1)}}{\beta}\int_0^{\infty} R^2\left[\nabla^2 V\right] g_0^{(2)}\,dR\right]$$

$$= \frac{4\pi\rho^{(1)} m}{3}\int_0^{\infty} R^2\left[\frac{d^2V}{dR^2}+\frac{2}{R}\frac{dV}{dR}\right] g_0^{(2)}\,dR. \qquad (110)$$

The radial distribution function (103) gave as a preliminary estimate for this friction constant:

$$\xi = 4.84 \times 10^{-10} \text{ gm/sec.}, \tag{111}$$

so that

$$\varkappa = 1.35 \times 10^{-5} \text{ cal./gm. sec. } ^\circ\text{C}. \tag{112}$$

Due to the experimental difficulties, no measurement has been carried out for this quantity, so it is only possible by various analogies to surmise whether this value is correct at least in the order of magnitude. One such applicable analogy is the principle of corresponding states which holds for any two parameter intermolecular potential. As has been pointed out in part I of this thesis, the two non-dimensional parameters significant to the Lennard-Jones potential (90) are $\frac{a^3}{v}$ and $\beta\varepsilon$, where a is some characteristic distance of the potential. Fluids possessing this same form of the potential have the same properties when $\frac{a^3}{v}$ and $\beta\varepsilon$ are the same. For the case at hand, the only monatomic liquid for which the coefficient of thermal conductivity is experimentally known is helium I, for which, unfortunately, quantum effects are not negligible. The available value(9) at 3.3 °K is 6×10^{-5} c.g.s. It is almost certain that quantum effects make this value too large since helium II at still lower temperatures has an enormously larger conductivity. Anyway, if it is assumed that the conductivity of argon is the calculated value, the principle of corresponding states gives as the conductivity of helium I 1.6 x 10^{-5} c.g.s. at 4.5 °K. This is in reasonable agreement in view of the sign of the quantum effects and the higher corresponding state temperature. In order to show what the application of the principle of corresponding states would yield in the case of the viscosity, where all necessary experimental values are known, the following comparison was carried out starting with the experimental viscosity of argon at 89° K. At 4.5 °K the calculated viscosity of He is .25 x 10^{-3} instead of .11 x 10^{-3} poises. Again quantum effects could cause this discrepancy, but in any case the significance of the order of magnitude of such a calculation is demonstrated. It is interesting to note that the thermal conductivity of most liquids is between 10^{-3} and 10^{-4} and that the rare gas liquids have a smaller value by a factor of 10. This may not be surprising since the rare gases show the same tendency compared to other gases.

To eliminate the uncertainty in the friction constant it is possible to make an experimental comparison without knowing its value since the product of the coefficient of viscosity and thermal conductivity is very nearly independent of ξ. If the small momentum contribution to the viscosity is neglected, the viscosity is proportional to ξ while the thermal conductivity, as has been seen, is inversely proportional to the friction constant. Thus for helium I we would get:

$$\begin{aligned}(\xi\eta)_{calculated} &= 4 \times 10^{-7}\ \text{c.g.s.} \\ (\xi\eta)_{experimental} &= 6.6 \times 10^{-7}\ \text{c.g.s.},\end{aligned} \qquad (113)$$

where, as is necessary for consistency, the same radial distribution function has been used for the evaluation of both coefficients.

The uncertainty in the distribution function and therefore in the two integrals (105) evaluated with it might be quite large. It is interesting to note that if these two integrals were neglected entirely, that is if they proved to be negligibly small compared to the $\varkappa^{(1)}$ term, the coefficient of heat conductivity of argon would be equal to 3.1×10^{-5} c.g.s. and therefore the one for helium I would be 3.7×10^{-5} c.g.s., in better agreement with experiment.

APPENDIX I

If we define

$$g^{(2)} = g_0^{(2)}(\vec{R}, T(\vec{R}_1)) + g'^{(2)} \tag{114}$$

equation (63) and therefore (65) remain unaltered. However there is then no need to expand $\log g_0^{(2)}(\vec{R}_1, T(\vec{R}_1))$ about $T(\vec{R}_1)$, the temperature for molecule one, as was previously done. Therefore we can immediately write down the current density in pair space projected on the 3-space of molecule one by substituting (65) into (57)

$$\begin{aligned}\vec{j}_1^{(2)} - \vec{u}_1 \rho^{(2)} &= -\frac{\rho^{(1)}\rho^{(1)}}{\xi} kT\Big[-\nabla_{\vec{R}}\, g_0^{(2)} - \nabla_{\vec{R}}\, g'^{(2)} + \frac{1}{2}\nabla T\Big(\frac{\partial g_0^{(2)}}{\partial T}\Big)_p - \\ &\qquad - \big(g_0^{(2)} + g'^{(2)}\big)\nabla_{\vec{R}_1} \log g_0^{(2)}\Big] \\ &= -\frac{\rho^{(1)}\rho^{(1)}}{\xi} kT\Big[-\nabla_{\vec{R}}\, g'^{(2)} + g'^{(2)}\nabla_{\vec{R}} \log g_0^{(2)} + \frac{1}{2}\nabla T\Big(\frac{\partial g_0^{(2)}}{\partial T}\Big)_p\Big].\end{aligned} \tag{115}$$

For the corresponding equation for molecule two, however, it is necessary that $\log g_0^{(2)}(\vec{R}, T(\vec{R}_2))$ be expanded about $T(\vec{R}_1)$, so that analogously to (66)

$$\begin{aligned}&\nabla_{\vec{R}} \log g_0^{(2)}(R, T(\vec{R}_2)) = \\ &\nabla_{\vec{R}}\Big[\log g_0^{(2)}(\vec{R}, T(\vec{R}_1)) - (\vec{R}\cdot\nabla T)\Big[\frac{\partial}{\partial T}\log g_0^{(2)}(\vec{R}, T(\vec{R}_1))\Big]_p\Big].\end{aligned} \tag{116}$$

Therefore (72) becomes instead

$$\begin{aligned}\vec{j}_2^{(2)} - \vec{u}_2 \rho^{(2)} = -\frac{\rho^{(1)}\rho^{(1)}}{\xi} kT\Big[&\nabla_{\vec{R}}\, g'^{(2)} - g'^{(2)}\nabla_{\vec{R}} \log g_0^{(2)} + \\ &+ \frac{1}{2}\nabla T\Big(\frac{\partial g_0^{(2)}}{\partial T}\Big)_p - g_0^{(2)}\nabla_{\vec{R}}\Big\{(\vec{R}\cdot\nabla T)\Big(\frac{\partial \log g_0^{(2)}}{\partial T}\Big)_p\Big\}\Big].\end{aligned} \tag{117}$$

(79) will now read

$$-\rho^{(1)}\rho^{(1)}\frac{\partial g'^{(2)}}{\partial t} = \nabla_{\vec{R}}\cdot\left[\frac{\rho^{(1)}\rho^{(1)}}{\xi}kT\left\{-2\nabla_{\vec{R}}g'^{(2)} + 2g'^{(2)}\nabla_{\vec{R}}\log g_0^{(2)} + g_0^{(2)}\nabla_{\vec{R}}(\vec{R}\cdot\nabla T)\left(\frac{\partial\log g_0^{(2)}}{\partial T}\right)_P\right\}\right]. \tag{118}$$

The perturbation $g'^{(2)}$ arising from departures of equilibrium thus satisfies the partial differential equation

$$\nabla_{\vec{R}}\cdot\left[\nabla_{\vec{R}}g'^{(2)} - g'^{(2)}\nabla_{\vec{R}}\log g_0^{(2)}\right] - \frac{\xi}{2kT}\frac{\partial g'^{(2)}}{\partial t} = \frac{1}{2}\nabla_{\vec{R}}\cdot\left\{g_0^{(2)}\nabla_{\vec{R}}\left[(\vec{R}\cdot\nabla T)\left(\frac{\partial\log g_0^{(2)}}{\partial T}\right)_P\right]\right\}. \tag{119}$$

The solution satisfying the boundary condition is now of the following form:

$$g'^{(2)} = g_0^{(2)}(R)\,\frac{1}{2}\,(\vec{R}\cdot\nabla T)\left(\frac{\partial\log g_0^{(2)}}{\partial T}\right)_P. \tag{120}$$

If (120) is substituted into (114), equation (81) results.

GLOSSARY

a = distance occurring in the Lennard-Jones potential (90).

a_m, a_1 = constants occurring in an empirical radial distribution function (103).

b = coefficient of thermal expansion.

C_p = molar heat capacity at constant pressure.

E = internal energy density, also, thermodynamic internal energy.

$^{\circ}\langle\ \rangle$ = specifies equilibrium average of a quantity.

$^{\circ}\langle \vec{F}_a \rangle^{(n)}$ = equilibrium average force on molecule a in a set of n molecules.

$\vec{F}_a^{\dagger(n)}$ = perturbation force on a molecule a in a set of n molecules.

$\vec{F}_a^{(n)}$ total force acting on molecule a in a set of n molecules.

$\vec{F}^{(n)}$ total force in the configuration space of n molecules.

$f^{(N)}$ = probability density in phase space of N molecules.

$\bar{f}^{(N)}$ = time averaged $f^{(N)}$.

$\bar{f}^{(n)}$ = time averaged probability density in the phase space of n molecules in a system of N molecules.

$g^{(2)}$ = pair correlation function.

$g_0^{(2)}$ = equilibrium radial distribution function.

$g'^{(2)}$ = perturbation to the equilibrium radial distribution function.

H = enthalpy.

$\vec{j}^{(n)}$ = particle current density in the configuration space of n molecules.

$\vec{j}_a^{(2)}$ = particle current density in pair space projected on the singlet space of molecule a.

k = Boltzmann constant.

m = mass.

N = total number of molecules.

n = subset of total number of molecules.

$\vec{P}$ = momentum vector in N-n dimensional phase space.

$\vec{p}$ = momentum vector in n-dimensional phase space - or singlet space.

$\vec{P}_1, \vec{P}_2$ = the 2 momenta in 12-dimensional phase space.

p = pressure.

$\vec{Q}$ = position vector in N-n dimensional phase space.

$\vec{q}$ = position vector in n-dimensional phase space.

$\vec{q}$ = heat current density.

$\vec{q}_k$ = heat current density due to transport of thermal kinetic energy.

$\vec{q}_v$ = heat current density due to molecular interactions.

R = gas constant

$\vec{R}, \vec{R}_{12}$ = relative coordinate of molecules in a pair.

$\vec{R}_1, \vec{R}_2$ = the two positions in 12-dimensional phase space.

$\vec{r}$ = the positions in singlet configuration space.

s = constant occurring in an empirical radial distribution function (103).

T = absolute temperature.

t = time.

t = constant occurring in an empirical radial distribution function (103).

$\vec{u}$ = particle velocity.

V = pair interaction potential.

V_N = total intermolecular potential of N molecules.

v = molar volume.

$W^{(n)}$ = potential of mean force in the configuration space of n-molecules.

$\vec{X}$ = external force per unit volume.

β = 1/kT

ε = energy occurring in the Lennard-Jones potential (90).

η = coefficient of viscosity.

Θ = correlation time.

θ, φ = angles in polar coordinates.

$\varkappa$ = coefficient of thermal conductivity.

$\varkappa_{\kappa}$ = kinetic part of the coefficient of thermal conductivity.

$\varkappa_{v}$ = intermolecular part of the coefficient of thermal conductivity.

$\varkappa_{v}^{(1)}$ = a part of the intermolecular part of the coefficient of thermal conductivity as defined by (92).

$\varkappa^{(1)}$ = a part of the coefficient of thermal conductivity as defined by (100).

ζ = friction constant.

$\underset{\sim}{\zeta}^{(2)}$ = friction tensor.

$\underset{\sim}{\bar{\zeta}}_{a}^{(2)}$ = friction tensor in pair space projected on the singlet space of molecule a.

$\vec{\Pi} = \vec{P}/m - \vec{u}$

ρ = mass density

$\rho^{(n)}$ = number density in the configuration space of n molecules.

$\underset{\sim}{\sigma}$ = symmetric stress tensor.

τ = time smoothing interval.

REFERENCES

1. J. G. Kirkwood, F. P. Buff, and M. S. Green, J. Chem. Phys. 17, 988 (1949).

2. J. H. Irving and J. G. Kirkwood, J. Chem. Phys., 18, 817, (1950).

3. J. G. Kirkwood, J. Chem. Phys., 3, 300, (1935).

4. M. Born and H. S. Green, Proc. Roy. Soc. A, 188, 10 (1946); 190, 455, (1947).

5. J. G. Kirkwood, J. Chem. Phys., 14, 180 (1946).

6. K. Clusius, Zeit. Phys. Chem. B 31, 467, (1935).

7. E. Mathias, H. K Onnes, and C. A. Crommelin, Proc. Roy. Acad. Amsterdam, 5, 667, (1912).

8. A. Eisenstein and N. S. Gingrich, Phys. Rev., 62, 261, (1942).

9. W. H. Keesom and A. P. Keesom, Physica 3, 359, (1935).

PROPOSITIONS

1. I propose that a model theory for the viscosities of pure liquids be:

   a) tested by trying to correlate the viscosity and hydrolytic stability of tetrasilicates;

   b) used to assess the aggregation state of molecular species in the liquid;

   c) extended into a parachor scheme to predict viscosities.

2. I propose that a model theory for the viscosity of liquid mixtures be:

   a) tested by trying to correlate the concentration-dependence of the viscosity with that of the thermodynamic functions;

   b) used to define a new ideal norm for the viscosity of a liquid mixture;

   c) used to test the assumption that only binary interactions are significant in the liquid.

3. The formula for the ~~specific~~ intrinsic viscosity, $[\eta]$, in terms of the molecular weight M and the constants K and α, $[\eta] = KM^{\alpha}$, used for polymer solutions, may also apply to some substances of low molecular weight.

4. The Monte Carlo method can be used to evaluate the radial distribution function of a hard sphere fluid and of hard sphere fluid mixtures. I.B.M. equipment can be used for the calculations, and the results may be compared with those of this thesis.

5. The general integral equation for the radial distribution function of a two component fluid mixture should to set up and solved in the hard sphere approximation. These radial distribution functions can then be used to study the effect of molecular size on the thermodynamic functions of fluid mixtures.

6. An electrical analog computer may be used to evaluate the three-dimensional Ising model of ferromagnetism. This method can take into account interactions between other than nearest neighbors.

7. An approximate order-disorder treatment of a crystalline isotopic mixture of A and B supports the conclusion that the equilibrium form (with respect to pure A and pure B) is a superlattice at 0°K.

8. The "heat mole" of a component in a multicomponent mixture may be defined as the molecular weight times the ratio of the partial enthalpy of the component to that of the reference component. This "heat mole" is useful in multicomponent distillation calculations to compensate approximately for the heat balance. This definition of the "heat mole" increases the accuracy of the calculations but none of the tedium usually associated with a heat balance calculation is involved.

9. I propose that the radial distribution functions in the metastable gas-liquid region of the phase diagram (this thesis) might be used in a theory of cavitation.

10. A critical examination of the Jones-Ray controversy, which is concerned with the change of surface tension with concentration of an electrolyte, yields the conclusion that faults can be found for all the many explanations except Langmuir's. (Langmuir, Science 88, 430, 1938.)